NASA CR-72643

A STUDY OF THE EFFECT OF DOPING ON A CAST LOW-CHROMIUM HIGH STRENGTH, NICKEL-BASE ALLOY

N70.24295

CASE FILE COPY

by

C. S. Wukusick

GENERAL ELECTRIC COMPANY

Prepared For

NATIONAL AERONAUTICS AND SPACE ADMINISTRATION

FINAL REPORT

A STUDY OF THE EFFECT OF DOPING ON A CAST LOW-CHROMIUM,
HIGH STRENGTH, NICKEL-BASE ALLOY

by

C. S. Wukusick

GENERAL ELECTRIC COMPANY
MATERIAL AND PROCESS TECHNOLOGY LABORATORIES
CINCINNATI, OHIO 45215

Prepared For

NATIONAL AERONAUTICS AND SPACE ADMINISTRATION

December 4, 1969

Contract NAS3-11149

TABLE OF CONTENTS

ABSTRACT

The objective of this program was to develop improved cast nickel-base superalloys through additions of reactive metals to improve oxidation/corrosion resistance.

A total of 27 alloys based on modification of the NASA-TRW-VI-A alloy were evaluated in tensile, stress rupture, oxidation and hot corrosion tests. La additions were effective in improvement of the short-term hot corrosion resistance. However, in long-time tests the results were negative. Also, mechanical properties were seriously degraded. Modifications in the investment casting practice resulted in improved structures and mechanical properties but not equivalent to the base alloy.

The doping additions apparently affect hot corrosion behavior through their effects on surface oxide adherence rather than on overall composition. It is concluded that the concept is not adaptable to present investment casting practice.

LIST OF TABLES

LIST OF TABLES (CONTINUED)

LIST OF FIGURES

1. SUMMARY

The objective of this program was to increase the oxidation/corrosion resistance of a cast high strength nickel-base superalloy by addition of reactive (doping) elements.

The NASA-TRW-VI-A (less Re) alloy was selected as the base alloy for the program. Twenty-seven investment cast alloys were evaluated for oxidation/corrosion behavior and mechanical properties. In addition, 50 alloys were chill cast and evaluated for corrosion resistance. Alloying (doping) additions studied were Re, Mn, Y, Ce, Gd, Th and La. Investment casting procedures were varied to modify the cast structures of the alloys. Mechanical properties were evaluated through tensile tests at 1600F and stress-rupture tests at 1800F, 27.5 ksi. All the investment cast alloys were evaluated for static oxidation resistance at 1800F, 1000 hrs. and 2000F, 400 hrs. Hot corrosion tests were carried out in a flame tunnel facility at 1600F and 1750F with NaCl ingested into the gas stream at concentrations up to 100 ppm.

In the initial series of 17 alloys, individual dopants were added at concentrations of up to 0.8 w/o Mn, 0.5 w/o Re, and 0.30 w/o of Ce, Y, Gd, Th, and La. The addition of Re to the base alloy resulted in an increase in rupture life with 0.25 w/o as effective as 0.5 w/o. The rare-earth type elements lowered the rupture life from 50 to 90% and ductility without any significant improvement in corrosion resistance. It was concluded that the dopant levels were too low to affect the corrosion resistance. The degradation of mechanical properties was attributed to grain-boundary formations of low-melting Ni-rare earth compounds. Improvements in the distribution of the rare-earth containing phases were deemed necessary to retain useful mechanical properties.

In order to determine the optimum dopant concentration with near-ideal dopant distribution, a large number of chill-cast alloys were evaluated for corrosion resistance. It was determined that about 0.5 w/o La was required to significantly improve corrosion resistance. Also, it was found that Mn was generally detrimental particularly in combination with the rare-earth elements. The final series of 10 investment cast alloys contained 0.4 to 0.6% La or La + Y. Investment casting procedures were also varied in order to obtain a better dopant distribution. The use of a mold imbedded in nickel shot resulted in a faster freezing rate and a better structure. Mechanical properties, while improved, were still poorer than the base alloy. Hot corrosion resistance also was not significantly improved in the investment cast alloys, particularly in long-time low salt tests.

The results of the oxidation/corrosion studies indicated that the dopants act to improve surface stability principally through their effects on surface oxide characteristics, i.e. by formation of adherent oxides.

It is concluded that successful application of the doping concept will require consolidation techniques other than conventional investment casting. Also the base alloy should exhibit relatively good corrosion resistance, so that oxide fracture will not result in catastrophic failure. The objective should be to extend life through formation of spalling-resistant surface oxides.

2. INTRODUCTION

Nickel-base superalloys are utilized extensively in the "hot" components of aircraft gas turbine engines. The successful utilization of the alloys is attributed to their unexcelled combination of high temperature strength and corrosion resistance. The continuing need for improved turbine materials is well known, and one of the most critical needs is for stronger turbine blade alloys. Increased strength can result in improved performance through increased thrust but it must be accomplished without too great a sacrifice in corrosion resistance.

It is generally known that in complex turbine blade alloys, the chromium content determines to a great extent the resistance to corrosion by the turbine atmosphere. In general, the higher the Cr content the greater is the resistance to corrosion. However, when faced with the problem of increasing the strength of Ni-base alloys, it is advantageous to lower the Cr content since it is not as effective a strengthener as other, more refractory elements; Mo, W, etc. Over the years as the strength of Ni-base superalloys has been increased, the Cr content has been correspondingly lowered. There has been a progression from U-500 (20 Cr) to Rene' 77 (15 Cr) to Rene' 100 (9 Cr) to NASA-TRW-VI-A (6 Cr). The resistance to corrosion (sulfidation) has decreased although the resistance is not always directly proportional to the Cr content. It is clear, however, that in order to utilize alloys containing 6-9% Cr in long-life engines, the resistance to sulfidation must be improved. Even when considering the alternate route of coating for corrosion resistance, the base alloy must exhibit adequate resistance to prevent catastrophic failure. This is because turbine components such as blades are subject to ballistic impact and erosion conditions which can result in coating penetration and failure. In such instances the corrosion resistance of the base alloy is quite important.

Several approaches to improved turbine blade materials are possible, and include directional solidification, dispersion strengthening, composites and other alloy bases. However, the most attractive route, considering timing and economy is in precision casting. This approach has the very important advantage of capitalizing on an already-existing production technology. However, in view of the dilemma caused by low Cr contents, it is imperative that an adequate substitute for Cr be found. As a result of extensive studies of the surface stabilities of superalloys,[1,2] a possible substitute for a portion of the Cr was found. For certain alloys practically all of the major oxidation/corrosion problems or characteristics (i.e. heterogeneous oxides, spalling, internal oxidation and oxide volatility) can be significantly improved by "doping" or minor additions of Th, Y and rare-earths. Combinations of rare-earth elements and Mn have been particularly effective in certain alloys. The alloy HS-188 developed by Union Carbide Company owes its excellent oxidation resistance to La + Mn additions. Apparently the La improves oxide adherence and promotes the formation of a spinel oxide Mn Cr_2O_4 which is less volatile in high-velocity environments than Cr_2O_3.

2

While the precise mechanisms by which the minor additions improve surface stability are not fully established, it has been shown that doping is capable of altering the nature and adherence of major scaling products. Therefore, the objective of the present work was to combine the high strength of a low-Cr turbine blade alloy with hot corrosion resistance conferred by "doping" element additions. Preliminary studies demonstrated very significant improvements in the corrosion resistance of the NASA-TRW-VI-A and other alloys when proper amounts of dopants were added (Figure 1).[2] The rare-earth type elements exhibit very limited solubility in Ni-base alloys and as a result exhibit marked segregation. Therefore, since a possible detrimental effect on mechanical properties could be expected, a major objective of the present program was to obtain improved surface stability without loss in strength.

2.1 Program Goals

In order to represent a significant advance to turbine materials technology, an alloy must exhibit as a minimum, the following properties:

(1) Strength: The high temperature strength as measured by creep and stress rupture must be increased to a point which will result in an increase in temperature capability of approximately 50F as indicated in Figure 2 over existing alloys such as Rene' 100. (The increased strength can result in a nearly tripled service life.)

(2) Hot Corrosion Resistance: Rene' 77 alloy is a good example of commercially available alloys which have exhibited adequate surface stability in service. The Cr content of U-700 is 15% and probably represents nearly a lower limit for service in most turbine applications. The resistance of a newly developed alloy should be at least equivalent to that of Rene' 77 alloy.

(3) Ductility: The ductility of the alloy should be adequate to provide sufficient resistance to low cycle fatigue including thermal fatigue. The minimum ductility value has not been determined but it should be at least high enough to insure that fracture does not occur during the 2nd stage of creep.

(4) Cost: With the strength increase outlined above the cost of the alloy in part form should not be more than double that of presently available alloys. This requirement effectively limits the selection of production techniques to conventional precision casting since other processes would lessen the economic advantage.

3. TECHNICAL PLAN

The objective of this program was to establish the effects and develop an understanding of doping elements, singly and in combination, on the oxidation/corrosion behavior, structural stability and mechanical properties of a selected NASA-TRW developed alloy.

3.1   Alloy Selection

3.1.1   Base Alloy

As stated in the goals, the base alloy selected for the program must exhibit a 50F advantage in strength capability over existing alloys. Alloy development programs in progress at the start of this study had progressed to a point where the development of alloys having strengths equal to Rene' 100 and surface stability equal to Rene' 77 seemed assured. Therefore, the strength of Rene' 100 was used in establishing a base for the program. A survey of available alloys (both commercial and experimental) indicated that the NASA-TRW-VI-A alloy[3] (hereafter referred to as VI-A) exhibited the required strength on a strength/density basis as indicated in Figure 3. The chemical compositions of several turbine blade alloys are presented in Table I. From available data the VI-A alloy is about equivalent to Rene' 100 alloy in resistance to hot corrosion even though its Cr content is lower.

In addition to the above comparisons, preliminary studies of a number of alloys indicated that the VI-A alloy could be greatly improved in surface stability by doping additions. A typical result of the preliminary work is shown in Figure 4.

The VI-A alloy contains a small amount of Re, a rather expensive alloying element. In this study Re was considered a dopant and the base alloy was the VI-A alloy (less Re).

3.1.2   Alloying Additions

The rare-earth type elements were selected from the data presented in Table II in which the elements are separated into five distinct groups based on their physical-chemical properties. The elements are grouped primarily with regard to oxidation states. In addition the first group (Y-Sc) of elements exhibit relatively high melting and boiling points. The next two groups (Ce-Nd) exhibit low melting but high boiling points. The fourth group (Sm-Yb) exhibit both low melting and boiling points. The last two elements are similar to the first group except for the variation in oxidation states.

Elements from each of four groups were selected for this study. The group consisting of Sm, Er and Yb were eliminated from consideration because of their low boiling temperatures. The elements, Y, Gd, Ce, La and Th were selected from cost, availability and prior study[2] considerations. Manganese was selected as a doping element based on its demonstrated beneficial effects when present in Rene' Y, HS-188 and Rene' 100 alloys. Rhenium, being quite similar chemically to Mn might be expected to affect surface reactions in a similar manner, and so was considered as a doping element although its primary role in VI-A alloy is that of a strengthener.

4

The optimum concentration of rare-earth type doping elements based on past experience at the start of the program lay between 0.1 and 0.4 atom percent (a/o). Concurrent work with Rene' 100 alloy indicated that in order to retain adequate strength the concentration should be kept on the low side. (2) Therefore, in the initial alloys the concentration of rare-earth type elements was kept below 0.3 a/o.

The effect of Mn concentration was generally not well defined except 1 w/o had been found effective. Since Mn is highly soluble in the matrix, it could have a significant effect on matrix strength and stability. For this reason initial Mn concentrations were set at 0.4 and 0.8 w/o.

Rhenium is present in VI-A alloy primarily as a strengthening element although some effect on corrosion behavior was anticipated. Prior studies indicated that the strengthening effect of Re was about constant at 0.25 to 0.50% Re. Therefore, these levels were included in the initial alloys.

The initial additions to alloy VI-A are listed in Table III (a). All of the doping elements were evaluated singly in the initial series. Upon completion of the evaluation of the first series of alloys, modifications in doping element concentrations and combinations of doping elements were prepared and evaluated. The alloys are listed in Table III (b) which also lists changes in casting practice which will be discussed in a later section.

3.2   Alloy Preparation

3.2.1   Master Alloy

The VI-A master alloy (less Re) was prepared by TRW Inc. using standard vacuum induction melting procedures. Four 150 -lb. heats of the alloy were cast into 2 3/4" diameter bars suitable for remelting. Vendor analyses of the four heats are listed in Table IV. The analyses were all within specification for the alloy (except for Re).

Master alloys of the doping elements were prepared by arc-melting Ni-dopant alloys in an inert atmosphere. Chemical compositions of the resultant master alloys are listed in Table V. The use of master alloys tends to reduce crucible reactions and increases the alloying rate of high-melting point elements such as Re.

3.2.2   Investment Castings

The procedures utilized in casting the experimental alloys are listed in Table VI. Molds were designed to provide the necessary test specimens. The molds were innoculated with cobalt oxide to control grain size. The melting procedure was determined from initial casting trials carried out at both G.E.-M&PTL and Misco Division of Howmet Corporation. The initial casting of the base alloy at Misco was cast with a 275F superheat into a mold heated to 1800F. The grain size, as measured at the surface was extremely small, approximately 1/64" diameter. In order to produce the desired 1/16-1/32" grain size a 325F superheat was found necessary. The melting procedure for the first 17 alloys was as follows:

5

1.   The master alloy charge consisted of equal amounts of four (4) heats, F4063, 64, 66 and 67.

2.   The master alloy and the doping additions were charged into an alumina crucible and meltdown was completed in 3 to 5 minutes.

3.   After adjustment of the superheat, the alloys were cast into molds preheated to 1800F. A light wrapping of asbestos on the mold was removed four minutes after pouring of the heats.

During melting and casting, vacuum was maintained at less than 0.5 microns. The melts were generally free of slag indicating a minimum of melt-crucible reaction. All the test bars were inspected by x-ray and dye-penetrant (zyglo) at Misco. One specimen from alloy #11 was scrapped due to failure to pass zyglo inspection. Typical castings are shown in Figures 5 and 6. The casting procedures were varied for alloys 18-27. The modifications were introduced to obtain variations in alloy structure, as will be discussed more fully in succeeding sections.

3.2.3   Chill Castings

A number of the alloys were prepared as "drop" or "chill" castings. The procedure consisted of arc-melting 50 gram charges in a cold-copper crucible in a helium atmosphere. The resultant buttons were then placed over the cavity of a shaped mold, remelted and "dropped" into the copper mold. Typical castings are shown in Figure 7. The resultant 3/16" diameter cast pins were centerless ground prior to testing. The chill castings were introduced to provide a more homogeneous distribution of the dopants in the alloys. Nominal compositions of the chill castings are listed in Table VII.

3.3   Alloy Evaluations

3.3.1   Chemical Analyses

Each of the investment cast alloys was analyzed for dopant concentration. Also, the base alloy and one of the doped alloys were evaluated for complete chemistry. Chemical analyses for the dopants were performed at G.E.-M&PTL using a quantitative spectrographic technique.

3.3.2   Heat Treatment Response

Specimens of each alloy were heated for 1 hour at temperatures between 2000 and 2300F to determine (a) the incipient melting temperature and (b) other microstructural changes such as solutioning of gamma prime and carbides. Selected alloys were also given extended aging treatments to determine effects on microstructures.

3.3.3   Mechanical Properties

Duplicate specimens of each alloy were tested in air for tensile and stress rupture properties.

6

(a) Stress rupture at 1800F, 27.5 ksi; a condition which results in at least a 100 hour life for the base VI-A alloy.

(b) Tensile tests at 1600F; a temperature which usually yields minimum ductility in the base alloy.

3.3.4 Oxidation/Hot Corrosion

All the investment cast alloys were screened for oxidation/hot corrosion properties as outlined below. The test specimens were either flat plates (.080" X .5" X .6") or pins 1/8 to 3/16" diameter. All specimens were ground, then polished through 600 grit paper and rinsed in acetone prior to test. Duplicate specimens were tested in most cases and after test the specimens were examined metallographically to determine metal loss and internal oxidation behavior.

(a) Cyclic static oxidation tests were conducted at 2000F for a total of 400 hours in 25 hour cycles and at 1800F for 1000 hours in 100 hour cycles. Some of the alloys were also exposed isothermally for 400 hours at 2000F, and 1000 hours at 1800F to evaluate the effect of cycling on oxide adherence. Weight changes, spalling tendencies and general oxide appearance were recorded.

(b) All the alloys were screened for hot corrosion resistance in a flame tunnel facility in an atmosphere containing a high concentration of NaCl ingested into the gas stream. The specimens were mounted in a rotating test fixture. The flame velocity was about 75 ft./sec. Initially all the alloys were tested for 50 hours in an atmosphere formed by combustion of JP-5 fuel at a 30/1 air/fuel ratio and containing 100 ppm synthetic sea salt prepared according to ASTM D665-60. Test temperatures were 1550 and 1725F.

Selected alloys were subjected to a planned 1000 hour test at 1600F, 1 ppm salt in a similar test rig. The test was terminated after 450 hours due to failure of most of the alloys.

4. RESULTS

4.1 Chemical Compositions

Chemical analyses of the master heats and master alloys were presented in Tables IV and V. Chemical analyses of the alloys after casting (alloys 1 and 8) are presented in Table VIII. No significant changes in base alloy chemistry occurred during the investment casting process.

Chemical analyses of the alloys for dopant concentrations are presented in Table IX. In general little or no loss of dopants occurred during the casting process. The fact that some analyses are higher than expected from the amounts

added probably reflects on segregation of dopants in the sample used for chemical analysis. There was a consistent loss of about 20% of the Mn during melting owing to the high vapor pressure of the element.

4.2   Heat Treatment Response

The as-cast microstructures of the investment cast alloys are presented in Figures 8 through 23. Some variation in carbide and γ-γ' eutectic morphology is observed in the various alloys but no systematic trend is evident. The distribution of the rare-earth containing phases is interdendritic and closely associated with γ-γ' eutectic nodules and carbides.

The alloys contain a large amount of γ-γ' eutectic nodules which vary from a finely divided structure at the origin to a coarse γ' with only a small amount of γ at the outer edge. It is evident that after the nodules were solidified, some liquid remained and other phases, such as those containing rare-earth elements were formed adjacent to the γ-γ' nodules. Even in the base alloy an unidentified phase, presumably a boride, formed adjacent to the γ-γ' nodules.

Two types of carbides were formed, blocky and script. In general the script carbides were formed in the dendrite cores while the blocky ones were randomly distributed.

Alloys 18-20 which were cast into 2000F molds with reduced superheat (225, 125, 50F) exhibited a large amount of interdendritic porosity and casting shrink. Also present were indications of mold-metal reaction which tended to result in a porous surface (Figure 14). The changes in structure did not correlate very well with degree of superheat; the greatest degree of structure refinement was obtained with 125F superheat. The differences may be related to minor variations in melting and pouring time which could cause varying mold temperatures during casting. In this series of heats the molds were heated to 2000F in a separate facility, and transferred to the casting chamber just prior to casting.

Alloys 22 through 27 which were cast into molds imbedded in Ni-shot exhibited somewhat more refined microstructures than the alloys cast under standard mold conditions as shown in Figure 15.

In order to determine heat treat potential and incipient melting characteristics, the alloys were heated for 1 hour at temperatures between 2000 and 2300F. Metallographic observations are summarized in Table X. The base alloy and the alloys containing Re exhibited little or no incipient melting at temperatures up to 2300F. All the doped alloys exhibited varying degrees of melting at 2300F and some at 2200F. Melting occurred primarily in regions adjacent to the γ-γ' eutectic nodules. Alloys containing Ce additions exhibited the greatest indication of melting, while Yttrium and Thorium are probably the least detrimental of the rare-earth type elements. The degree of melting increased as the amount of rare-earth phase was increased. This was particularly evident for the La-containing alloys.

8

The heat treatment study demonstrated that the alloys cannot be solutioned with respect to the γ' precipitate. Microstructures are shown in Figures 24 through 28, after high temperature heat treatments. The heat treatments tend to coarsen the γ' in the eutectic nodules by solutioning of the network. In some areas, particularly adjacent to the $\gamma-\gamma'$ eutectic nodules, it appears that beta phase (NiAl) may be formed. The study indicates that the alloy should not be given a high temperature solution treatment since this only coarsens the $\gamma-\gamma'$ eutectic structure and most probably causes a loss in ductility which is already marginal.

One of the effects of intermediate temperature heat treatments (1600-1900F) on superalloys is the formation of a γ' envelope in the grain boundary due to the reaction:

$$\text{MC} + \gamma \longrightarrow M_{23}C_6 + \gamma'$$
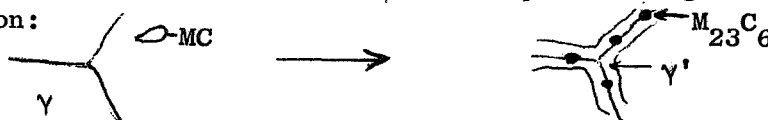
The γ' forms around $M_{23}C_6$ particles. Since the rare-earth phases were generally located in the grain boundaries, an attempt was made to form γ' around the R.E. phases and thus reduce their detrimental effects on high temperature strength. However, extended heat treatments (1000 hours at 1700 and 1800F) did not result in any envelopment of the R.E. phases by γ'. As indicated in Figure 29, the carbide particles were enveloped but the La-containing phase was not. The heat treatments also were not effective in spheroidization of the rare-earth-containing phases. It is clearly evident that the morphology of the rare-earth containing phases must be controlled during the casting processes principally through control of the freezing rate.

4.3   Mechanical Properties

The results of 1600F tensile tests performed on the alloys are presented in Table XI. In general, all the dopants reduced the tensile ductility although Re and Mn exerted a relatively minor effect. Most of the test specimens fractured near the end of the gage. Some specimens were machined to insure alignment but the ductilities were still low.

The results of the stress rupture tests are presented in Table XII. The addition of Re to the base alloy resulted in a slight increase in rupture life, with 0.25% Re more effective than 0.50% Re. Mn progressively decreased the life although the differences are not great. The rare-earth type elements generally lowered rupture life and ductility. Rupture life decreased as the dopant content was increased. Of the doping additions, Y, Gd and Th were about equal in reducing rupture life. La and Ce exhibited a more pronounced effect in reducing rupture life than the other additions. It is apparent that, due to the location of the rare-earth containing compounds in the grain boundaries, the strength of the boundary regions is decreased. Therefore, the alloys are ductility limited. The base alloy itself is very close to being ductility limited due to the large amount of $\gamma-\gamma'$ eutectic nodules in the boundary regions. Extensive inter-granular cracking occurs during testing as shown in Figure 30. Improvements in the distribution of the rare-earth phases by utilization of mold chilling (alloys 22-27) resulted in minor increases in rupture life. However, the strengths are well below the base alloy.

The very low strengths of the alloys cast with a high mold temperature and low superheat might be attributed to the porosity present in the test bars. It is also suspected that alloy-mold reaction could have resulted in contamination of the alloys.

4.4   Oxidation

All the investment cast alloys were evaluated for oxidation behavior at 1800 and 2000F. The weight change data for the cyclic 1800F tests are presented in Tables XIII and XIV. In Table XIII the total or gross weight changes are recorded. The gross changes include both the oxide retained on the specimen as well as the spalled product. The net weight changes are recorded in Table XIV. The difference between the two tables is the spalled product. In general, the gross weight gains for the doped alloys were larger than for the base alloys but the oxide adherence was improved. Some of the alloys were oxidized isothermally and comparisons between isothermal and cyclic data are presented in Table XV. In general the gross weight gains in the cyclic tests are about 2X those in the isothermal tests except for alloys 12, and 14 which exhibited good oxide adherence.

The weight change data for the 2000F cyclic oxidation tests are presented in Table XVI. Examination of the data indicates that Mn is detrimental to the oxidation resistance with the biggest effect between 0.2 and 0.4% Mn. Re also appears to be detrimental. Yttrium and Gd appear to provide the most improvement in oxidation resistance. The results for alloys 18 through 25 were quite variable. These alloys contain combinations of Re, La and in some cases Mn, all of which seem to impair oxidation resistance.

A comparison of isothermal and cyclic tests data is made in Table XVII. As in the case of the 1800F tests, Yttrium appears to provide the greatest improvement in oxidation resistance at 2000F. Specimen appearance after cyclic oxidation is indicated in Figure 31, and after isothermal oxidation in Figure 32. The improvement in oxide adherence provided by the rare-earth element additions is clearly evident. In attempting to explain the causes of the differences in oxidation behavior, oxides from several of the alloys were analyzed by x-ray diffraction and emission spectrography. Alloys 1, 3, 6, 8, 10, 12, 13 and 14 were examined after 400 hours at 2000F. The surface oxides contained α Al_2O_3 and a spinel which from spectrographic analysis probably contained Ni, Cr, Co and Al. The spinel was probably $Ni(AlCr)_2O_4$; (a_o = 8.05-8.15 $\mathring{A}$). Also present was an oxide which is isostructural with $ZrSiO_4$ contained in the crucible material. Analysis also indicated the presence of NiO and traces of rare-earth elements in the spalled residue from the alloys which contained rare-earth additions. The x-ray diffraction data obtained from the base alloy and alloy 12 (0.21 Y) are presented in Tables XVIII through XXI. The only apparent difference is the presence of NiO in the oxide spalled from the doped alloy #12.

Metal loss data determined metallographically are presented in Table XXII. Rather high metal losses in the Mn and Re doped alloys suggests oxide volatility since all of the losses cannot be attributed to spalled oxides. The best alloys appear to be those containing Y, Ce, Gd and small amounts of La, although, internal oxidation is evidently relatively deep. As an example, in Figure 33, the La

10

containing alloys exhibited a small amount of alloy depletion but significant
intergranular oxidation. The structures are typical of the most of the doped
alloys. In Figure 34 are shown typical examples of alloys which exhibited high
metal losses. Oxidation was general, without marked intergranular attack.

4.5 Hot Corrosion

Hot corrosion testing included not only the investment cast alloys, but
also series of "drop" cast alloys prepared to evaluate compositional and struc-
tural effects.

Initially the first 17 alloys were evaluated in corrosion tests at 1550F
and 1725F, 50 hours in 100 ppm salt. In these tests the alloys all exhibited
rather poor corrosion resistance with some alloys worse than the base alloy. In
order to determine if structural effects were responsible the alloys were also
evaluated in the drop-cast condition. The results of the tests are presented
in Table XXIII. Drop-casting of the alloys to improve the distribution of the
doping elements in most cases caused a decrease in corrosion resistance at 1725F.
The reason for this is not clear. Photographs of the tested drop-cast specimens
are presented in Figure 35. Examples of microstructures of corroded specimens
are shown in Figure 36. Note, that once accelerated corrosion is initiated, the
microstructures in the corrosion zone are similar even though the initial micro-
structures are quite different. Apparently, recrystallization or fragmentation
has occurred and the resultant particle or grain size is the same in the two alloys.
This indicates that structural effects are important only in the initial stages
of corrosion, most probably in how they affect oxide film formation.

As a result of the poor corrosion resistance of the initial alloys con-
taining single doping additions, an additional series of drop-cast alloys con-
taining RE + Mn combinations were evaluated. Prior work[2] had indicated that
in some alloys, such combinations were more effective than single additions. The
results as shown in Figure 37 were negative, however, and it was concluded that
the RE content was too low to effectively improve the corrosion resistance. A
third series of drop-castings were prepared to evaluate larger RE additions and
combinations of RE + Mn. The base alloys of the series contained 0.25% Re (Alloy 5).
The results are summarized in Table XXIV and photographs are presented in Figures
38-40. The results demonstrate that Mn additions are detrimental. There appeared
to be an optimum La level at about 0.5-0.75 w/o, with 1% La detrimental. Several
of the alloys exhibited better corrosion resistance at 1725F than the base Rene' 77
alloy included as a standard. Photomicrographs of selected alloys are shown in
Figures 41 and 42. In Figure 41, the 0.5% La alloy exhibited a thin adherent
oxide and small amount of internal oxidation and/or sulfidation. The 0.75% La
alloy was quite variable as shown in Figure 42. The attack varied from negligible
to extensive internal sulfidation and corrosion. Indications are that in the
drop-castings, extensive internal sulfidation can occur prior to accelerated oxi-
dation. The internal sulfidation in the absence of oxidation is occurring in the
base as well as the doped alloys as shown in Figure 42. It is much more pronounced
in the drop cast alloys than in investment castings.

As a result of the preceeding tests, it was concluded that the La content of the investment cast alloys should be increased to about 0.5 w/o regardless of effects on mechanical properties. Concurrently, it was decided to evaluate further effects of casting procedures on mechanical properties. The resultant alloys (Nos. 21-27) were investment cast and evaluated. Some of the alloys were also drop-cast for comparison of corrosion behavior. The overall appearance of the specimens after a 1725F corrosion test is shown in Figure 43. The test was terminated after 30 hours because of significant corrosion of most of the specimens. The results demonstrate again the beneficial effect in drop-casting of the alloys. The one alloy (#25) which contained Mn exhibited very poor resistance even in the drop-cast condition, thus duplicating the results of earlier tests.

At this point in the program, the best alloys were selected for a long time (1000 hours), low salt (1 ppm) test at 1600F. The selected alloys are listed in Table XXV along with metallographic observations. The test was terminated after 450 hours because of significant corrosion of the test specimens. A photograph of the test specimens is shown in Figure 44. The alloy containing yttrium was probably the best overall but probably not significantly superior to the base alloy containing Re. The base alloy (#1) was quite variable as shown in Figure 45. The 0.25% Re alloy exhibited relatively good corrosion resistance while the 0.5 Re alloy exhibited extensive blisters and intergranular attack (I.G.A.) as indicated in Figure 46. The alloy containing Y exhibited I.G.A. (Figure 47) which accounted for the relatively high metal loss. Also shown is an etched specimen of an 0.5% La alloy containing I.G.A. and alloy depletion. The high La alloys generally exhibited poor resistance to the low-salt environment with the 0.6% La alloy much poorer than the base alloys.

5.   DISCUSSION

The results obtained in this study indicate that, whereas reactive metal additions can markedly improve the surface stability of a number of alloy systems,[1,2,4,5] care must be taken in the application of the concept. Unless properly applied, the additions can drastically impair both mechanical properties and surface stability. The first important requirement to be achieved is the proper dispersion of the doping elements. The doping elements as a family are soluble in the alloy only when in the molten state. Upon freezing the elements form a stable M-RE compound which has a low freezing temperature and tends therefore to form in dendrite and grain boundaries. Because of the very low solubility in the solid state, the distribution of the rare-earth phases cannot be significantly changed through heat treatment. In a casting, therefore, the distribution is fixed during the freezing process.

Most successful applications of "doping" have been in wrought alloys, where the RE-containing phases are distributed more uniformly through the working processes. Examples of successful applications of the doping concept are the FeCrAlY, and HS-188 (Cobalt Base) alloys which are used in the wrought form. Turbine blade alloys are generally stronger in the cast than in the

wrought form. Also the strongest alloys, such as VI-A are of limited
workability. In addition there is a very important economical advantage
in the utilization of precision castings particularly of turbine blades
of complex configurations. For these reasons, the present program was
limited to the evaluation of cast alloys. Modifications of the present
investment casting process to achieve a highly significant improvement
in dopant dispersion does not appear feasible. Even if successful, it
appears unlikely that adequate mechanical properties could be retained
or developed. In order to retain high temperature strength, a coarse
grain size is required and in the VI-A alloy the presence of excess gamma
prime would prevent the growth of large grains in a fine grained casting.

The detrimental effect of the rare-earth type elements on mechanical
properties is attributed to their location in the interdendritic and grain
boundary areas. At high temperatures, high strength nickel-base superalloys
characteristically fail due to grain boundary separation. This may be due
to an inbalance in strength between grains and grain boundaries. The base
alloy VI-A exhibits quite low ductility due to the presence of a large amount
of γ-γ' eutectic in the boundaries. The addition of a small amount of a
weak or brittle phase in the boundaries might be expected to seriously impair
the ductility. It is not clear whether the RE-containing phases are weak
and ductile, or are brittle. The net effect, that of reduced overall alloy
ductility, would be the same in either case. In Ni-base superalloys, extended
high temperature heat treatments (1600-1800F) tend to result in precipitation
of grain boundary carbides and formation of γ' envelopes around the carbide
particles. Such reactions in some cases improve the high temperature ductility.
In this study, it was found that little or no reaction occurred between the
RE-containing phases and the matrix, and no envelopment of the particles occurred.
This is probably a result of the very low solubilities of the RE elements
in the Ni-base matrix. Previous work[2] indicated that the RE-containing
phases are of compositions near Ni_5M_{RE} as predicted from the binary phase
diagrams. The high stability of the RE-containing phases provides an
inherent advantage in that the RE elements apparently do not effect γ' solu-
tioning and precipitation reactions. γ' growth during aging at 1700-1800F
was not affected by the RE additions. Therefore, it is tentatively concluded
that the decrease in strength caused by the RE additions is not as a result
of a change in γ' characteristics, but is strictly a grain boundary phenomenon.
In order to minimize effects on strength, the RE phase must be distributed
more uniformly throughout the structure - both matrix and grain boundary.
This cannot be achieved with present casting practice or with relatively simple
modifications of existing practice.

The distribution of the RE-containing phases is also very important
in surface reactions, both oxidation and hot corrosion. Pronounced intergranular
attack (I.G.A.) can occur as a result of the location of the RE in the grain
boundaries. Because of the segregation, the RE elements cannot participate
very effectively in the surface reactions. The mechanism through which the
RE elements improve the oxidation/corrosion behavior of alloys has not been
completely defined. It has been fairly well established that the RE elements

13

do not change the major oxides formed but act in a secondary manner. There is good evidence in some systems (for example FeCrAlY) that the RE diffuses to the sub-scale region and precipitates as a finely dispersed internal oxide.[4] The oxide particles may act as "roots" for the growing surface oxide film. Whatever the exact mechanism, the net result is an adherent oxide film. In this study the improvement (when it occurred) might also be related to the formation of more adherent oxides (Figure 41). The results obtained tend to support this supposition. First, the microstructures of corroded specimens were quite similar, indicating that once accelerated corrosion was initiated, it progressed in a manner independent of the doping content. Secondly, we might expect adherent oxide formation during the initial stages of corrosion testing. However, in long-time tests, as the oxide film thickens, spalling of the oxide during thermal cycling would be expected. We might expect then that doping would not be as effective in long-time tests. Once oxide spalling or erosion occurs, the alloy would corrode at a rate which may even be higher than normal because of the depletion of critical elements, (Al, Cr) in the underlying metal.

Relatively poor behavior in long-time, low-salt tests has recently been noted for Rene' 100 based alloys.[2] The results of the present investigation thus indicate similar behavior for the VI-A type alloys. In order to further verify the effect of oxide adherence on corrosion resistance, a series of FeCrAlY alloys were tested in the bare and pre-oxidized conditions. Alloy compositions and test results are shown in Figure 48. The yttrium additions result in the formation of adherent, coherent Al_2O_3 surface oxide. In the absence of the Al_2O_3 film only the alloys with high Al + Cr contents resisted the corrosion environment. The principal effect of the Y addition in the low Cr + Al alloys was in regard to formation of a protective Al_2O_3 oxide film.

In the long-time, low-salt test, the TRW-base alloys corroded initially near the bottom or top of the specimens. In the test fixture top and bottom rings of Hastelloy X were utilized to hold the specimens in place. Corrosion was initiated at the contact points indicating that abrasion of the surface oxide results in accelerated corrosion. It thus appears that the reliability of a doped blade alloy in a corrosive environment would be expected to be quite low. The best application of the concept would appear to be to prolong the life of an alloy which already exhibits relatively good corrosion resistance. It is unlikely that a small amount of RE can be effectively substituted for a relatively large amount of Cr and/or Al in an alloy.

One of the more important observations noted in this program was that combinations of Mn and RE elements were detrimental to the oxidation/corrosion resistance of the VI-A alloy. This is contrary to the results[2] obtained on other alloys such as Rene' 100 where Mn was found to be necessary. The most logical explanation for the Mn effect is that it must be related to the type of surface oxides formed. In other (higher Cr) alloys, Mn has been found to promote the formation of $NiCr_2O_4$ type spinel oxide, and thus improve oxidation resistance. In an alloy like VI-A which has a low Cr and a high Al content, the formation of Al_2O_3 or $NiAl_2O_4$ is likely. Mn may interfere with $NiAl_2O_4$ formation. Work by

14

Kvernes and Kofstad[5] indicates that Mn supports formation of $NiCr_2O_4$ and yttrium-modified alloys support the formation of $NiAl_2O_4$. It is also known that yttrium additions to FeCrAl alloys promote the formation of γ-Al_2O_3 surface oxide. The x-ray diffraction data obtained from the oxides on the VI-A alloy indicated the presence of both Ni $(CrAl)_2O_4$ spinel and γ-Al_2O_3 oxides. It is expected that Al-rich oxides should predominate and doping additions which stabilize such oxides should be utilized. From the results obtained in this study, it appears that yttrium may be the most effective doping element in improving overall oxidation/corrosion resistance.

The depression of the melting point of the alloy by RE additions is troublesome. Even in alloys without excessive γ-γ' eutectic, the γ' solution temperature will be above the incipient melting temperature. More refractory doping elements or compounds must be utilized. Since the mechanism by which RE elements are effective may be dependent on the precipitation of subscale oxide particles, there is a distinct possibility that the elements could be added in the form of a finely dispersed oxide, such as Y_2O_3. This, of course, would require a basic process different from precision casting.

6.   CONCLUSIONS

From the results obtained in this study, the following conclusions are offered:

1.   The addition of rare-earth type elements to a cast Ni-base superalloy in amount sufficient to improve the surface stability (0.5 w/o) seriously impairs the mechanical properties.

2.   Rare-earth elements, if not well-dispersed, do not effect significant improvements in surface stability.

3.   Rare-earth type elements improve surface oxide charact-teristics, principally oxide adherence. Improvements in corro-sion resistance are believed related to improved surface oxides rather than to the changes in alloy chemistry.

7.   RECOMMENDATIONS

It is recommended:

1.   Future work on the application of the doping concept should be concerned with more refractory doping compounds such as oxides.

2.   The base alloy selected for study should exhibit rela-tively good corrosion resistance, so that oxide fracture will not result in catastrophic failure. The objective should be to extend life through formation of spalling-resistant surface oxides.

8. ACKNOWLEDGMENTS

9. REFERENCES

1. Wasielewski, G.E., "Nickel-Base Superalloy Oxidation", Summary Report AFML-TR-67-30. Contract AF (615)-286, Jan., 1967.

2. Wasielewski, G.E., Wukusick, C.S., "Nickel-Base Superalloy Oxidation", Technical Report AFML-TR-69-27, February, 1969.

3. Collins, H.E., Quigg, R.J., Dreshfield, R.L., "Development of a Nickel-Base Superalloy Using Statistically Designed Experiments", Trans. Quarterly ASM, Vol. 61, No. 4, Dec. 1968.

4. Wukusick, C.S., "The Physical Metallurgy and Oxidation Behavior of Fe-Cr-Al-Y Alloys", G.E. Co. Report GEMP-414, June 1, 1966. (available from GE-NSP, Evendale, Ohio)

5. Knernes, I., Kofstad, P., "Studies on the Behavior of Nickel-Base Superalloys at High Temperatures", Progress Report #8, Contract F610526700057, CIIR Publication No. 596. January 31, 1969.

16

TABLE I

COMPOSITIONS OF NICKEL-BASE SUPERALLOYS

Alloy	Cr	Al	Ti	Co	Mo	W	Ta	Cb	V	C	Other
Rene' 100	9.0	5.5	4.2	15.0	3.0	-	-	-	1.0	0.17	
NASA-TRW-VI-A	6.0	5.4	1.0	7.5	2.0	6.0	9.0	0.5	-	0.13	0.5 Re, 0.4 Hf
Mar-M-200	9.0	5.0	2.0	10.0	-	12.5	-	1.0	-	0.15	
Inco 713-C	13.6	6.0	1.0	-	5.5	-	-	2.5	-	0.14	
Rene' 77	15.0	4.3	3.4	15.0	4.2	-	-	-	-	0.07	

TABLE II

SOME PROPERTIES OF THE RARE EARTHS Y, Sc AND Th

Element	At No	MP (°F)	BP (°F)	ΔH_{vap} (Kcal/mole)	Oxidation States	Ionic Radii (Å)	Metal Crystal Structure [a]	Transition Temp (°F)	Atomic Radii (Å) [b]	R_2O_3 Oxide Crystal Structure [a]	R_2O_3 Oxide Transition Temp (°F)	$\Delta H_{298}R_2O_3$ (Kcal/mole)
Y	39	2748	5486	85	3	0.88	hcp/bcc	2714	1.801/1.83	bcc	–	−455.45
Gd	64	2394	4946	73	3	0.94	hcp/bcc	2307	1.802/1.81	bcc/mono	∼2460	−433.94
Dy	66	2565	4226	67	3	0.91	hcp	–	1.773	bcc	–	−445.84
Ho	67	2662	4226	67	3	0.89	hcp	–	1.766	bcc	–	−449.55
Er	68	2727	4766	67	3	0.88	hcp	–	1.757	bcc	–	−453.59
Tm	69	2813	3130	56	3	0.87	hcp	–	1.746	bcc	–	−451.4
Lu	71	3006	3506	59	3	0.85	hcp	–	1.734	bcc	–	−452.8
Sc	21	2802	4946	75	3	0.68	hcp/fcc	2433	1.641/1.605	bcc	–	−410.0
Ce	58	1479	6278	93	3,4	1.02/0.92	fcc/bcc	1346	1.825/1.84	hcp/bcc	–	−435.0
Pr	59	1686	5468	79	3,4	1.00/0.90	hcp/bcc	1458	1.828/1.84	hcp/bcc	–	−435.8
La	57	1688	6278	90	3	1.05	hcp/fcc/bcc	590/1587	1.88/1.90	bcc/hcp	∼890	−428.57
Nd	60	1866	5746	70	3	1.00	hcp/bcc	1584	1.82/1.84	bcc/hcp	∼1075	−432.15
Sm	62	1962	2966	46	2,3	1.11/0.97	rhom/bcc	1683	1.80/1.81	bcc/mono	∼2015	−433.89
Eu	63	1519	2712	41	2,3	1.09/0.96	bcc	–	2.042	bcc/mono	∼2015	–
Yb	70	1515	2786	39	2,3	0.93/0.86	fcc/bcc	1468	1.94/1.98	bcc	–	−433.68
Tb	65	2472	4586	70	3,4	0.92/0.84	hcp/	2403	1.782/	bcc	–	−436.8
Th	90	3182	7592	130	4	–	fcc/bcc	2552	1.80/1.82	–	–	−293.2

[a] Above room temperature

[b] Calculated from Lattice Constants Assuming CN = 12

TABLE III

NOMINAL ADDITIONS TO ALLOY VI-A

(a) FIRST SERIES OF ALLOYS

Alloy No.	Heat No.	Alloy Addition (wt. %)
1	S488	Base
2	S491	0.2 Mn
3	S492	0.4 Mn
4	S493	0.8 Mn
5	S494	0.25 Re
6	S495	0.5 Re
7	S496	0.065 Ce
8	S497	0.2 Ce
9	S498	0.3 Ce
10	S499	0.04 Y
11	S500	0.14 Y
12	S501	0.21 Y
13	S502	0.23 Gd
14	S503	0.31 Th
15	S959	0.065 La
16	S960	0.2 La
17	S961	0.3 La

TABLE III - CONT'D

(b) SECOND SERIES OF ALLOYS

Alloy	Heat No.	Dopant Addition (w/o)	Comments
18	S409	0.5 La, 1 Mn	225°F S.H.
19	S433	0.5 La, 1 Mn	125°F S.H.
20	S451	0.5 La, 1 Mn	50°F S.H.
21	205	0.5 La	Standard Mold
22	206	0.5 La	Shot-backed Mold
23	218	0.4 La	" "
24	219	0.6 La	" "
25	220	0.6 La + 1 Mn	" "
26	221	0.2 La + 0.2 Y	" "
27	222	0.3 La + 0.15 Y	" "

* All contain 0.25 Re

TABLE IV

VENDOR ANALYSES OF MASTER ALLOY HEATS

Heat No.	C	Cr	Al	Ti	Co	Mo	W	Ta	Cb	Zr	Hf	B	Re	Fe	S	Si	Mn
F-4063	.14	6.26	5.53	1.02	7.51	2.01	5.86	9.25	.46	.12	.43	.022	<.10	<.10	.006	<.05	<.02
F-4064	.13	6.16	5.58	.95	7.46	1.99	5.79	8.66	.45	.13	.41	.016	<.05	.10	.005	<.10	<.05
F-4065	.13	6.17	5.53	.96	7.48	2.01	5.99	9.22	.45	.15	.44	.016	.07	.10	.005	<.10	<.05
F-4066	.14	6.30	5.53	.96	7.47	2.02	5.83	8.77	.43	.14	.43	.016	<.05	<.10	.005	<.10	<.05
F-4067	.13	6.15	5.58	.97	7.50	2.02	5.98	9.04	.47	.13	.43	.019	<.05	<.10	.005	<.10	<.05

TABLE V

COMPOSITIONS OF MASTER ALLOYS

Additive	Wt.% in Ni
Mn	50.0
La	32.1
Ce	32.3
Y	23.0
Gd	34.8
Th	44.2
Re	50.0

TABLE VI

INVESTMENT CASTING PROCEDURES

Alloy No.	Heat No.	Dopant Additions (w/o)	Mold Temp. (°F)	Superheat (°F)	Remarks
1-17	S488-503 S959-961	Various Dopants	1800	325	Standard Procedure
1	S962	Base (Coarse Grain)	1800	375	
18	S409	0.5 La + .25 Re + 1.0 Mn	2000	225	
19	S433	0.5 La + .25 Re + 1.0 Mn	2000	125	(Shrink)
20	S451	0.5 La + .25 Re + 1.0 Mn	2000	50	(Shrink)
21	205	0.5 La + .25 Re	1800	325	Standard
22	206	0.5 La + .25 Re	1500*	350	Small Grain Size
23	218	0.4 La + .25 Re	1500*	400	
24	219	0.6 La + 0.25 Re	1500*	375	
25	220	0.6 La + .25 Re + 1.0 Mn	1500*	400	
26	221	0.2 La + .25 Re + 0.2 Y	1500*	400	
27	222	0.3 La + .25 Re + .15 Y	1500*	400	

* Mold imbedded in Ni shot during casting

TABLE VII

CHILL CAST ALLOYS

Casting No.	Base Alloy	Dopant Additions (w/o)
1A	1	Base
2A	2	0.2 Mn
3A	3	0.4 Mn
4A	4	0.8 Mn
5A	5	0.25 Re
6A	6	0.50 Re
7A	7	0.065 Ce
8A	8	0.2 Ce
9A	9	0.3 Ce
10A	10	0.04 Y
11A	11	0.14 Y
12A	12	0.21 Y
13A	13	0.23 Gd
14A	14	0.31 Th
15A	15	0.035 La
16A	16	0.12 La
17A	17	0.27 La
13B	13	0.23 Gd + 0.4 Mn
13C	13	0.23 Gd + 0.8 Mn
5B	5	0.25 Re + 0.4 Mn
5C	5	0.25 Re + 0.8 Mn
10B	10	0.04 Y + 0.4 Mn

(Continued)

TABLE VII – CONT'D

Casting No.	Base Alloy	Dopant Additions (w/o)
10C	10	0.04 Y + 0.8 Mn
11B	11	0.14 Y + 0.4 Mn
11C	11	0.14 Y + 0.8 Mn
12B	12	0.21 Y + 0.4 Mn
12C	12	0.21 Y + 0.8 Mn
14B	14	0.31 Th + 0.4 Mn
5D	5	0.25 Re + 0.5 La
5E	5	0.25 Re + 0.75 La
5F	5	0.25 Re + 1.0 La
5G	5	0.25 Re + 0.5 La + 0.5 Mn
5H	5	0.25 Re + 0.75 La + 0.5 Mn
5I	5	0.25 Re + 0.75 La + 1.0 Mn
5J	5	0.25 Re + 0.5 Y
5K	5	0.25 Re + 0.75 Y
5L	5	0.25 Re + 1.0 Y
5M	5	0.25 Re + 0.5 Y + 0.5 Mn
5N	5	0.25 Re + 0.75 Y + 0.5 Mn
5O	5	0.25 Re + 0.75 Y + 1.0 Mn
5P	5	0.25 Re + 0.5 Ce
5Q	5	0.25 Re + 0.75 Ce
5R	5	0.25 Re + 1.0 Ce
5S	5	0.25 Re + 0.5 Ce + 0.5 Mn
5T	5	0.25 Re + 0.75 Ce + 0.5 Mn
5U	5	0.25 Re + 0.75 Ce + 1.0 Mn
21A	21	0.25 Re + 0.5 La
24A	24	0.25 Re + 0.6 La
25A	25	0.25 Re + 0.6 La + 1.0 Mn
26A	26	0.25 Re + 0.2 La + 0.2 Y

TABLE VIII

CHEMICAL ANALYSES OF CAST ALLOYS

Element	(Alloy 1) Aim	(Alloy 1) Anal.	(Alloy 8) Aim	(Alloy 8) Anal.
C	0.13	0.16		0.15
Cr	6.2	6.05		6.11
Mo	2.0	2.05		2.16
Ti	1.0	0.99		1.03
Co	7.5	7.43		7.51
W	6.0	5.76		5.75
Ta	9.0	7.95		8.18
Al	5.5	5.45		5.48
Cb	0.5	0.50	Same As S488	0.55
Hf	0.45	0.44		0.48
Si	< 0.10	0.043		0.035
B	0.02	0.023		0.027
Mn	< 0.05	< 0.01		< 0.01
Zn	0.15	0.082		0.10
Ce	< 0.05	< 0.05	0.20	0.23

TABLE IX

CHEMICAL ANALYSES FOR DOPANTS IN INVESTMENT CAST ALLOYS

Alloy No.	Heat No.	Alloy Composition**		
		Aim (w/o)	Anal. (w/o)	Anal. (a/o)
1	S488	Base		
1	S962	Base		
2	S491	0.2 Mn	0.2 Mn	
3	S492	0.4 Mn	0.37 Mn	
4	S493	0.8 Mn	0.78 Mn	
5	S494	0.25 Re	0.27 Re	
6	S495	0.5 Re	0.48 Re	
7	S496	0.065 Ce	0.08 Ce	0.04 Ce
8	S497	0.2 Ce	0.23 Ce	0.11 Ce
9	S498	0.3 Ce	0.32 Ce	0.16 Ce
10	S499	0.04 Y	0.06 Y	0.04 Y
11	S500	0.14 Y	0.12 Y	0.09 Y
12	S501	0.21 Y	0.21 Y	0.15 Y
13	S502	0.23 Gd	0.23 Gd	0.10 Gd
14	S503	0.31 Th	0.34 Th	0.11 Th
15	S959	0.065 La	0.034 La	0.15 La
16	S960	0.2 La	0.12 La	0.06 La
17	S961	0.3 La	0.27 La	0.14 La
18	S409	0.5 La, *1 Mn	0.61 La, 0.72 Mn	0.30 La
19	S433	0.5 La, *1 Mn	0.71 La, 0.98 Mn	0.35 La
20	S451	0.5 La, *1 Mn	0.55 La, 0.76 Mn	0.27 La
21	205	0.5 La*	0.52 La	0.26 La
22	206	0.5 La*	0.53 La	0.26 La
23	218	0.4 La*	0.46 La	0.23 La
24	219	0.6 La*	0.75 La	0.37 La
25	220	0.6 La + 1.0 Mn*	0.59 La + 0.74 Mn	0.30 La
26	221	0.2 La + 0.2 Y*	0.20 La + 0.11 Y	0.10 La + 0.08 Y
27	222	0.3 La + 0.15 Y*	0.25 La + 0.10 Y	0.12 La + 0.07 Y

** Quantitative Spectrographic Analyses at G.E., M&PTL

* All contain 0.25 w/o Re

TABLE X

RESULTS OF INCIPIENT MELTING STUDY (1 HR. AT TEMP.)

Alloy No.	Nominal Comp.	H.T. Temp. °F			
		2000	2100	2200	2300
1		No	No	No	VS
2	+0.2Mn	No	No	No	GB
3	+0.4Mn	No	No	VS	GB
4	+0.8Mn	No	No	VS	GB
5	+0.25Re	No	No	No	No
6	+0.50Re	No	No	No	VS
7	+0.065Ce	No	No	VS	MM
8	+0.20Ce	No	No	VS/GB	MM
9	+0.30Ce	No	No	GB	MM
10	+0.04Y	No	No	VS	GB
11	+0.14Y	No	No	No	GB
12	+0.21Y	No	No	VS	GB
13	+0.23Gd	No	No	VS	GB
14	+0.31Th	No	No	No	GB
15	0.065La	No	No	No	GB
16	0.2La	No	No	No	GB
17	0.3La	No	No	No	GB
18	0.5La + 0.25Re + 1Mn	No	No	GB	MM
19	0.5La + 0.25Re + 1Mn	No	No	GB	MM
20	0.5La + 0.25Re + 1Mn	No	No	GB	MM
21	0.5La + 0.25Re	No	No	VS	GB
22	0.5La + 0.25Re	No	No	VS	GB
23	0.4La + 0.25Re	No	No	VS	GB
24	0.6La + 0.25Re	No	No	GB	MM
25	0.6La + 0.25Re + 1Mn	No	No	No	GB
26	0.2La + 0.2Y + 0.25Re	No	No	No	GB
27	0.3La + 0.15Y + 0.25Re	No	No	No	GB

No - No Melting Observed
VS - Very Slight Melting Observed
GB - Grain Boundary Film Formed
MM - Massive Melting Observed

TABLE XI

1600°F TENSILE DATA

Alloy No.	Alloy	UTS (ksi)	0.2YS (ksi)	Elong. (%)	R of A (%)
1	Base	146.0	116.0	1.4	4.0
		126.0	124.0	0.4	4.0
		129.5	–	1.1	1.9
1	Base	116.5	94.0	1.6	3.1
		114.5	100.7	1.5	1.5
2	+0.2 w/o Mn	125.0	114.5	0.7	4.8
		125.0	115.0	1.4	5.6
3	+0.4 w/o Mn	131.0	120.0	2.4	4.8
		126.0	116.0	1.5	4.8
4	+0.8 w/o Mn	123.0	111.0	1.7	2.3
		121.0	113.0	1.1	2.4
5	+0.25 w/o Re	126.0	117.0	1.4	2.3
		126.0	118.0	1.1	3.2
6	+0.5 w/o Re	131.0	122.0	2.0	2.3
		129.0	115.0	1.8	4.8
7	+0.065 w/o Ce	97.0	N.A.	0.5	0.8
		127.0	115.0	1.2	1.6
8	+0.2 w/o Ce	106.0	N.A.	1.2	0.8
		115.0	111.0	0.1	0.0
9	+0.3 w/o Ce	127.0	115.5	0.8	2.3
		80.0	N.A.	0.4	0.0
10	+0.04 w/o Y	106.0	N.A.	0.6	0.8
		130.0	115.0	2.1	3.2
		119.0	104.0	0.9	0.6
11	+0.14 w/o Y	110.5	N.A.	0.9	0.6
		108.0	N.A.	1.1	0.8
		113.5	105.0	1.4	2.9

(Continued)

TABLE XI - CONTINUED

Alloy No.	Alloy	UTS (ksi)	0.2YS (ksi)	Elong. (%)	R of A (%)
12	+0.21 w/o Y	109.0	N.A.	0.5	0.8
		107.0	N.A.	1.1	0.8
		105.0	101.5	1.1	0.9
13	+0.23 w/o Gd	123.0	115.0	0.8	0.0
		120	112.0	1.7	2.4
		129.0	115.0	2.0	1.9
14	+0.31 w/o Th	126.0	116.0	0.8	0.8
		119.0	110.0	0.9	2.4
		120.0	113.5	1.2	0.9
15	+0.065 w/o La	113.0	99.0	2.2	3.1
		118.5	102.5	1.7	3.1
16	+0.2 w/o La	91.0	N.A.	1.3	1.7
		96.0	N.A.	1.2	1.5
17	+0.3 w/o La	98.5	96.0	1.0	1.7
		97.0	94.5	0.9	0.8
18	0.5 La + 1 Mn	88.5	–	0.7	0.0
		83.4	–	0.5	0.0
19	0.5 La + 1 Mn	82.6	–	0.3	0.0
		82.0	–	0.5	0.0
20	0.5 La + 1 Mn	57.3	–	0.5	0.0
		61.3	–	0.2	0.0
21	0.5 La	102.2	–	0.4	1.7
22	0.5 La	83.6	–	0.7	0.6
23	0.4 La	101.5	–	0.7	1.5
		83.8	–	1.2	1.5
24	0.6 La	94.4	–	0.8	0.8
		94.2	–	0.1	0.6
25	0.6 La + 1 Mn	78.9	–	1.1	1.5
		96.8	–	0.3	1.5
26	0.2 La + 0.2 Y	120.5	116.6	0.5	1.5
		107.2	–	0.8	1.5
27	0.3 La + 0.15 Y	107.1	105.2	1.5	1.5
		110.9	–	0.9	3.2

TABLE XII

STRESS RUPTURE DATA
1800°F/27.5 ksi

Alloy No.	Alloy Comp.	Life (hrs.)	Elong. (%)	R of A (%)
1	Base (Fine-Grained)	73.3	4.1	4.8
		63.9	3.6	6.4
		30.2	2.3	2.4
1	Base (Coarse-Grained)	47.1	3.0	1.6
		52.2	3.0	3.2
2	+0.2 w/o Mn	47.1	4.7	5.6
		81.48	4.8	6.4
3	+0.4 w/o Mn	57.9	5.3	2.8
		48.64	5.1	5.5
4	+0.8 w/o Mn	48.4	2.9	3.3
		33.1	3.1	2.4
5	+0.25 w/o Re	61.5	5.2	4.9
		113.4	6.2	8.2
6	+0.5 w/o Re	56.8	3.2	3.2
		92.9	8.5	4.0
7	+0.065 w/o Ce	16.5	1.4	0.9
		10.73	1.1	0.0
8	+0.2 w/o Ce	5.0	0.9	0.8
		4.33	1.1	0.8
9	+0.305 w/o Ce	3.3	0.5	0.8
		5.8	1.4	0.0
10	+0.04 w/o Y	16.0	1.9	1.6
		12.5	2.2	8.2
		7.0	2.5	2.3
11	+0.14 w/o Y	26.7	3.2	2.6
		9.42	1.6	2.8
		31.5	2.3	1.0

TABLE XII – CONTINUED

Alloy No.	Alloy Comp.	Life (hrs.)	Elong. (%)	R of A (%)
12	+0.21 w/o Y	13.2	1.8	0.8
		6.16	1.0	1.6
		9.4	0.9	0.0
13	+0.23 w/o Gd	20.8	1.0	0.8
		6.31	0.8	0.0
		20.8	1.9	0.0
14	+0.31 w/o Th	15.53	2.0	1.6
		12.37	1.5	1.6
		21.4	0.9	0.0
15	+0.065 La	7.3	1.2	2.4
		13.1	0.0	0.0
16	+0.2 La	3.5	0.0	0.0
		0.7	0.8	0.8
17	+0.3 La	2.1	0.6	1.6
		3.0	1.1	1.6
18	+0.5 La + 1 Mn	0.1	1.0	0.8
		0.1	0.9	0.8
19	+0.5 La + 1 Mn	0.1	0.9	0.0
		0.3	0.8	0.8
20	+0.5 + 1 Mn	0.7	0.7	1.4
		0.1	1.0	0.0
21	0.5 La	2.1	1.1	0.8
		4.0	0.7	0.0
		3.3	0.9	1.6 (25 ksi)
22	0.5 La	4.3	1.2	0.0
		1.7	1.5	0.0
		5.7	1.8	0.8 (25 ksi)
23	0.4 La	11.2	1.2	0.0
		12.5	1.0	0.0
24	0.6 La	10.7	0.9	0.8
		7.0	1.3	0.0
25	0.6 La + 1 Mn	4.7	1.0	0.0
		5.3	1.3	0.0
26	0.2 La + 0.2 Y	10.3	1.1	0.0
		18.9	0.6	0.0
27	0.3 La + 0.15 Y	18.7	1.5	0.8
		18.7	1.9	0.0

TABLE XIII

GROSS WEIGHT GAIN OCCURRING
DURING OXIDATION AT 1800°F, CYCLIC

Alloy No.		Total Wt. (mg/cm^2) (100 hr. cycles)									
		1	2	3	4	5	6	7	8	9	10
1	F.G.	0.66	1.11	0.97	1.60	1.84	1.78	2.09	2.11	2.17	2.13
1	C.G.	0.77	1.38	1.15	2.01	2.30	2.46	2.60	2.55	2.73	2.70
2	0.2 Mn	0.56	1.29	0.86	2.80	3.06	2.98	-	-	-	-
3	0.4 Mn	0.64	1.29	1.07	1.95	2.17	2.10	2.40	2.47	2.65	2.62
4	0.8 Mn	0.78	1.22	1.01	2.42	2.57	2.42	2.53	2.60	2.79	2.70
5	0.25 Re	0.73	1.26	1.05	1.83	2.0	1.89	2.12	2.03	2.12	2.14
6	0.50 Re	0.54	1.04	1.01	2.50	2.61	2.43	2.63	2.56	2.75	2.65
7	0.065 Ce	0.73	1.21	1.09	2.48	2.71	2.63	2.73	2.78	2.90	2.80
8	0.2 Ce	1.04	1.60	1.43	2.85	3.05	2.97	3.17	3.17	3.25	3.25
9	0.3 Ce	1.17	1.85	1.75	2.85	3.22	3.25	3.48	3.60	3.80	3.85
10	0.04 Y	0.69	1.32	1.13	2.82	3.05	3.0	3.05	3.08	3.21	3.29
11	0.14 Y	0.90	1.45	1.28	2.30	2.63	2.67	2.75	2.88	2.97	3.15
12	0.2 Y	0.36	0.66	0.64	1.56	1.54	1.54	1.60	1.60	2.0	1.90
13	Gd	0.91	1.73	1.52	2.55	2.83	2.77	2.87	3.00	3.24	3.32

(Continued)

33

TABLE XIII - CONTINUED

Alloy No.		1	2	3	4	5	6	7	8	9	10
				Total Wt. Change (mg/cm^2)			(100 hr. cycles)				
14	Th	0.70	1.32	1.17	2.22	2.40	2.44	2.55	2.60	2.85	2.93
15	0.05 La	-	-	2.0	2.34	2.71	2.41	2.85	2.60	2.20	2.94
16	0.2 La	-	-	2.51	2.83	3.32	2.79	3.37	3.19	2.71	4.06
17	0.3 La	-	-	1.98	2.40	2.40	2.30	2.61	2.32	1.91	2.47
18	225 0.5 La	-	-	2.88	3.44	3.88	3.55	4.21	3.95	3.60	4.32
19	125 0.5 La	-	-	3.47	4.05	4.51	4.20	4.85	4.60	4.24	5.35
20	50 0.5 La	-	-	5.5	6.4	7.0	6.8	7.5	7.3	7.2	7.98
21	0.5 La STD	-	-	3.39	3.70	4.33	3.93	4.69	4.34	3.90	5.00
22	0.5 La (SBM)	-	-	2.73	3.17	3.73	3.24	3.69	3.45	3.20	3.86
23	0.4 La	-	-	2.61	3.27	3.50	3.15	3.64	3.32	2.98	3.66
24	0.6 La	-	-	2.95	3.47	3.94	3.57	4.06	3.76	3.45	3.81
25	0.5 La + 1 Mn	-	-	3.16	3.95	4.34	3.81	4.56	4.19	4.03	4.82
26	La + Y	-	-	2.70	3.38	3.69	3.30	3.97	3.64	3.43	4.16
27	La + Y	-	-	2.83	3.05	3.67	3.12	3.76	3.49	2.80	4.00

TABLE XIV

NET WEIGHT GAINS OCCURRING
DURING OXIDATION AT 1800°F, CYCLIC

Alloy No.		Net Wt. Gain (mg/cm^2)					(After 100 hr. cycles)				
		1	2	3	4	5	6	7	8	9	10
1	F.G.	0.36	0.58	0.56	0.73	0.58	0.46	0.49	0.56	0.64	0.64
1	C.G.	0.41	0.70	0.68	0.77	0.68	0.61	0.52	0.61	0.64	0.62
2	0.2 Mn	0.28	0.66	0.63	0.74	0.68	0.60	0.52	0.62	0.66	0.68
3	0.4 Mn	0.33	0.67	0.67	0.74	0.60	0.46	0.48	0.53	0.52	0.60
4	0.8 Mn	0.48	0.59	0.52	0.63	0.55	0.48	0.55	0.70	0.81	0.75
5	0.25 Re	0.36	0.63	0.59	0.69	0.59	0.48	0.50	0.63	0.60	0.68
6	0.5 Re	0.34	0.56	0.59	0.70	0.58	0.45	0.45	0.52	0.50	0.40
7	0.065 Ce	0.34	0.57	0.60	0.84	0.74	0.64	0.77	0.95	0.97	0.98
8	0.2 Ce	0.70	1.09	1.1	1.35	1.32	1.26	1.34	1.57	1.65	1.70
9	0.3 Ce	0.88	1.22	1.26	1.43	1.46	1.47	1.63	1.88	1.95	2.07
10	0.04 Y	0.33	0.73	0.70	0.87	0.83	0.78	0.83	0.98	1.0	1.07
11	0.14 Y	0.65	0.84	0.88	1.07	1.06	1.08	1.12	1.31	1.40	1.49
12	0.21 Y	0.57	1.10	1.10	1.22	1.21	1.21	1.32	1.50	1.67	1.61
13	0.23 Gd	0.57	1.0	1.05	1.27	1.28	1.30	1.41	1.67	1.70	1.93

(Continued)

TABLE XIV - CONTINUED

Alloy No.		Net Wt. Change (mg/cm^2)					(After 100 hr. cycles)				
		1	2	3	4	5	6	7	8	9	10
14	0.31 Th	0.41	0.77	0.81	0.97	0.94	0.93	0.97	1.16	1.21	1.29
15	0.05 La	–	–	0.84	0.78	0.84	0.81	0.98	0.91	0.91	1.04
16	0.2 La	–	–	1.07	1.0	1.19	1.12	1.13	1.11	1.10	1.20
17	0.3 La	–	–	1.11	1.14	1.23	1.24	1.23	1.30	1.38	1.38
18	225F S.H. (0.5 La)	–	–	1.70	1.67	1.9	1.81	1.97	1.94	1.77	2.0
19	125 S.H. (0.5 La)	–	–	2.1	2.15	2.20	2.17	2.15	2.10	2.0	2.16
20	50 S.H. (0.5 La)	–	–	4.0	4.5	5.2	5.3	5.0	5.2	5.2	5.4
21	STD (0.5 La)	–	–	1.80	1.74	1.98	1.93	1.99	1.97	1.80	2.2
22	SBM (0.5 La)	–	–	1.50	1.36	1.52	1.44	1.52	1.46	1.35	1.49
23	SBM (0.5 La)	–	–	1.16	1.20	1.26	1.20	1.21	1.13	1.15	1.21
24	SBM (0.5 La)	–	–	1.50	1.57	1.59	1.56	1.48	1.40	1.45	1.47
25	SBM 0.5La + 1Mn	–	–	1.56	1.61	1.60	1.57	1.51	1.36	1.51	1.54
26	SBM 0.16La+0.13Y	–	–	1.23	1.31	1.27	1.14	1.0	0.87	1.0	0.96
27	SBM 0.16La+0.084Y	–	–	1.18	0.91	1.1	0.90	0.73	0.74	0.30	0.70

TABLE XV

COMPARISON OF ISOTHERMAL AND CYCLIC OXIDATION
AT 1800°F, 1000 HRS.

Alloy No.		Wt. Gain (mg/cm^2)			
		Isothermal		Cyclic	
		Gross	Net	Gross *	Net
1	Base F.G.	1.22	0.71	2.13	0.64
1	Base C.G.	1.09	0.71	2.70	0.62
2	0.2 Mn	0.97	0.52	–	0.68
3	0.4 Mn	1.00	0.60	2.62	0.60
4	0.8 Mn	1.06	0.69	2.70	0.75
5	0.25 Re	0.92	0.47	2.14	0.68
6	0.5 Re	1.38	0.56	2.65	0.40
7	0.065 Ce	1.25	0.75	2.80	0.98
8	0.2 Ce	1.66	1.27	3.25	1.70
9	0.3 Ce	2.01	1.62	3.85	2.07
10	0.04 Y	1.23	0.81	3.29	1.07
11	0.14 Y	1.68	1.24	3.15	1.49
12	0.21 Y	1.78	1.30	1.90	1.61
13	0.23 Gd	1.62	1.11	3.32	1.93
14	0.31 Th	1.69	1.10	2.93	1.29

* Includes spalled oxide wt.

TABLE XVI

WEIGHT CHANGES OCCURRING DURING OXIDATION AT 2000°F, CYCLIC

Alloy No.			100 Hrs.		200 Hrs.		300 Hrs.		400 Hrs.	
			Gross	Net	Gross	Net	Gross	Net	Gross	Net
1	Base	(Fine Grained)	1.80	-1.37	2.18	-2.22	1.49	-3.60	2.23	- 4.95
1	Base	(Coarse Grained)	1.87	-1.29	2.19	-2.27	1.53	-3.50	2.82	- 5.75
2	0.2 Mn		2.05	-1.74	2.46	-2.70	1.87	-4.21	2.99	- 6.87
3	0.4 Mn		1.99	-2.01	2.59	-3.10	1.99	-5.38	4.43	-10.18
4	0.8 Mn		1.82	-2.20	2.31	-3.30	1.91	-5.44	2.38	-11.21
5	0.25 Re		1.98	-2.07	2.46	-3.20	2.07	-6.05	3.10	-15.41
6	0.5 Re		2.03	-1.62	2.32	-2.52	1.68	-4.08	3.24	- 7.03
7	0.065 Ce		1.58	0.10	1.85	0.04	1.38	-0.08	1.73	0.24
8	0.2 Ce		2.07	0.17	2.39	-0.07	2.12	-0.03	2.95	- 0.02
9	0.3 Ce		2.18	0.44	2.56	-0.06	2.42	-0.17	3.56	- 0.34
10	0.04 Y		1.78	0.19	2.25	0.23	1.53	-0.16	2.46	0.14
11	0.14 Y		2.00	0.27	2.56	0.52	2.17	0.71	2.38	1.46
12	0.21 Y		2.16	0.29	2.65	0.52	2.29	0.66	2.69	1.18
13	0.23 Gd		2.02	0.15	2.55	0.31	2.23	0.57	2.69	1.19

(Continued)

TABLE XVI - CONTINUED

Alloy No.		Weight Change (mg/cm^2)							
		100 Hrs.		200 Hrs.		300 Hrs.		400 Hrs.	
		Gross	Net	Gross	Net	Gross	Net	Gross	Net
14	0.3 Th	2.27	-0.37	2.49	-0.72	3.39	-0.68	2.54	- 0.42
15	0.05 La	2.13	-0.27	3.95	-0.88	4.74	-1.06	5.50	- 1.16
16	0.2 La	2.78	-0.47	5.41	-1.14	7.03	-1.20	9.68	- 1.27
17	0.3 La	3.53	0.04	6.88	-1.37	9.16	-1.56	11.57	- 1.51
18	225F (Variable)	6.74	-83.9	11.06	-250.7	28.3	-378.5	45.04	-500.9
		4.87	-6.6	5.91	-10.9	6.96	-11.4	8.122	-10.9
19	125F (1 Spec)	6.63	-68.1	20.96	-209.7	30.43	-383.6	72.2	-432.0
20	50F (Variable)	9.77	-23.4	18.48	-49.8	23.65	-88.9	43.83	-160.9
		21.67	-64.0	68.71	-243.5	117.77	-365.5	178.37	-362.8
21	0.5 La STD	3.54	0.21	6.17	-1.54	7.38	-1.87	8.59	- 1.90
22	0.5 La SBM (Vari.)	3.45	-0.19	3.98	-2.07	4.56	-2.24	4.83	- 2.40
		6.59	-1.72	11.86	-2.60	13.51	-2.76	15.48	- 2.78
23	0.6 La (Variable)	2.21	0.45	3.25	-0.98	3.59	-1.39	3.98	- 1.38
		7.93	-0.70	17.72	-1.93	22.79	-2.05	26.09	- 2.15
24	0.4 La	3.79	-0.25	6.12	-3.29	7.68	-3.62	9.52	- 3.66
25	0.6 La + 1 Mn	13.53	-5.86	25.06	-9.11	31.58	-9.66	34.42	- 9.70
26	0.2 La + 0.2 Y	2.61	-0.43	4.65	-1.31	6.34	-1.52	7.70	- 1.38
27	0.3 La + 0.15 Y	2.23	-0.85	4.19	-1.47	5.08	-1.56	6.17	- 1.51

TABLE XVII

COMPARISON OF ISOTHERMAL AND CYCLIC OXIDATION
AT 2000°F, 400 HRS.

			Wt. Change (mg/cm^2)			
			Isothermal		Cyclic	
Alloy No.			Gross	Net	Gross	Net
1	Base	(Fine Grained)	1.44	-2.13	2.23	- 4.95
1	Base	(Coarse Grained)	1.68	-2.31	2.82	- 5.75
2	0.2 Mn		1.42	-2.64	2.99	- 6.87
3	0.4 Mn		1.53	-2.53	4.43	-10.18
4	0.8 Mn		0.18	-2.09	2.38	-11.21
5	0.25 Re		2.06	-2.73	3.10	-15.41
6	0.50 Re		1.89	-2.06	3.24	- 7.03
7	0.065 Ce		2.02	0.51	1.73	0.24
8	0.2 Ce		2.31	0.62	2.95	- 0.02
9	0.3 Ce		2.43	0.88	3.56	- 0.34
10	0.04 Y		2.05	0.40	2.46	0.14
11	0.14 Y		2.40	0.91	2.38	1.46
12	0.21 Y		2.81	1.36	2.69	1.18
13	0.23 Gd		2.22	0.92	2.69	1.19
14	0.31 Th		1.89	0.35	2.54	- 0.42

TABLE XVIII

X-RAY DIFFRACTION DATA - SURFACE OXIDE ON ALLOY #1

Radiation: CUK α

Alloy: T.R.W. (Alloy #1)
Condition: 2000°F, 400 hrs.
Pattern Quality: __
Pattern No.:   9039 (Oxide Sample)
Date: 7/31/68

d	I	Spinel HKL	$ZrSiO_4$ HKL	$\alpha\ Al_2O_3$ HKL		
4.7	w	111				
3.3	s		200			
2.87	w	220				
2.54	m			104		
2.45	m	311				
2.33	w	222				
2.23	vvw		202			
2.17	vvw					
2.09	vw			113		
2.03	w	400				
1.72	m		312			
1.65	w	422				
1.59	vvw			116		
1.56	w	511, 333				
1.51	vvw			122		
1.475	vw		420			
1.43	vw	440				
1.375	vw	531	332			
1.27	vvw	620				
1.23	vvw	533				
1.19	vvw		512			
1.17	vvw	444				
1.12	vvw			312		
1.06	vvw	553, 731				
0.93	vvw	751				
0.893	vvw	840		410		

s: strong,   m: medium,   w: weak,   v: very

TABLE XIX

X-RAY DIFFRACTION DATA, SPALLED OXIDE ON ALLOY #1

Radiation: CUK α
Conditions: 439K 19MA

Alloy: T.R.W.
Condition: 2000°F, 400 hrs.
Pattern Quality: ___
Pattern No.: 9039 (Spalling)
Date: 7/30/68

d	I	Spinel HKL	$ZrSiO_4$ HKL	$\alpha - Al_2O_3$ HKL		
4.65	w	111				
3.29	m		200			
2.85	w	220				
2.53	m			104		
2.44	m	311				
2.32	w					
2.21	vvw		202			
2.07	vw			113		
2.03	w	400				
1.71	vm		312			
1.64	w	422				
1.56	w	333,511				
1.51	vvw			122		
1.47	w		420			
1.43	w	440				
1.375	w	531				
1.26	vvw	620				
1.186	vvw		512			
1.165	vvw	444				
1.115	vvw			312		
1.057	vw	553,731				
0.892	vvw	840		410		
0.86	vvw					
0.834	vvw					

s: strong, m: medium, w: weak, v: very

TABLE XX

X-RAY DATA - SURFACE OXIDE ON ALLOY #12

Radiation: CUKα

Conditions: 2000 c/sec.

Alloy: T.R.W.

Condition: 2000°F, 400 hrs.

Pattern Quality: __

Pattern No.: 9044 (Sample Oxide)

Date: 7/31/68

d	I	Spinel HKL	ZrSiO$_4$ HKL	α Al$_2$O$_3$ HKL		
4.646	4	111				
3.284	21		200			
2.853	7	220				
2.542	20			104		
2.435	30	311				
2.06	7,100			113		
2.023	12	400				
1.787	25	420				
1.722	11		312			
1.653	5	422				
1.600	4			116		
1.556	8	511,333				
1.475	4		420			
1.431	12	440				
1.266	14	620				
1.119	5			312		
1.067	9	553,731				

s: strong,   m: medium,   w: weak,   v: very

TABLE XXI

X-RAY DATA - SPALLED OXIDE ON ALLOY #12

Radiation: CUK

Alloy: T.R.W.
Condition: 2000°F, 400 hrs.
Pattern Quality:
Pattern No.: 9044 (Spalling Oxide)
Date: 8/5/68

d	I	Spinel HKL	ZrSiO$_4$ HKL	Al$_2$O$_3$ HKL	NiO HKL	
4.7	vw	111				
3.3	m		200			
2.9	w	220				
2.55	w			104		
2.47	m	311				
2.41	w				111	
2.35	vw	222				
2.09	m			113	200	
2.04	w	400				
1.72	m		312			
1.65	vw	422				
1.57	w	511, 332				
1.475	w		420		220	
1.44	w	440				
1.38	vw	531				
1.26	vvw				311	
1.205	vvw				220	
1.195	vvw		512			
1.12	vvw			312		
1.10	vvw					
1.065	vw	731, 553				
1.045	vvw				400	
1.960	vvw				311	
0.935	vvw	751			420	
0.893	vvw			410		
0.853	vvw	931			422	

s: strong,   m: medium,   w: weak,   v: very

44

TABLE XXII

METAL LOSS DATA - 2000F OXIDATION

Alloy	Dopant Content	Surface Loss mils/side	Maximum Penetration mils/side
1	Base	1.1	2.1
2	0.2Mn	0.8	2.0
3	0.4Mn	1.3	2.8
4	0.8Mn	1.2	2.5
5	0.25Re	1.8	2.4
6	0.50Re	2.5	3.8
9	0.30Ce	0.4	2.8
10	0.04Y	0.5	3.3
11	0.14Y	0.6	3.5
12	0.21Y	0.4	2.8
13	0.23Gd	0.5	4.2
14	0.31Th	1.1	3.0
15	0.065La	0.9	2.6
16	0.2La	0.9	2.5
17	0.3La	0.9	3.6
18	0.5La + 0.25Re + 1Mn	1.3 / 34.2 Variable	3.8 / 35.0
19	0.5La + 0.25Re + 1Mn	40.0	41.5
20	0.5La + 0.25Re + 1Mn	20.2	25.5
21	0.5La + 0.25Re	0.9	3.4
22	0.5La + 0.25Re	0.9	2.6
23	0.4La + 0.25Re	0.9	2.2
24	0.6La + 0.25Re	0.8	2.6
25	0.6La + 0.25Re + 1Mn	0.9 / 5.5 Variable	3.3 / 7.5
26	0.2La + 0.2Y + 0.25Re	0.8	2.7
27	0.3La + 0.15Y + 0.25Re	0.8	2.9

TABLE XXIII

HOT CORROSION DATA FOR INITIAL ALLOYS
100 PPM NaCl

Alloy	Composition (w/o)	Metal Loss (mils/side)			
		1550°F/50 hrs.		1725°F/50 hrs.	
		Investment Cast	Drop Cast	Investment Cast	Drop Cast
1	Base (Fine Grain)	2	1 (irregular)	4.0	5.0 (irregular)
1	Base (Coarse Grain)	29	–	8.0	–
2	0.2 Mn	2	–	2.5	–
3	0.4 Mn	1	1	7.0	14.0
4	0.8 Mn	2	1	8.0	25.0
5	0.25 Re	1	1	2.5	28.0 (irregular)
6	0.5 Re	2	1.5	5.0	10.0 (irregular)
7	0.065 Ce	1	1 (irregular)	5.0	–
8	0.2 Ce	30	–	6.0	–
9	0.3 Ce	1	1 (irregular)	10.0	5.0 (irregular)
10	0.04 Y	1	1 (irregular)	6.0	5.5
11	0.14 Y	1	1 (irregular)	4.5	21.0
12	0.21 Y	1	1 (irregular)	0.5	23.0
13	0.23 Gd	1	1 (irregular)	7.0	8.0
14	0.31 Th	28	35	4.0	11.5
15	0.065 La	23	–	6.0	33.5
16	0.2 La	27	–	10.5	18.0
17	0.3 La	28	–	4.0	5.5
Rene' 77		0.5 (wrought)	–	10.0 (wrought)	–

46

TABLE XXIV

HOT CORROSION TEST RESULTS, 1725°F/50 Hrs./100 ppm

Alloy No.	Composition* (nominal) (w/o)	Results
D	0.5 La	O.K., with blisters at base
E	0.75 La	Corrosion at top
F	1.0 La	General Corrosion
G	0.5 La + 0.5 Mn	Corroded bottom half
H	0.75 La + 0.5 Mn	General Corrosion
I	0.75 La + 1.0 Mn	General Corrosion (worse than H)
J	0.5 Y	General Corrosion
K	0.75 Y	General Corrosion (better than I)
L	1.0 Y	General Corrosion
M	0.5 Y + 0.5 Mn	General Corrosion (worse than J)
N	0.75 Y + 0.5 Mn	General Corrosion
O	0.75 Y + 1.0 Mn	General Corrosion (worse than M & N)
P	0.5 Ce	all severely corroded
Q	0.75 Ce	Mn detrimental
R	1.0 Ce	
S	0.5 Ce + 0.5 Mn	
T	0.75 Ce + 0.5 Mn	
U	0.75 Ce + 1.0 Mn	
	U-700 Base (wrought)	severely corroded

* TRW-VI-A alloy containing 0.25 Re

TABLE XXV

METAL LOSS DATA

HOT CORROSION, 1600°F, 1 PPM NaCl, 450 Hrs.

Alloy	Heat	Composition	Metal Loss (mils/side)[*]		Comments
			Max.	Min.	
1	S488	Base	13.7	13.7	Variable
			6.6	6.6	
4	S493	0.8 Mn	1.3	~0.3	Variable
5	S494	0.25 Re	1.5	0.4	Good
			0.6	–	Very Little I.G.A.
6	S495	0.5 Re	4.0	0.4	Blisters, I.G.A.
			2.8	0.6	
11	S500	0.14 Y	2.0	0.4	Good, I.G.A.
			2.2	0.3	
14	S503	0.31 Th	2.1	0.4	Blisters
			2.3	0.4	
17	S961	0.27 La	1.5	0.3	Variable
			1.7	0.4	
21	205	0.25 Re + 0.5 La Standard	21.1	21.1	Variable
			3.0	~0.3	
22	206	0.25 Re + 0.5 La S.B. Mold	16.1	16.1	Variable
			16.6	16.6	

(Continued)

48

TABLE XXV - CONTINUED

Alloy	Heat	Composition	Metal Loss (mils/side)[*]		Comments
			Max.	Min.	
23	218	0.25 Re + 0.4 La S.B. Mold	12.8	12.8	Variable
			15.3	15.3	
24	219	0.25 Re + 0.6 La S.B. Mold	-	-	Completely Corroded
25	220	0.25 Re + 1.0 Mn + 0.6 La S.B. Mold	14.3	14.3	Variable
			2.3	∿0.6	
26	221	0.25 Re + 0.2 La + 0.2 Y S.B. Mold	8.4	8.4	Variable
			1.3	0.4	
27	222	0.25 Re + 0.3 La + 0.15 Y S.B. Mold	6.8	6.8	Variable

Max. = Scale + Intergranular Oxid. (I.G.A.)

Min. = Scale Loss Only (Except in Severely Corroded Spec. Where Internal Sulfidation is Included)
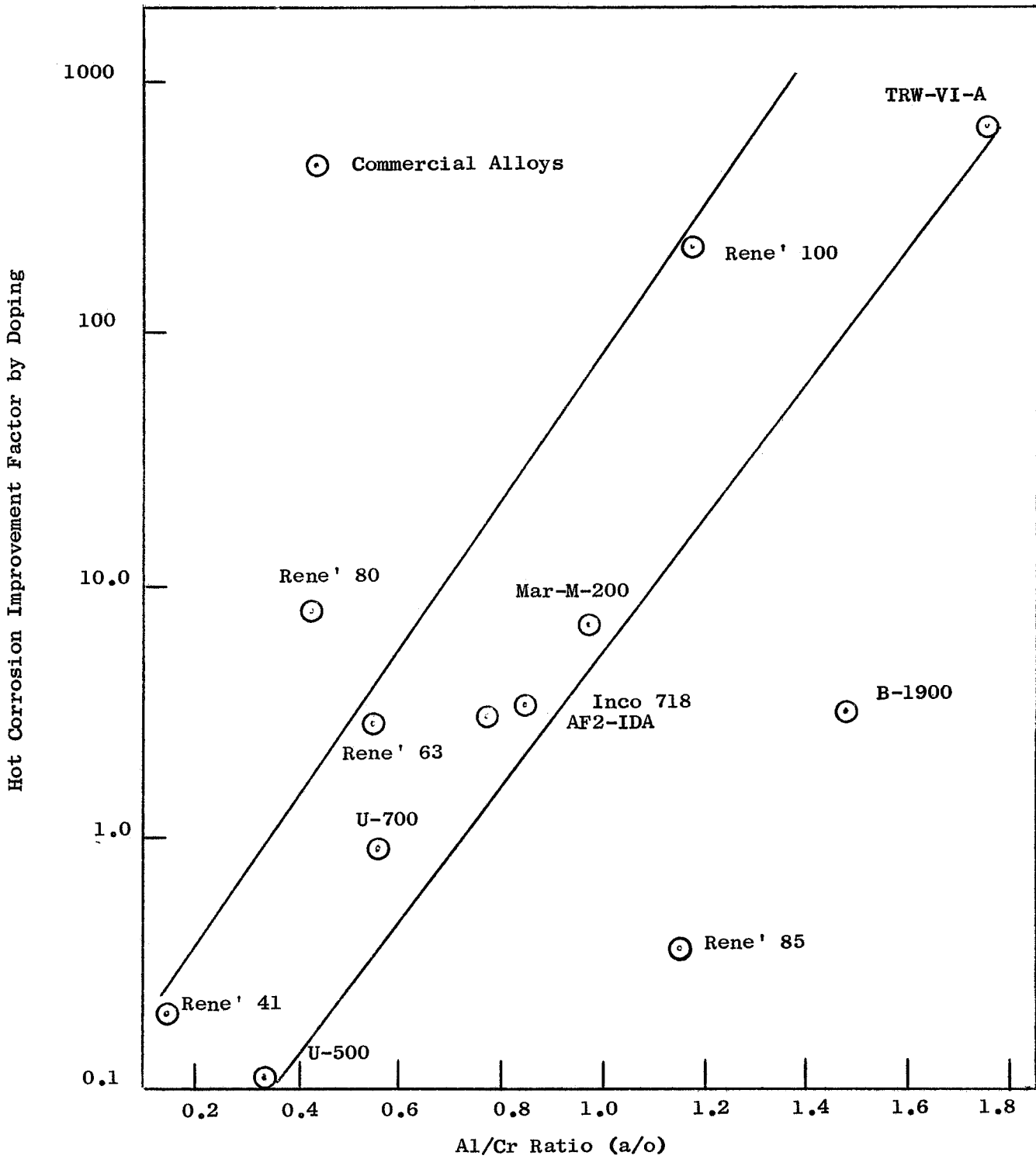
Figure 1: Relation Between Al/Cr Ratio in Alloy and
Benefit Derived from Doping
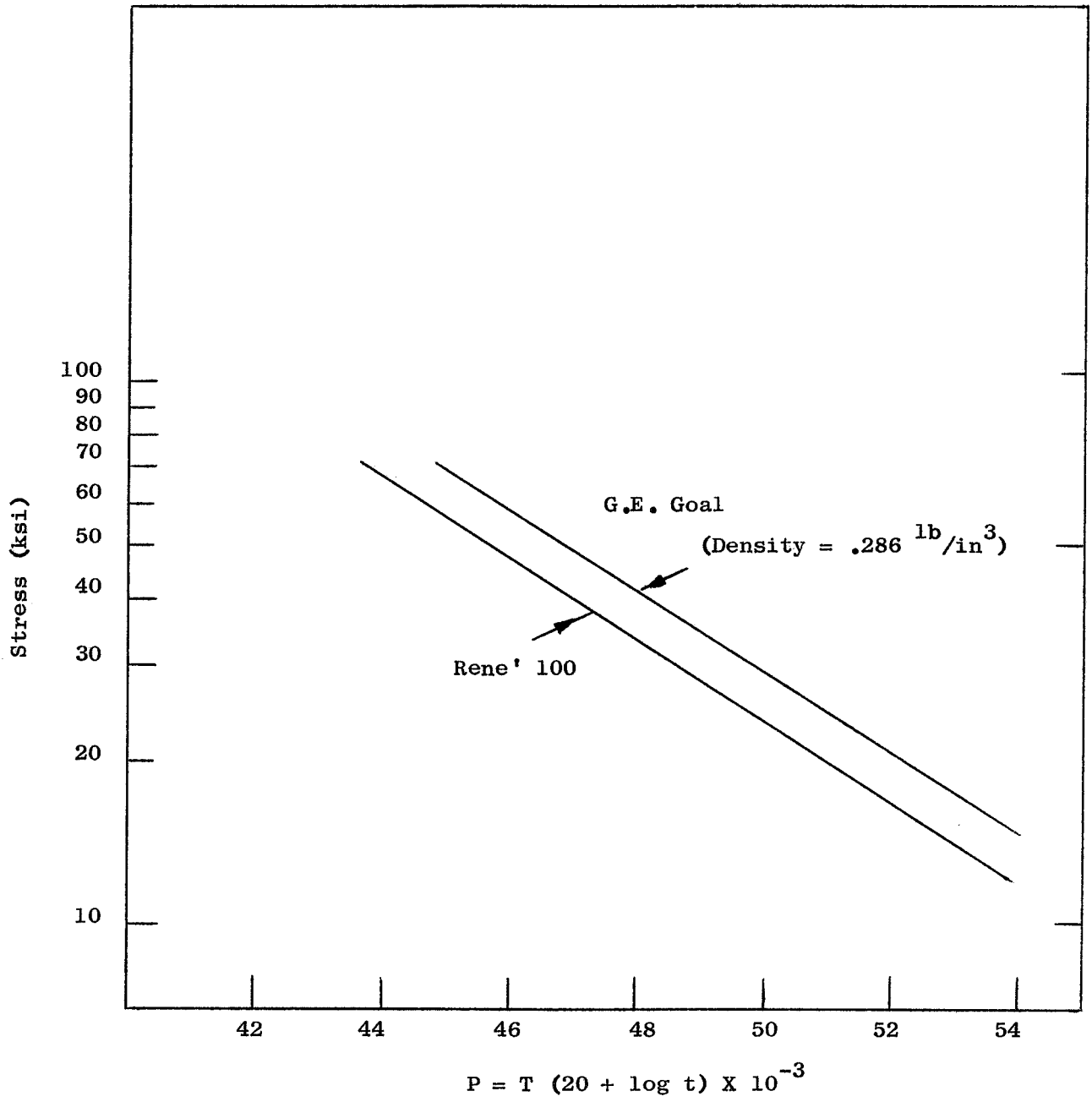
Figure 2:   Stress Rupture Strength of Rene' 100 and Advanced
Alloy Goal

The y-axis is labeled Stress (ksi) with values 100, 90, 80, 70, 60, 50, 40, 30, 20, 10. The x-axis is labeled $P = T \ (20 + \log t) \ X \ 10^{-3}$ with values 42, 44, 46, 48, 50, 52, 54.

G.E. Goal
$(\text{Density} = .286 \ ^{lb}/in^3)$

Rene' 100
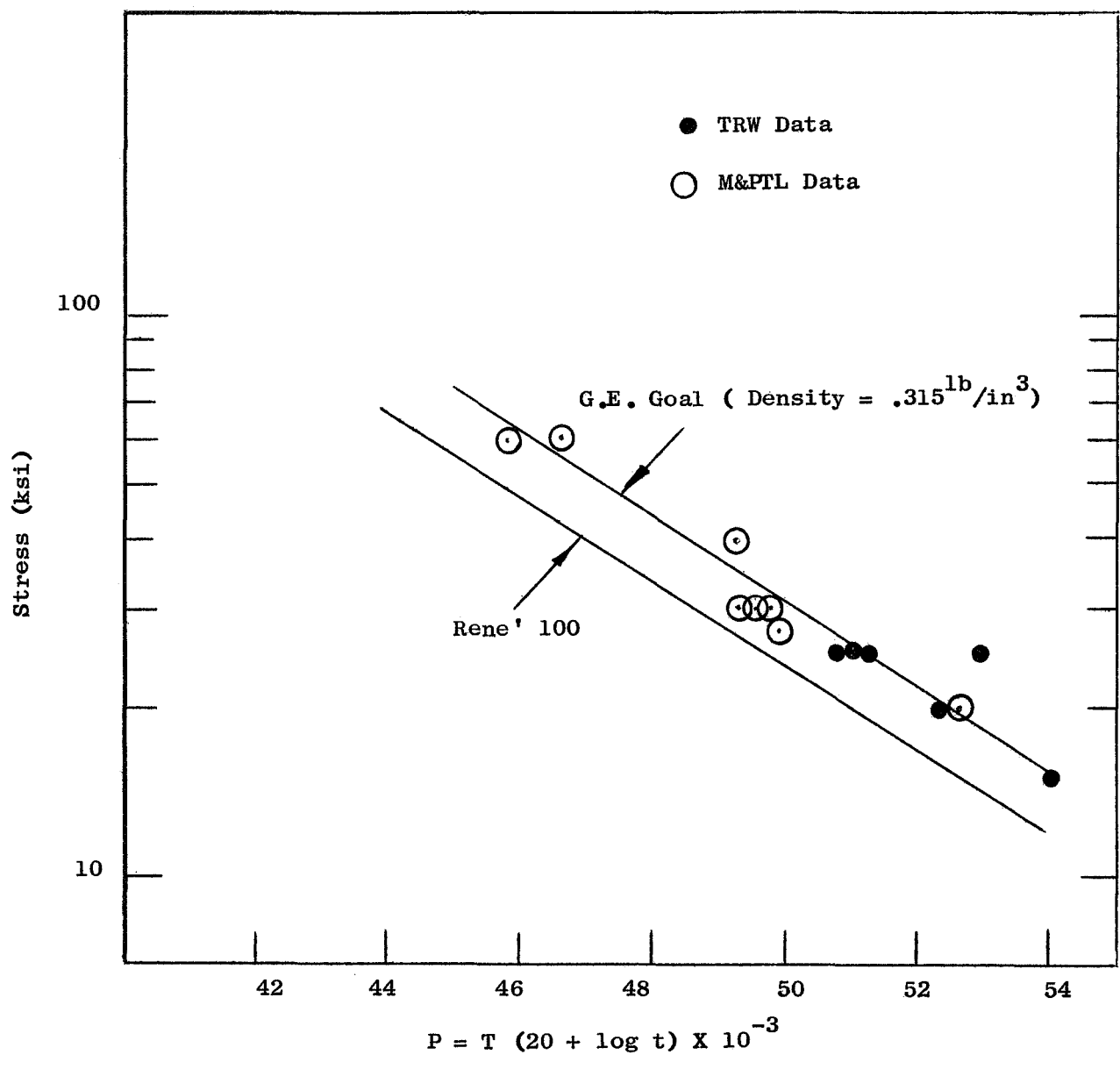
Figure 3: Rupture Strength of VI-A Alloy

250X   Ni 737

VI-A + R.E. + Mn

50X   N2004-05
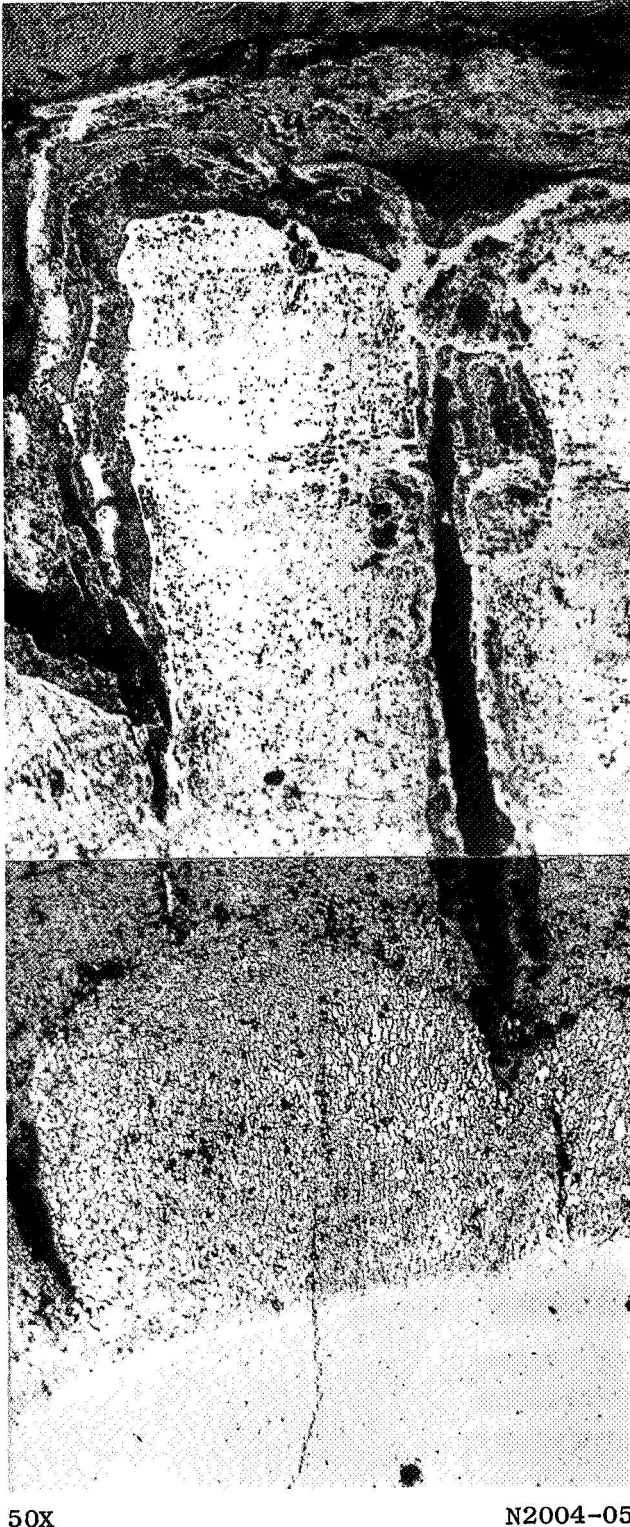
VI-A Base Alloy
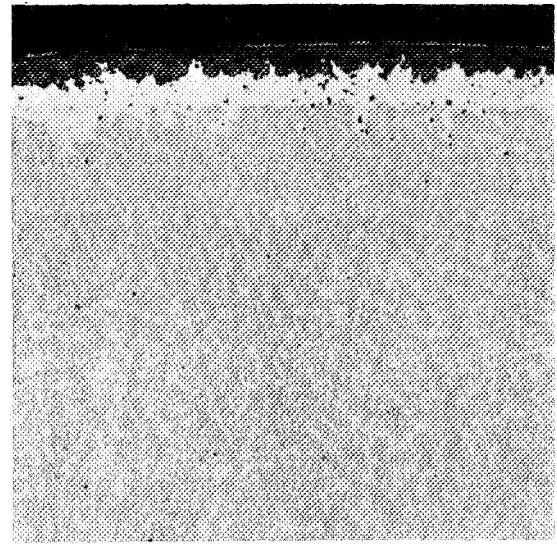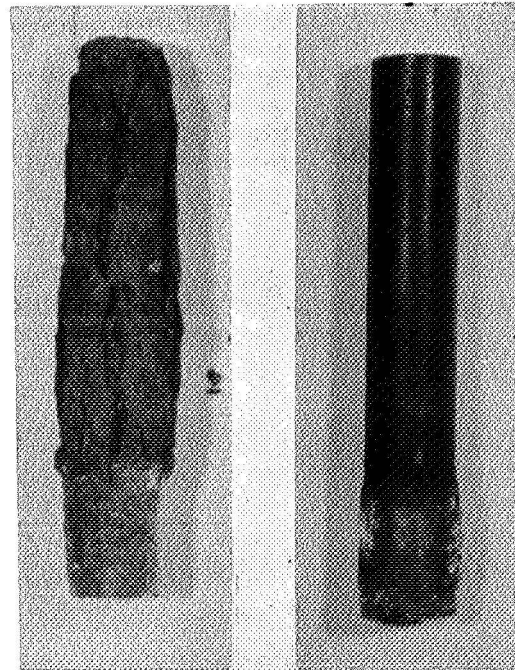
(-133.7 Mils/Dia.)   (-0.5 Mils/Dia.)

Figure 4:   Effect of Reactive Metal Additions on the Hot Corrosion Resistance
of Chill-Cast VI-A after 50 hrs./1700F. (Note: Difference in Magnifications)
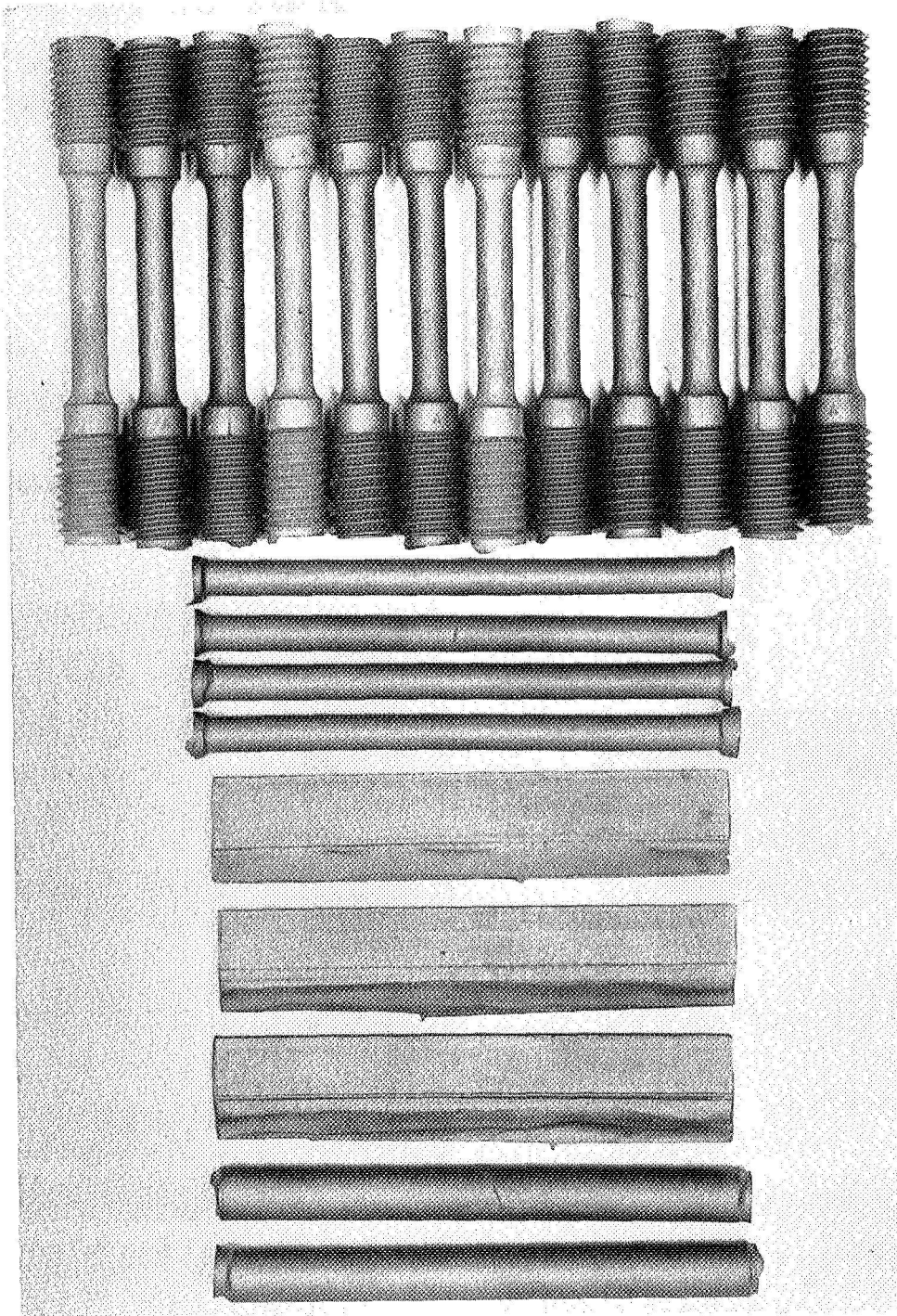
C68052273

Figure 5: Typical Castings, Products of One Mold.
Alloy No. 1
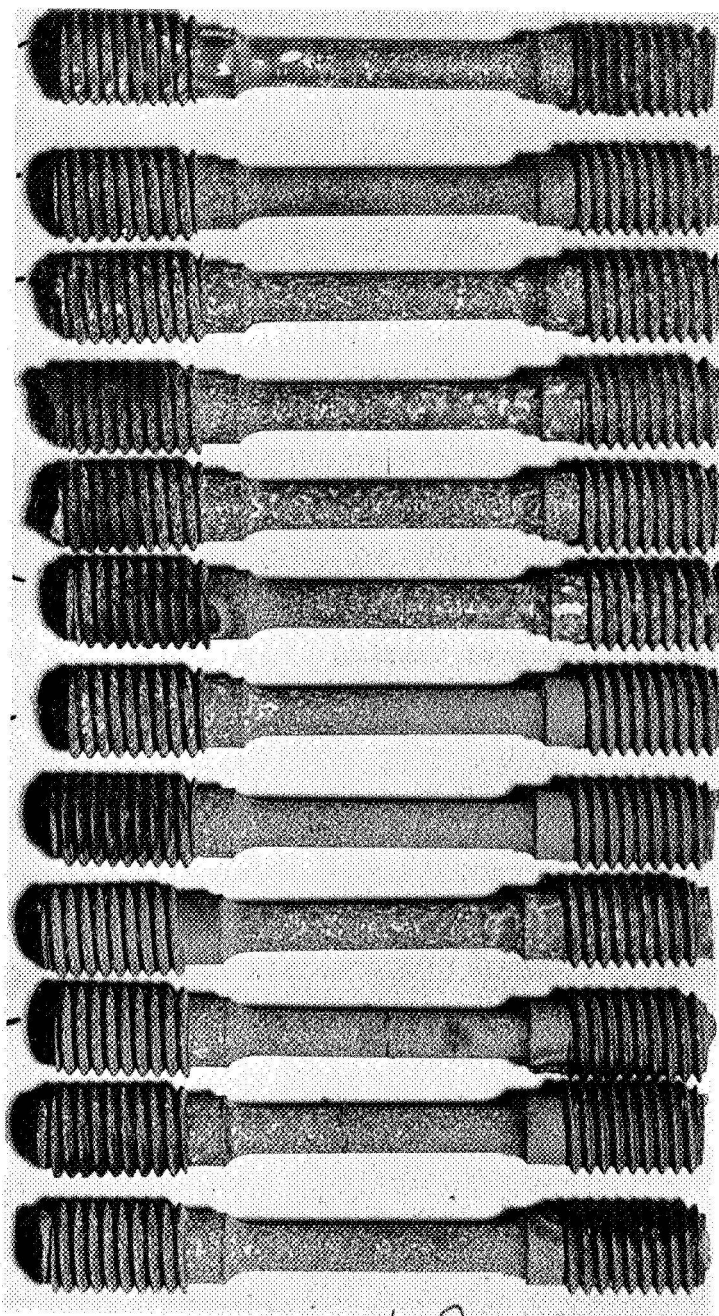
1X   C68061350

Figure 6:   Etched Test Bars of Some of the Experimental Alloys
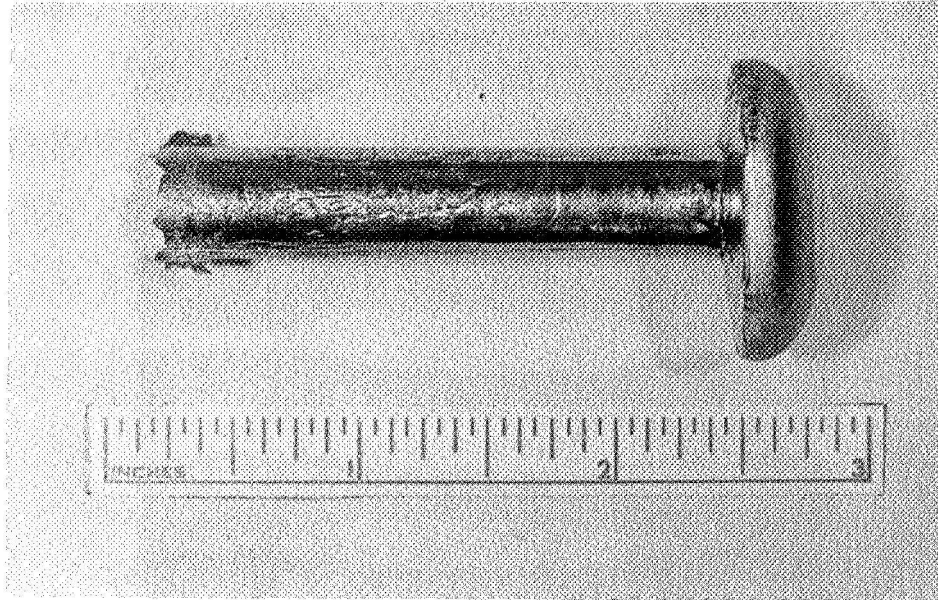
(a)   Straight Cylindrical Casting
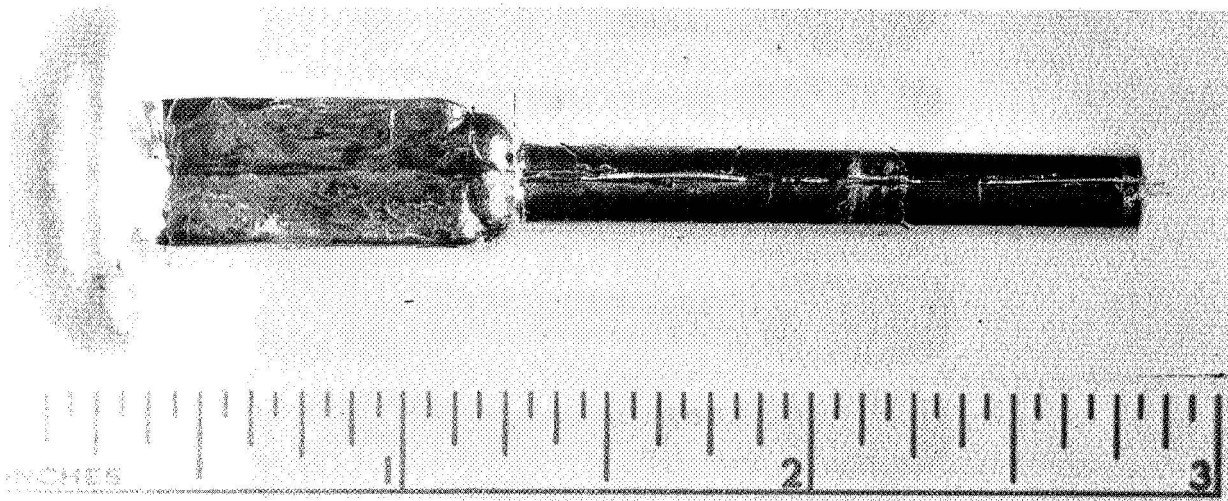
(b)   Step Cylindrical Casting

Figure 7:   Configuration of Laboratory Chill-Castings Used in this Study.

(a)   250X   Neg. No. P4550
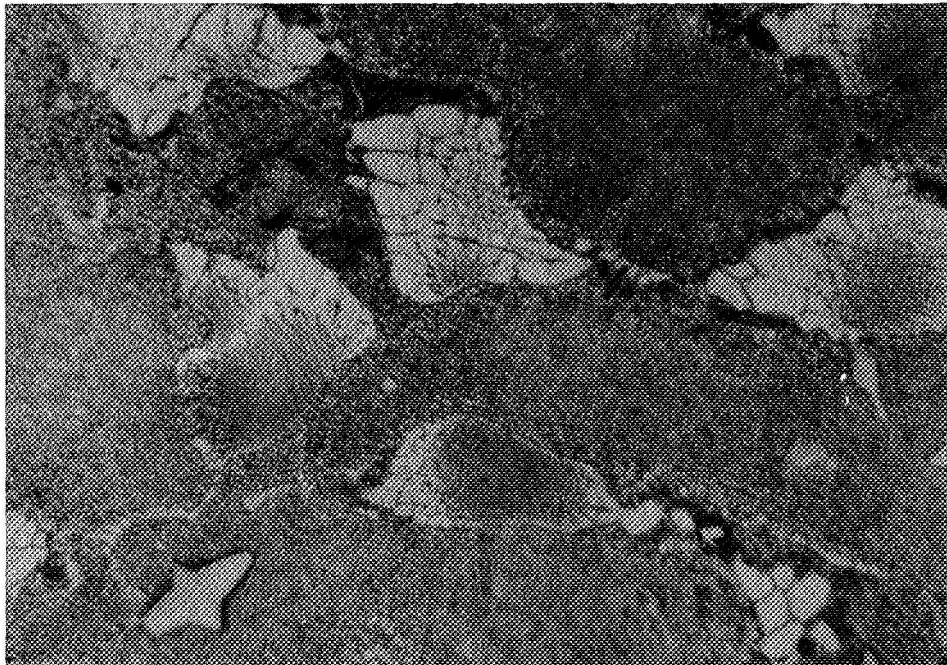
(b)   1000X   Neg. No. P4729

J-4139

Figure 8: Alloy #1 (Base) – Microstructure As–Cast – Etched
8-1 Phos.
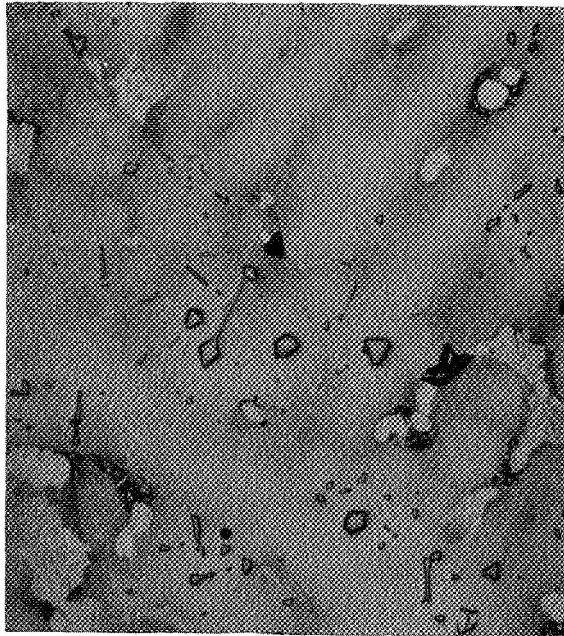
J4140
(a)   0.2 w/o Mn

P4551
250X
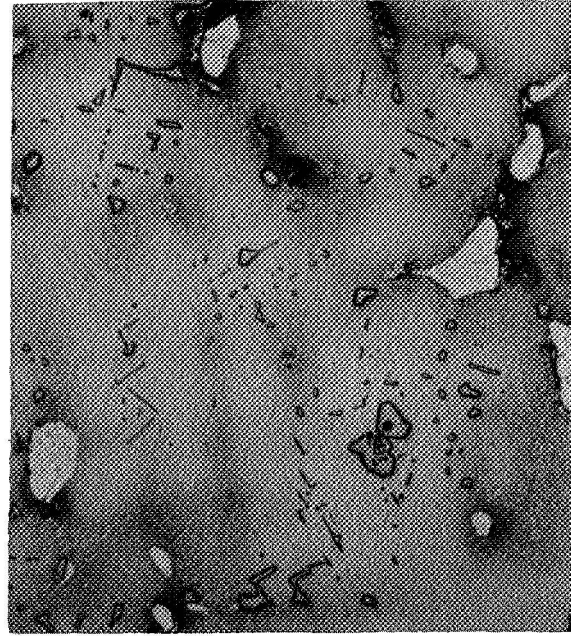
J4141
(b)   0.4 w/o Mn

P4553
250X
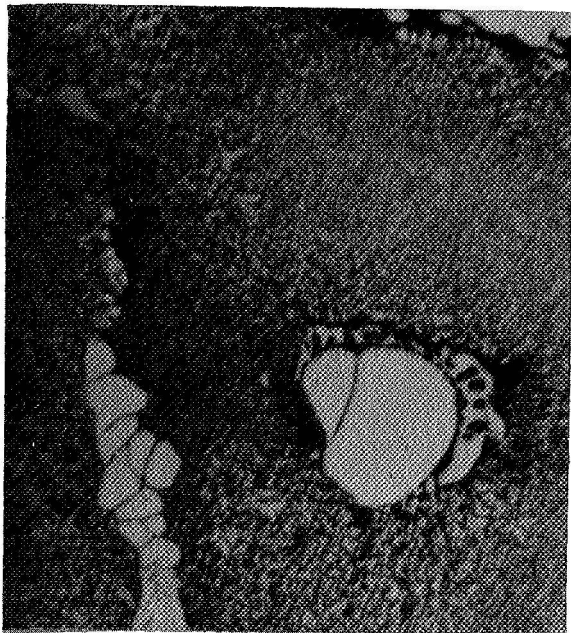
J4141
(c)   0.4 w/o Mn

P4731
1000X
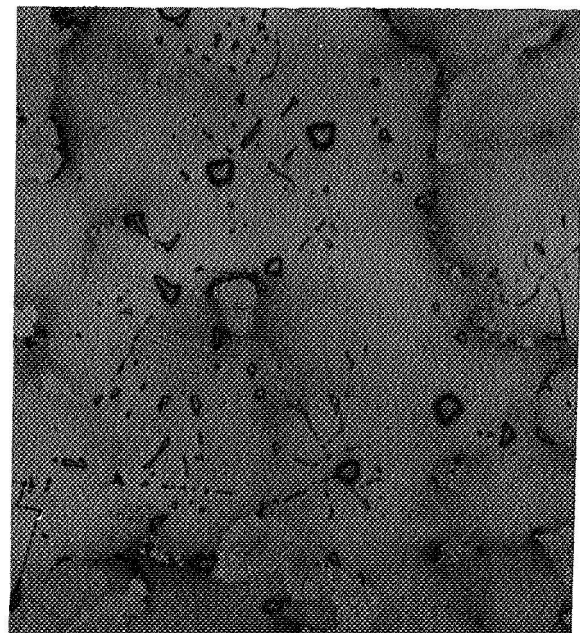
J4142
(d)   0.8 w/o Mn

P4555
250X

Figure 9:   Microstructures of Exp. Alloys Containing Mn As-Cast.
Etched 8-1 Phos.
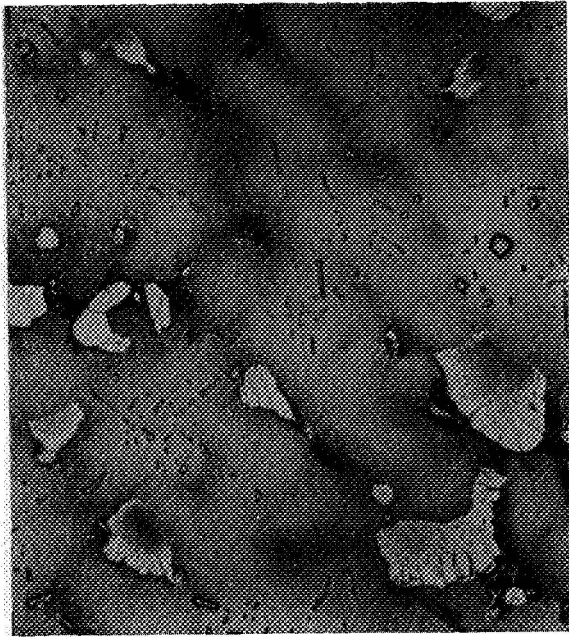
J4143   P4554
(a)   0.25 w/o Re   250X

J4143   P4735
(b)   0.25 w/o Re   1000X

J4144   P4560
(c)   0.5 w/o Re   250X
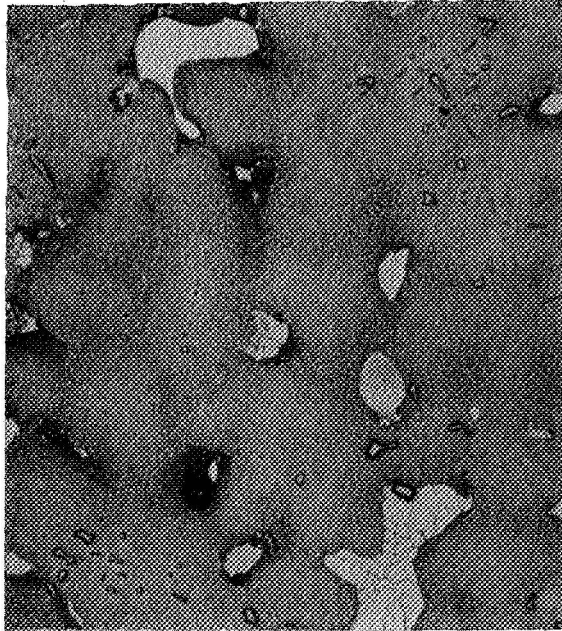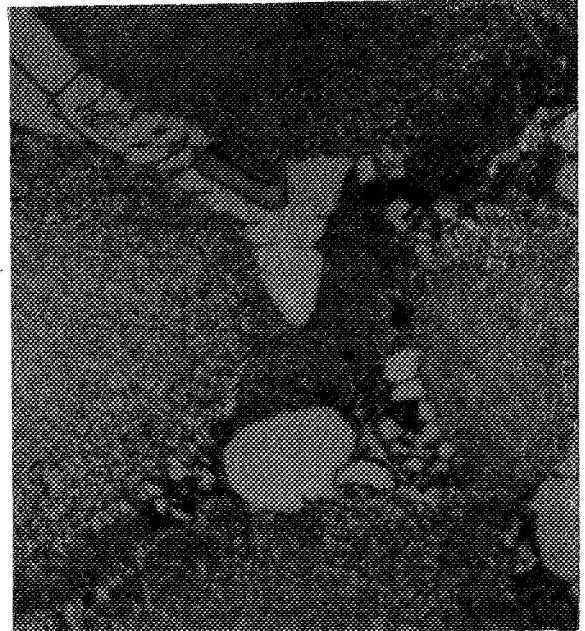
J4144   P4736
(d)   0.5 Re   1000X

Figure 10: Microstructures of Exp. Alloys Containing Re As-Cast. Etched
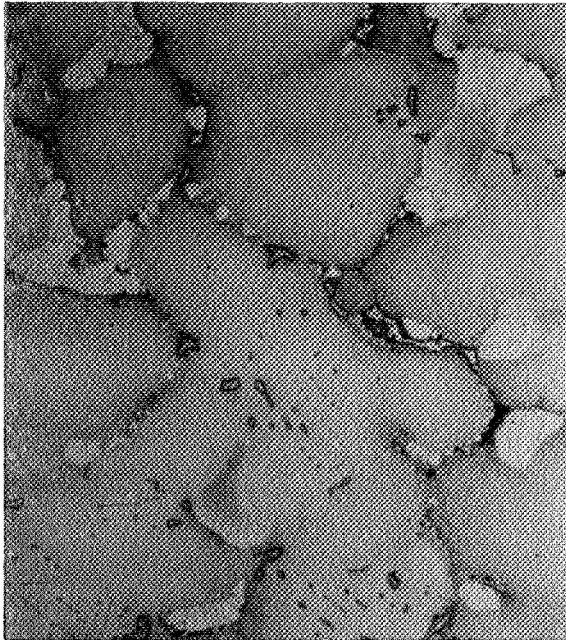
59

J4145   P4571
(a)   0.065 w/o Ce   250X

J4145   P4738
(b)   0.065 Ce   1000X

J4147   P4575
(c)   0.3 w/o Ce   250X
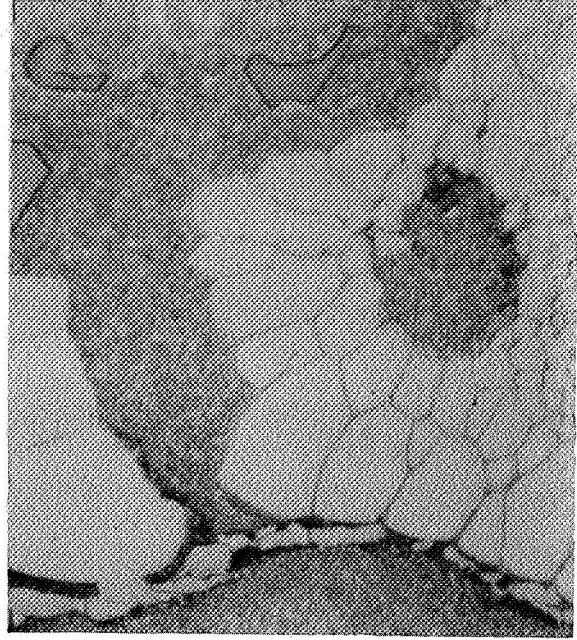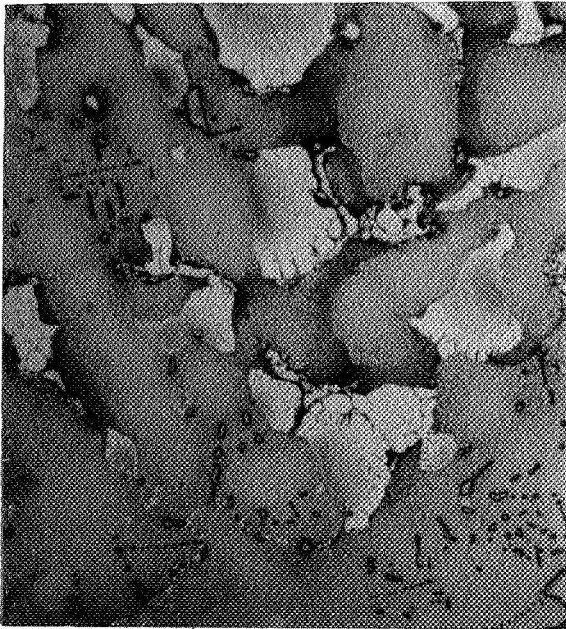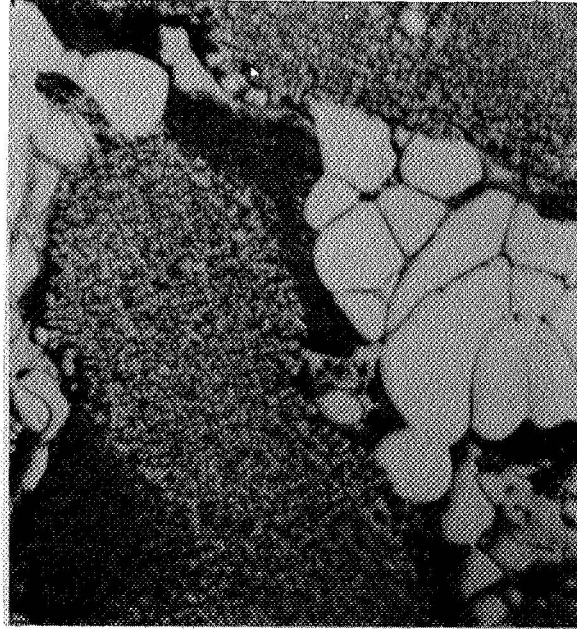
J4147   P4740
(d)   0.3 Ce   1000X

Figure 11: Microstructure of Exp. Alloys Containing Ce. As-Cast. Etched.
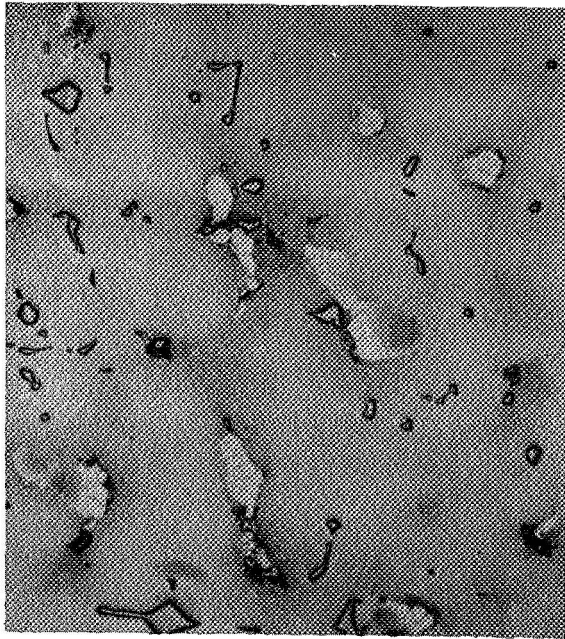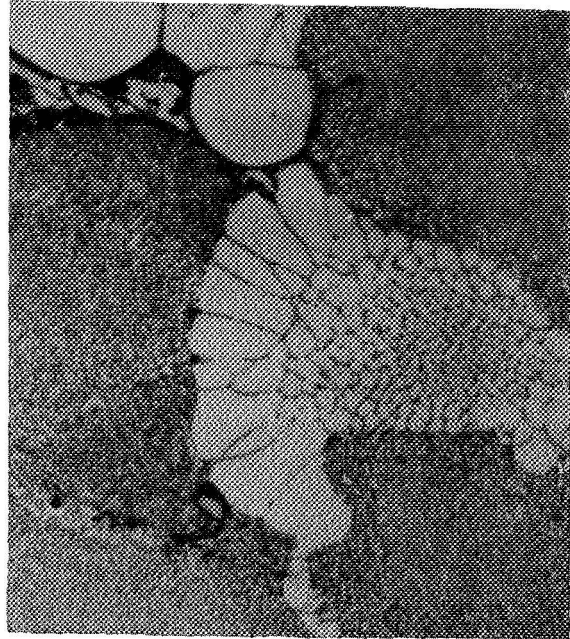
J4148   P4577   J4148   P4769
(a)   0.04 w/o Y   250X   (b)   0.04Y   1000X
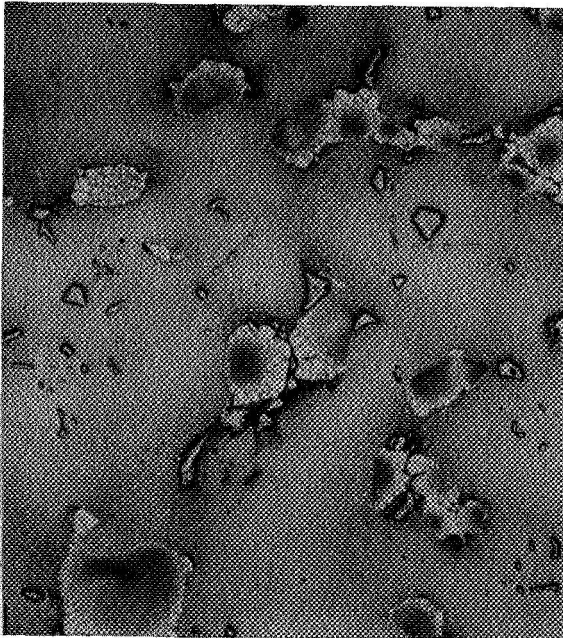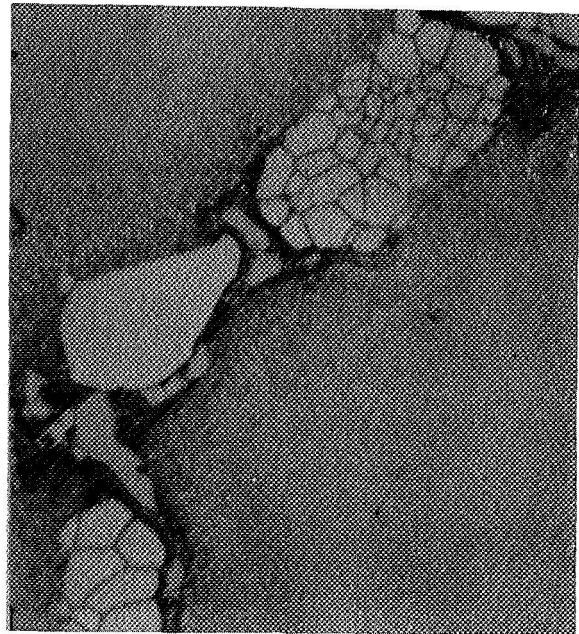
J4150   P4581   J4150   P4771
(c)   0.21 w/o Y   250X   (d)   0.21 w/o Y   1000X

Figure 12:   Microstructures of Exp. Alloys Containing Y.   As-Cast -Etched

61

J4151   P4584
(a)   0.23 w/o Gd   250X
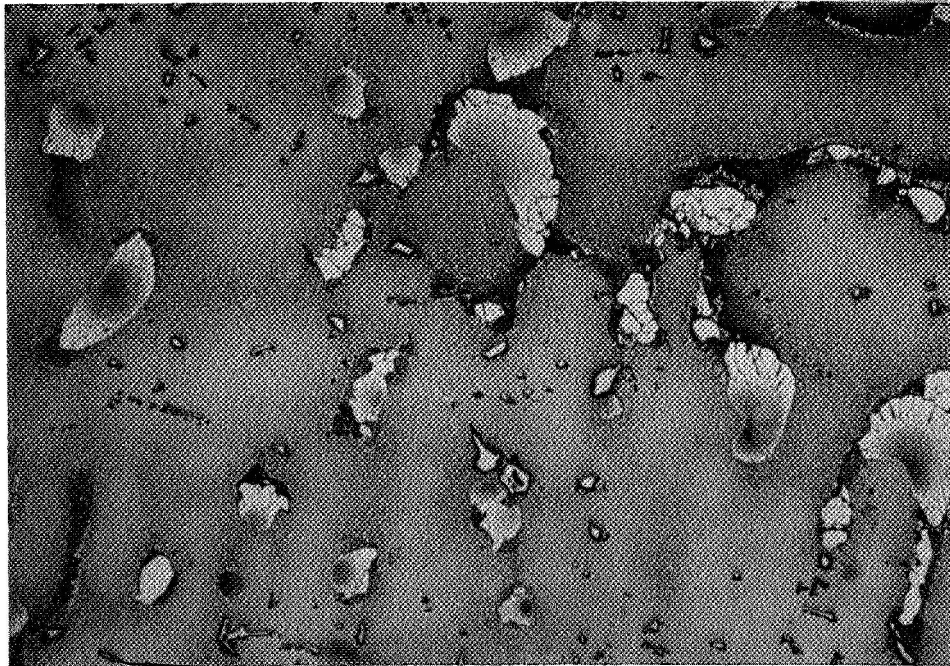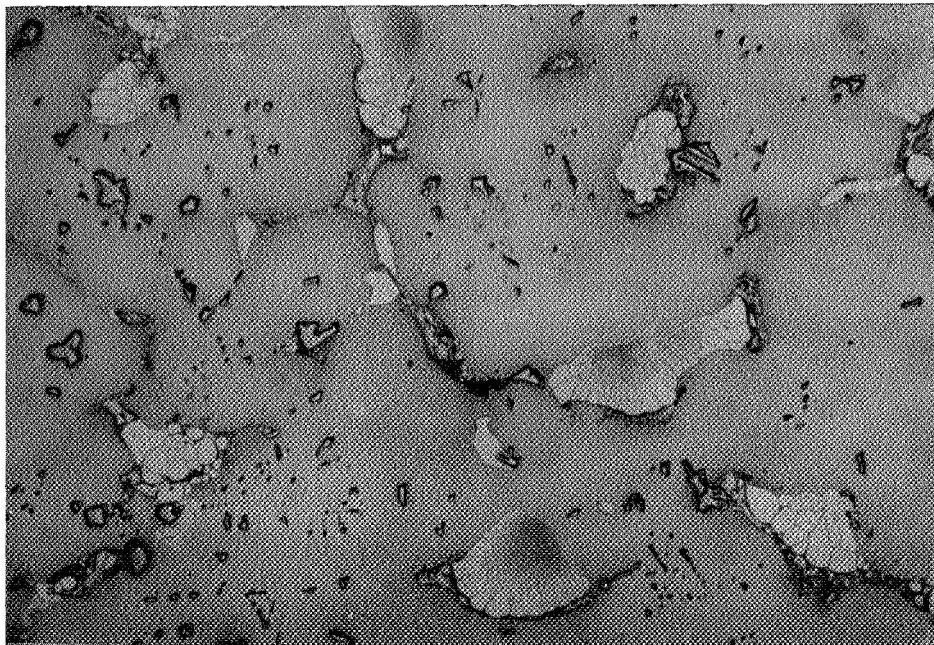
J4152   P4586
(b)   0.31 w/o Th   250X

Figure 13:   Microstructures of Exp. Alloys #13 & 14 As-Cast.   Etched.
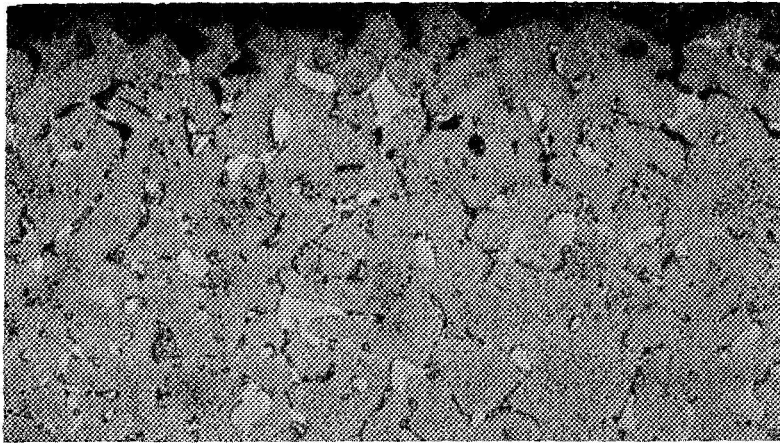
A1016   P1383
(a)   225F Superheat

A1015   P1382
(b)   125F Superheat

A1014   P1381
(c)   50F Superheat
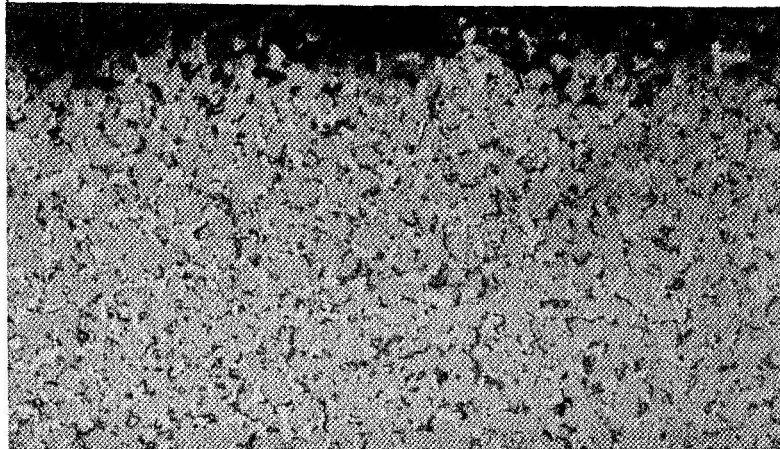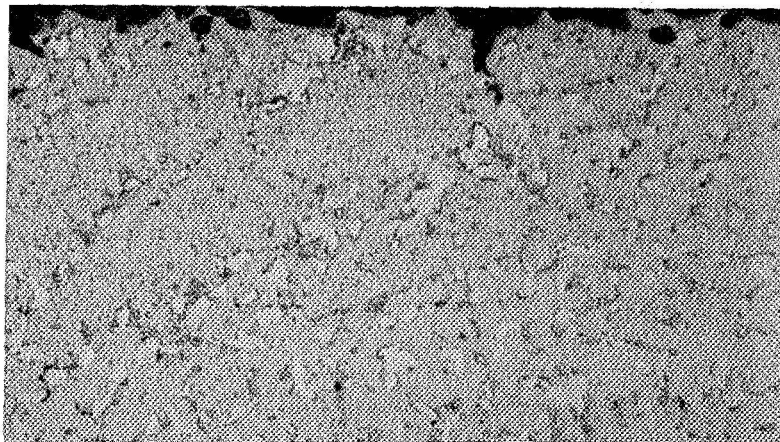
Figure 14:   Microstructures of VI-A & 0.5La + 0.25Re + 1Mn Alloy Cast With
             Varying Degrees of Superheat (Alloys 18-20)   100X
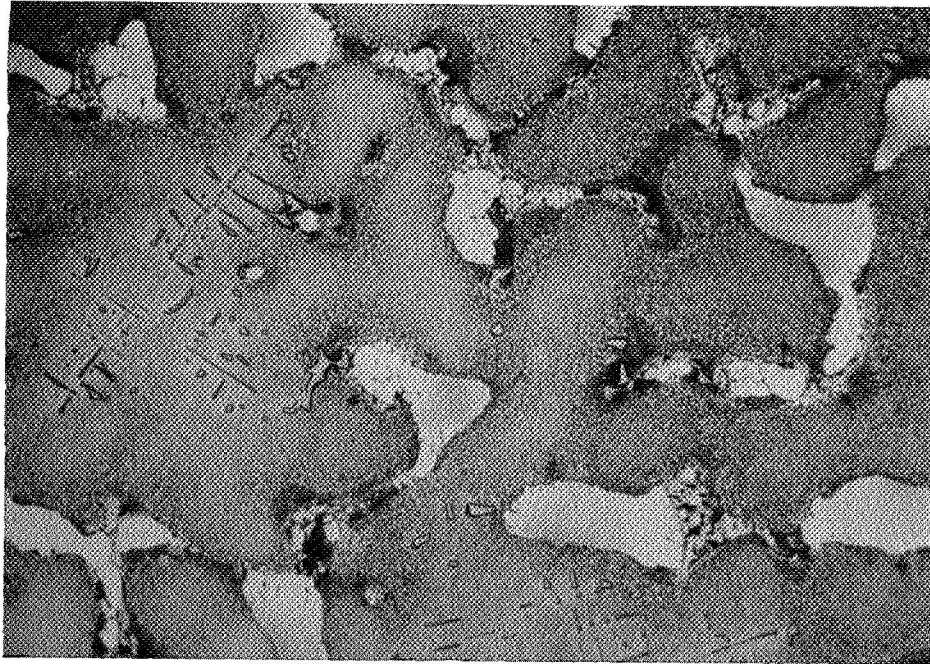
A8050   B10372
(a)   Alloy 21, 0.5 w/o La.   Standard Melting Practice
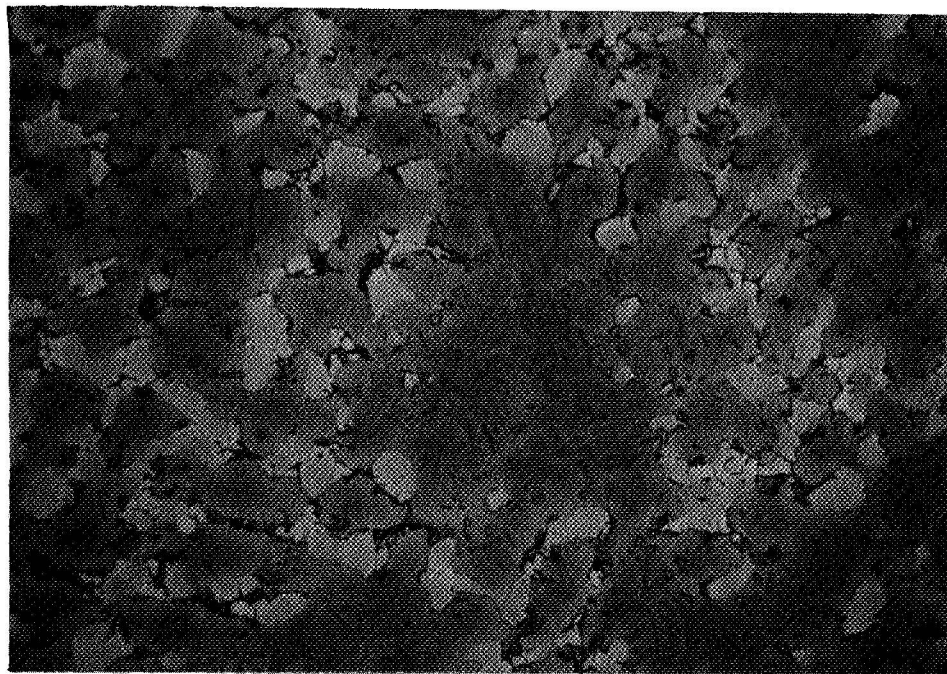
A8050   B10373
(b)   Alloy 22, 0.5 w/o La, Chilled Mold

Figure 15:   Microstructures of Alloys 21 & 22 As-Cast - Etched.   250X
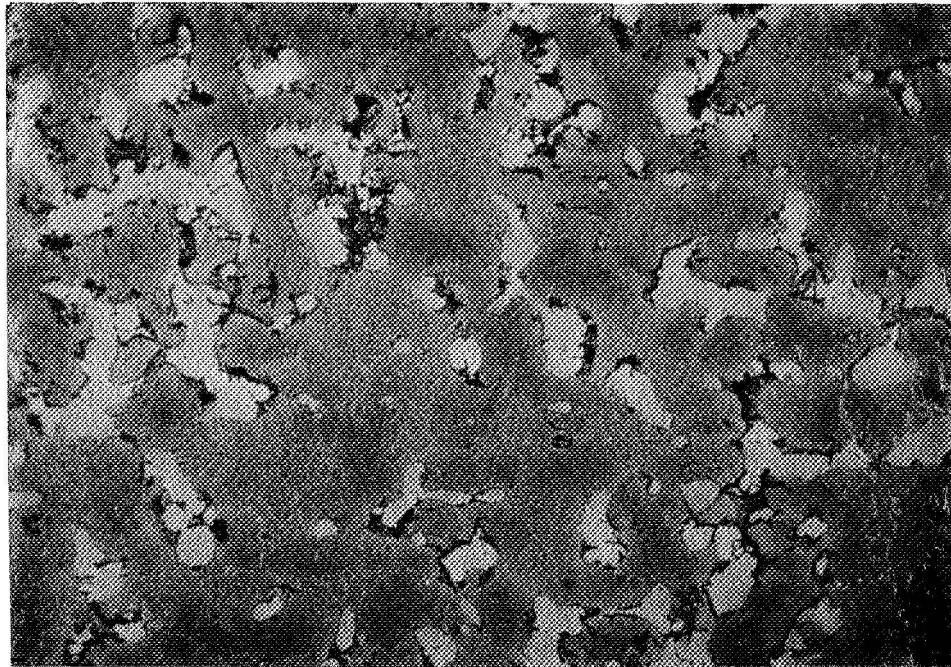
A8052   B10374
(a)   Alloy 23, 0.4% La
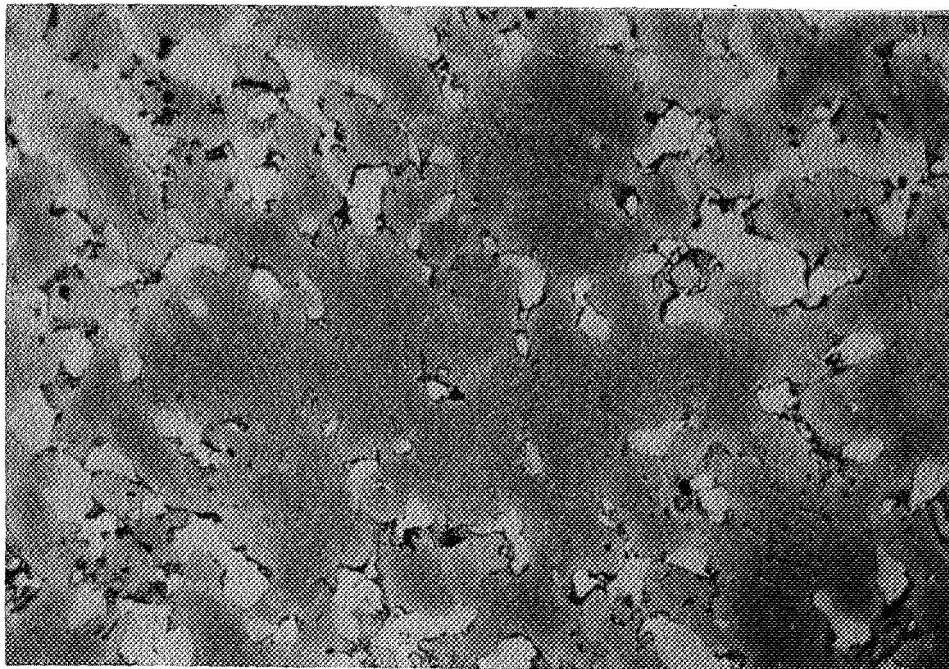
A8053   B10375
(b)   Alloy 24, 0.6% La

Figure 16:   Microstructures of Alloys 23 & 24 As-Cast - Etched.   250X
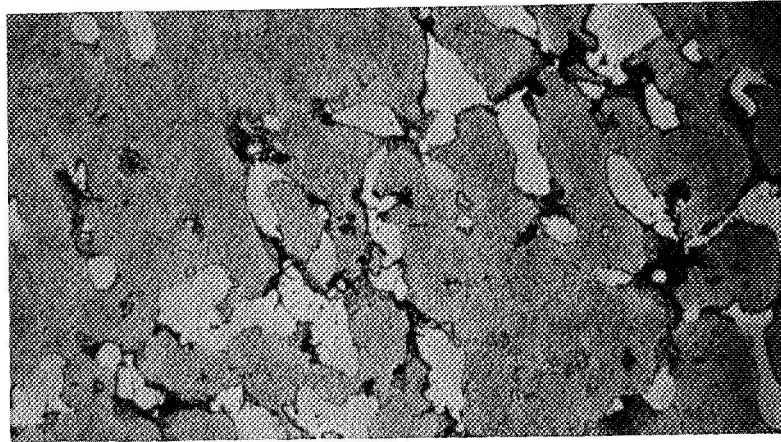
A8054   B10376

(a)   Alloy 25, 0.6 La + 1.0 Mn
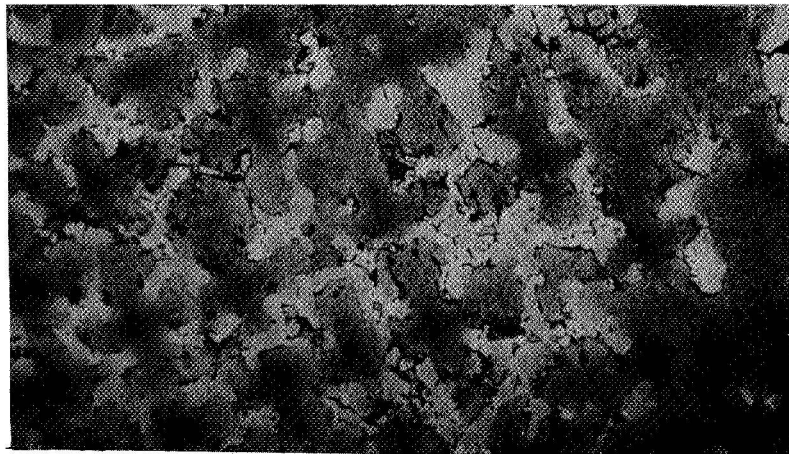
A8055   B10377

(b)   Alloy 26, 0.2 La + 0.2 Y
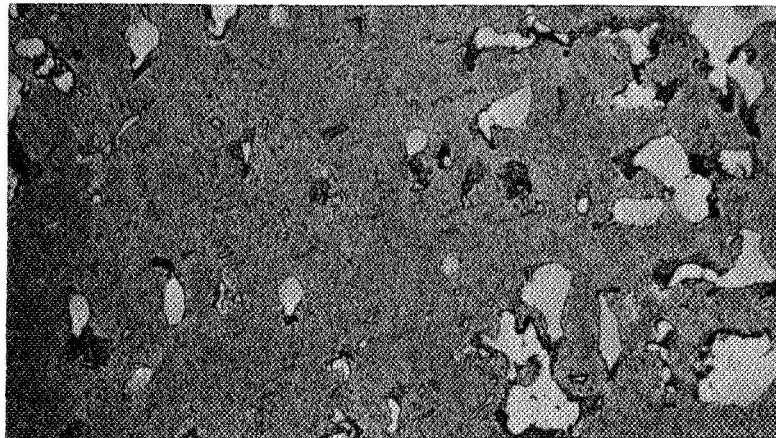
A8056   B10380

(c)   Alloy 27, 0.3 La + 0.15 Y

Figure 17:   Microstructures of Alloys 25-27 As-Cast - Etched.   250X
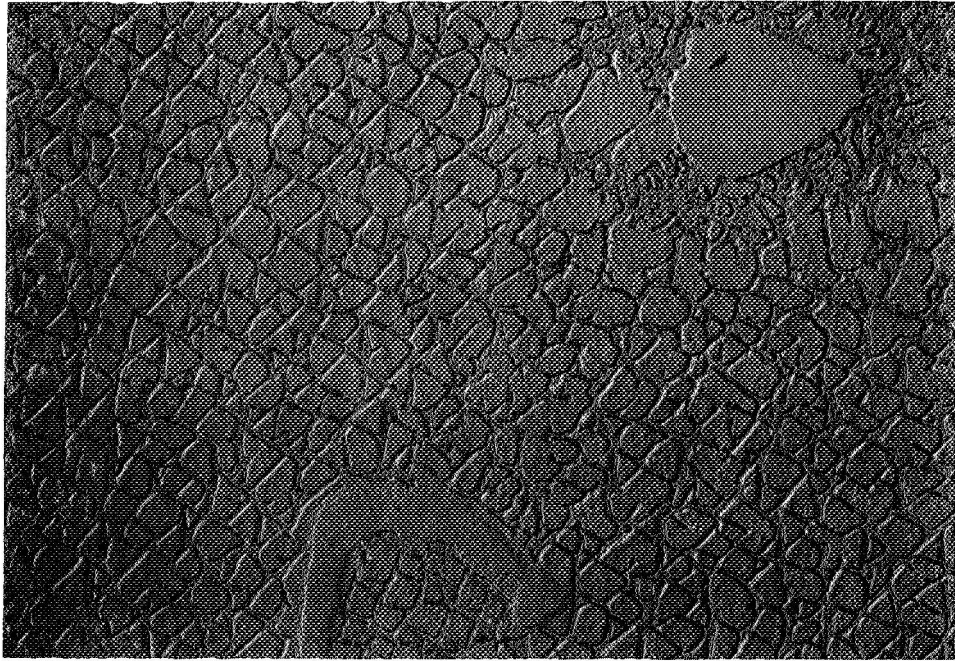
H-29-3
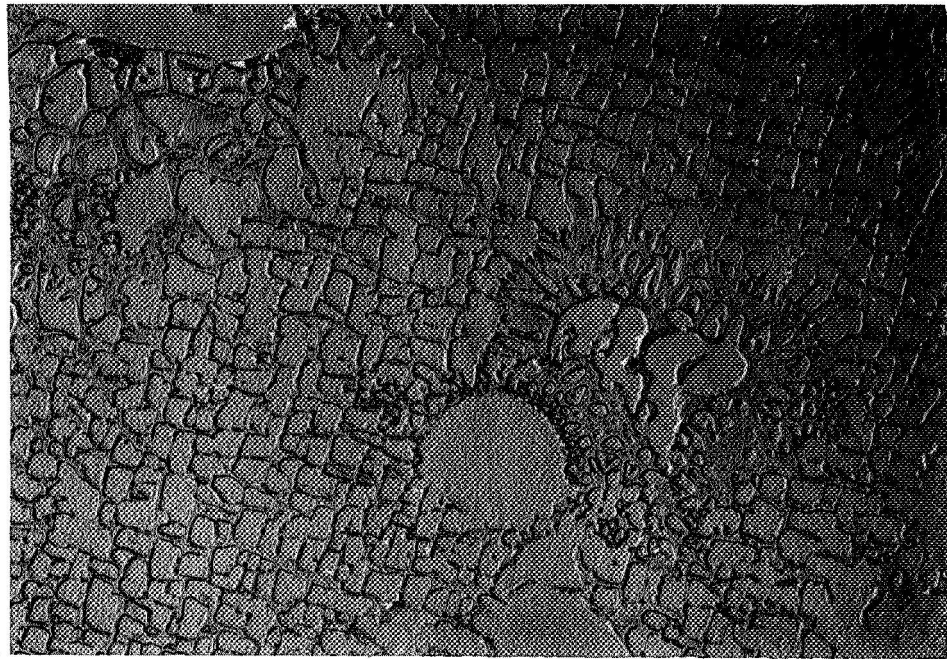
H-29-6

Figure 18: Electron Micrographs of Base Alloy (#1)   5000X
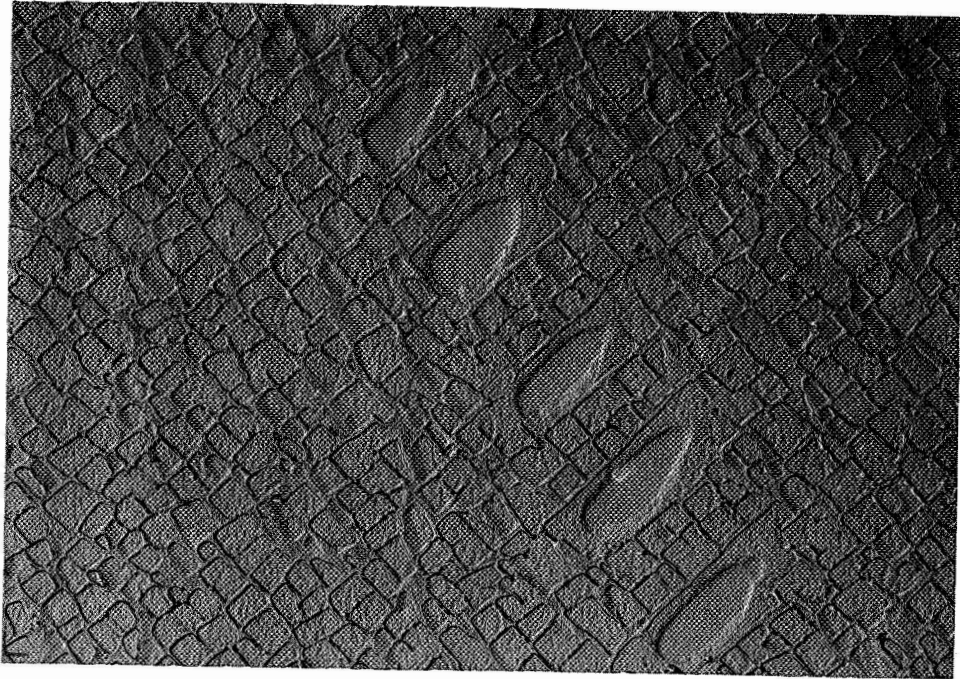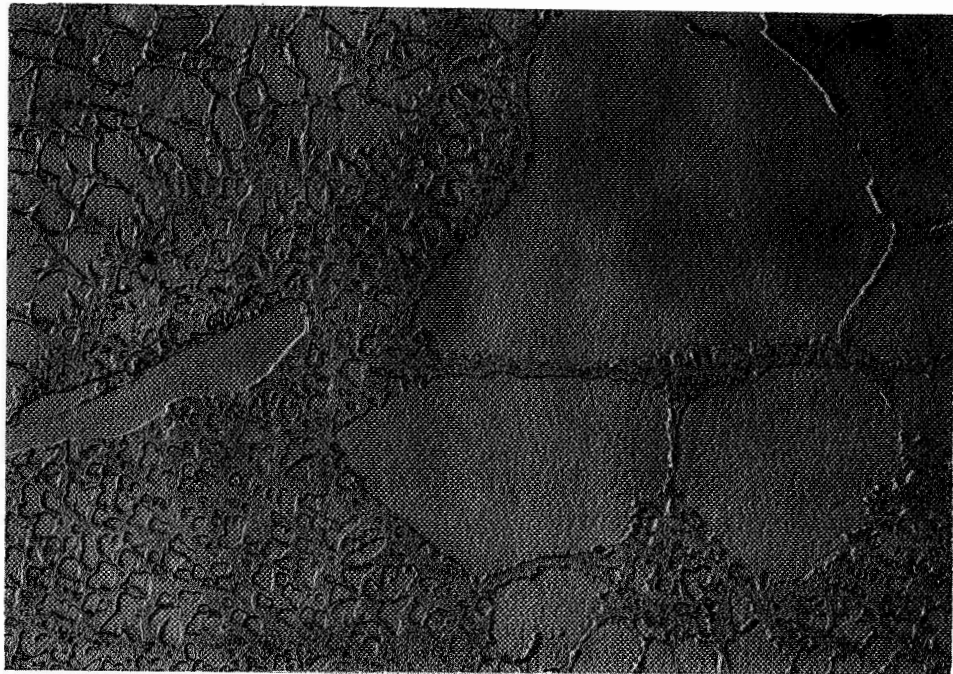
H-29-1

H-29-4

Figure 19:   Electron Micrographs of Base Alloy #1 - 5000X

H-29-15
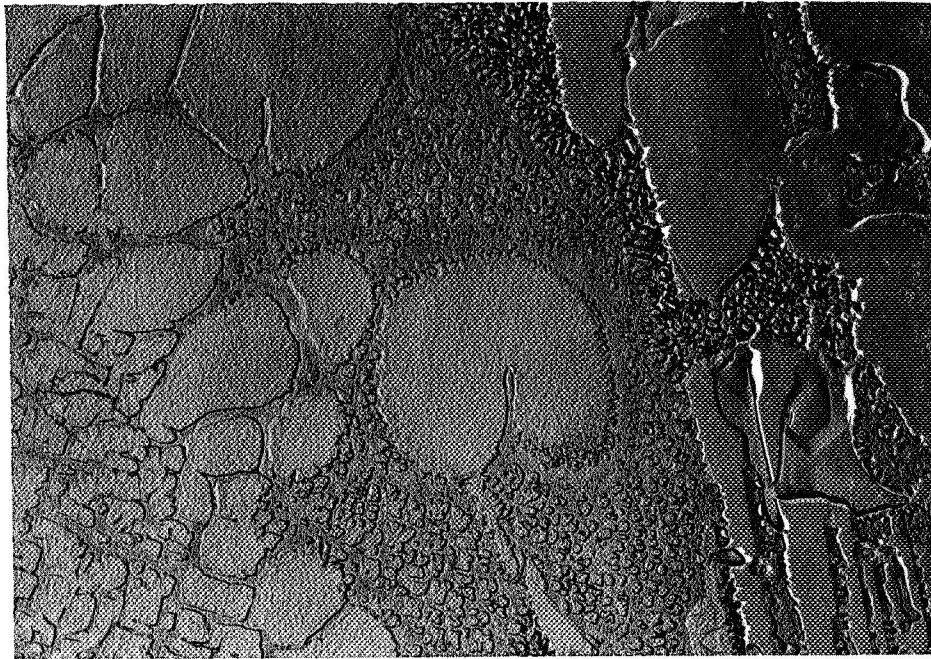
H-29-12

Figure 20:   Electron Micrographs of Alloy #5.
             Base + 0.5% Re.   5000X
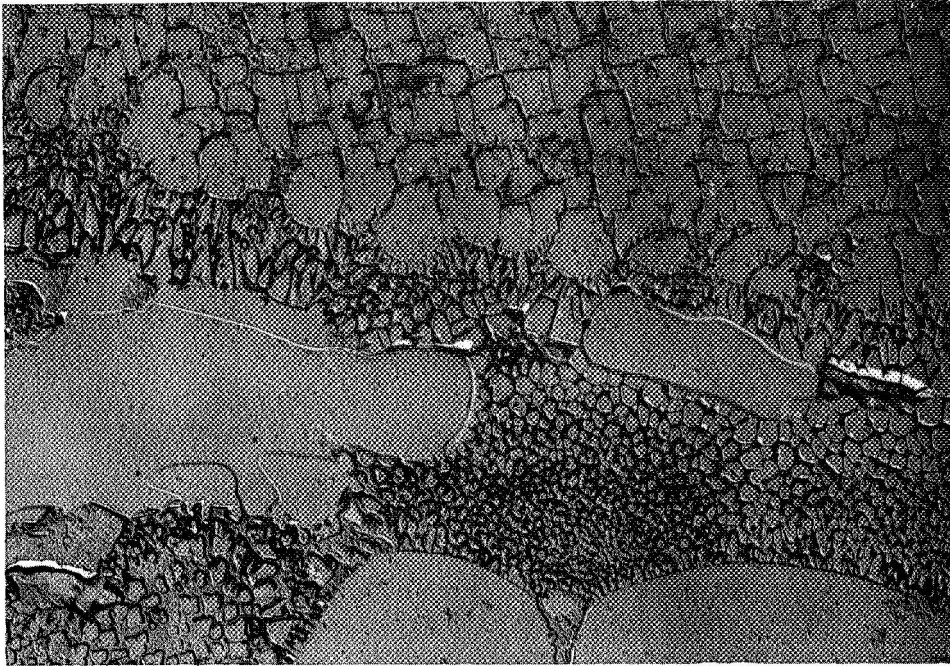
H-30-3
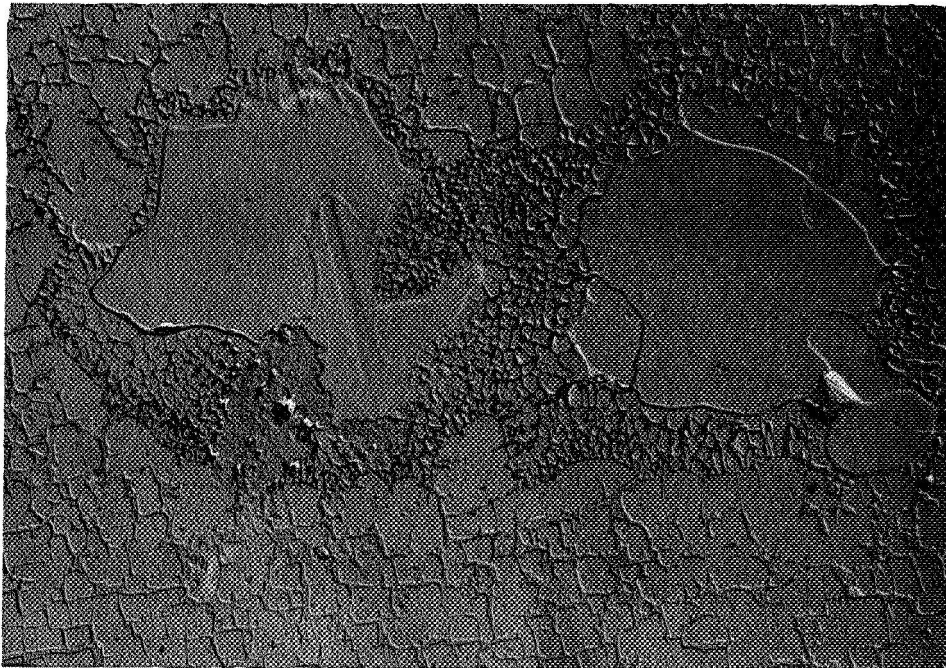
H-30-2

Figure 21: Electron Micrographs of Alloy 11
Containing 0.14% Y.   5000X

70
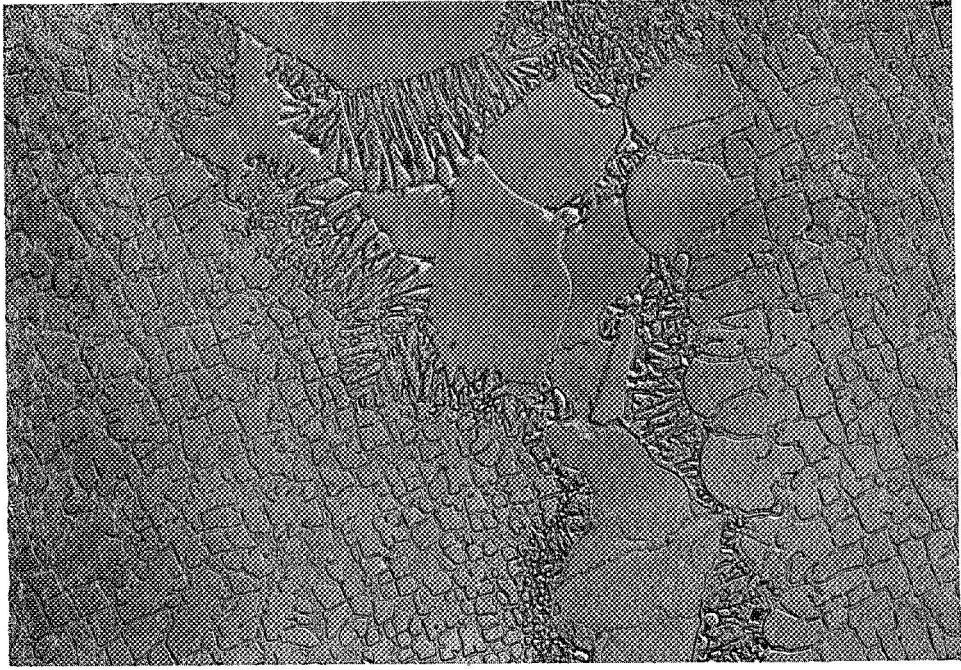
H-27-15
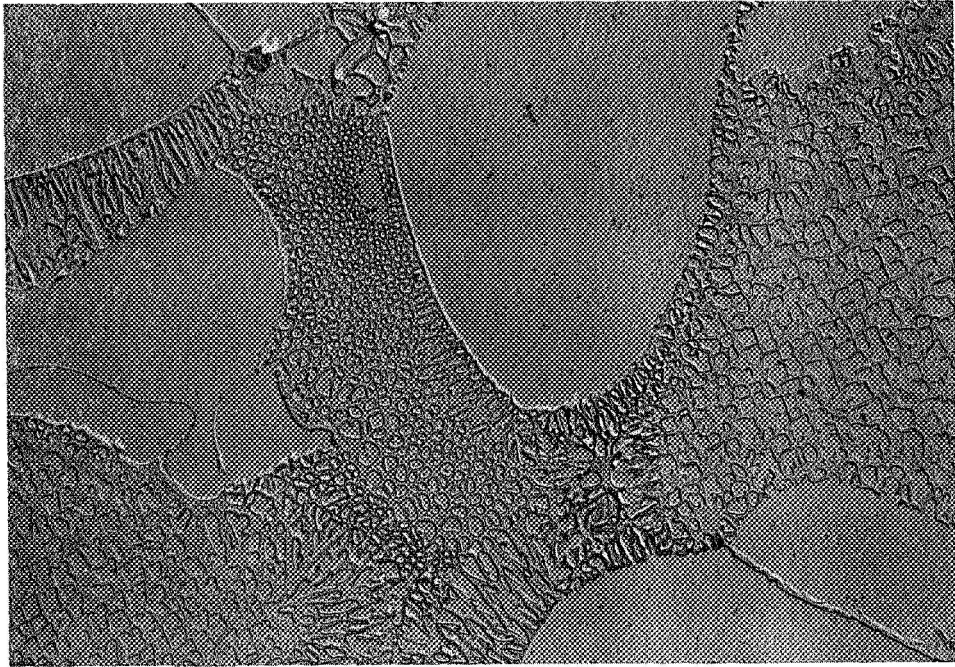
H-27-17

Figure 22: Electron Micrographs of Alloy 13 Containing 0.23% Gd.   5000X
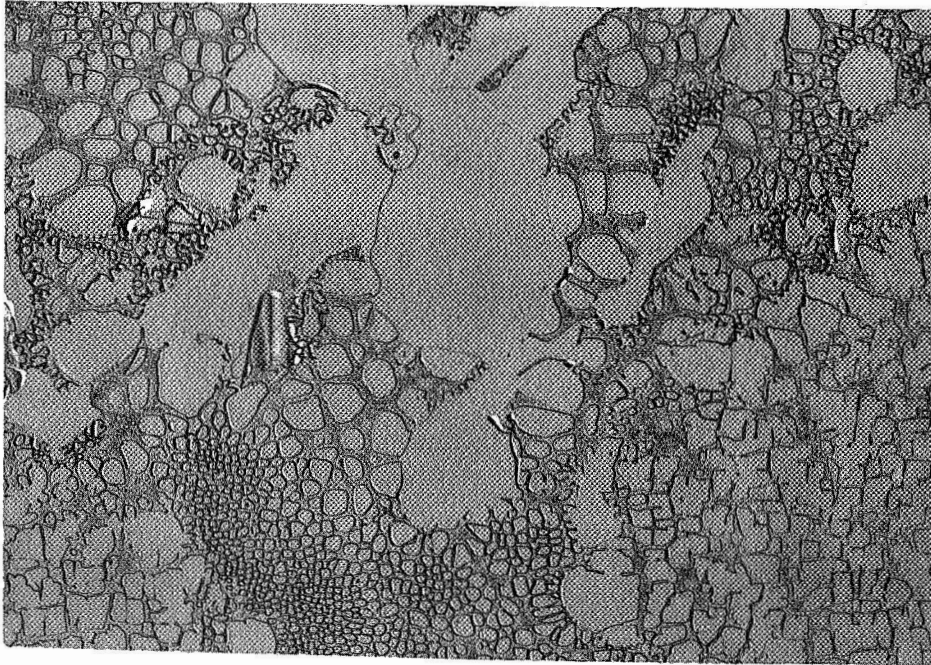
H-30-9
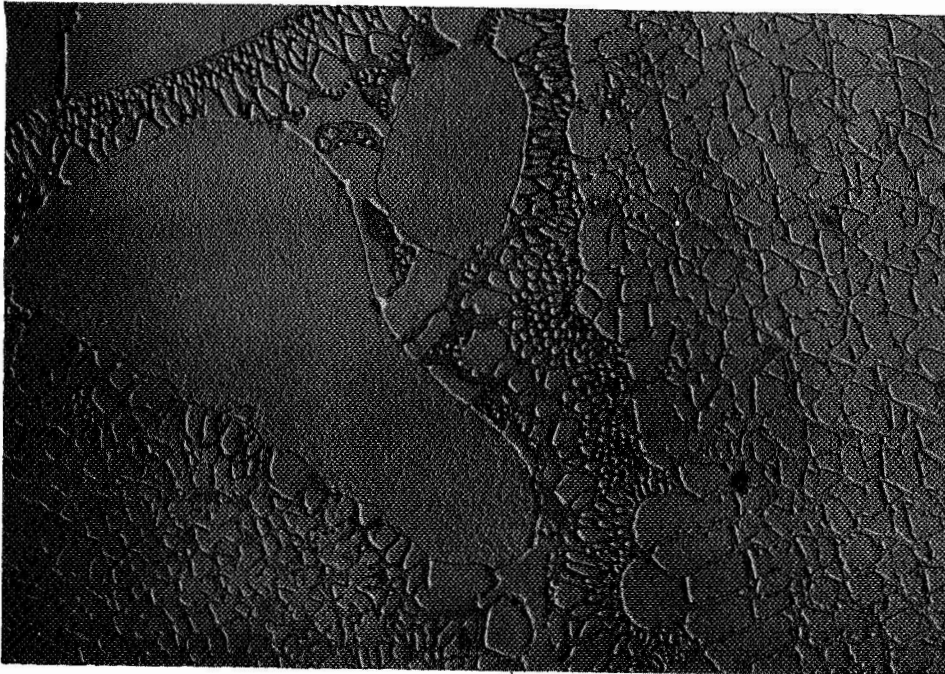
H-30-7

Figure 23: Electron Micrographs of Alloy No. 14 Containing 0.3 Thorium.

5000X

A4223   P6153
(a)   2200F, 1 hr.

A4224   P6154
(b)   2300F, 1 hr.
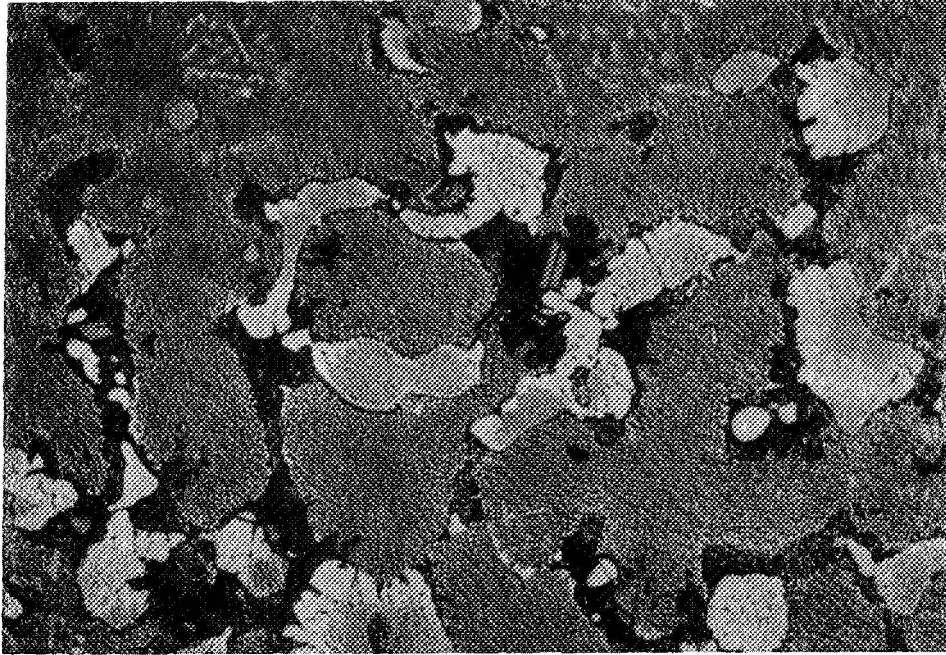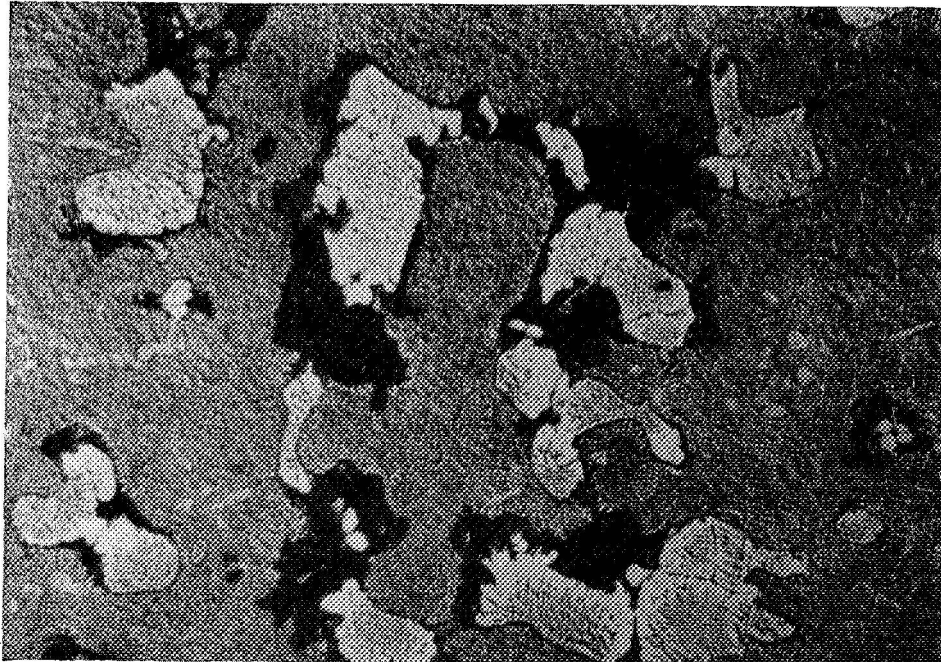
Figure 24:   Microstructure of Base Alloy after Heat Treatment
            at 2200 & 2300F, 1 hr. Etched, 500X

A4244   P6166
(a)   Alloy 5, 0.25% Re

A4224   P6165
(b)   Alloy 6, 0.5% Re
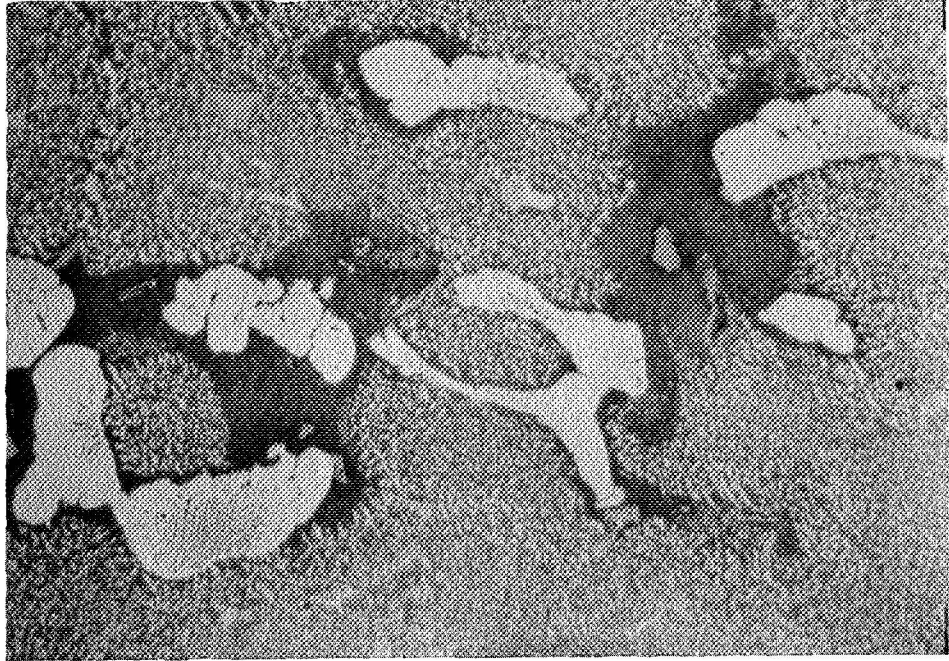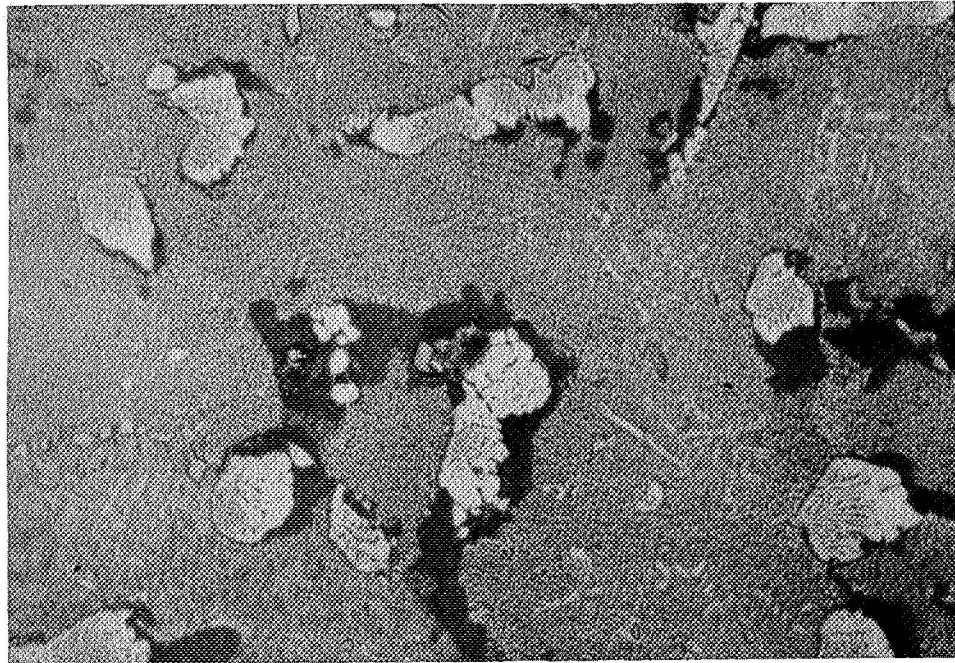
Figure 25:   Microstructures of VI-A Alloys after Heat Treatment,
              1 hr. @ 2300F.   Etched,   500X
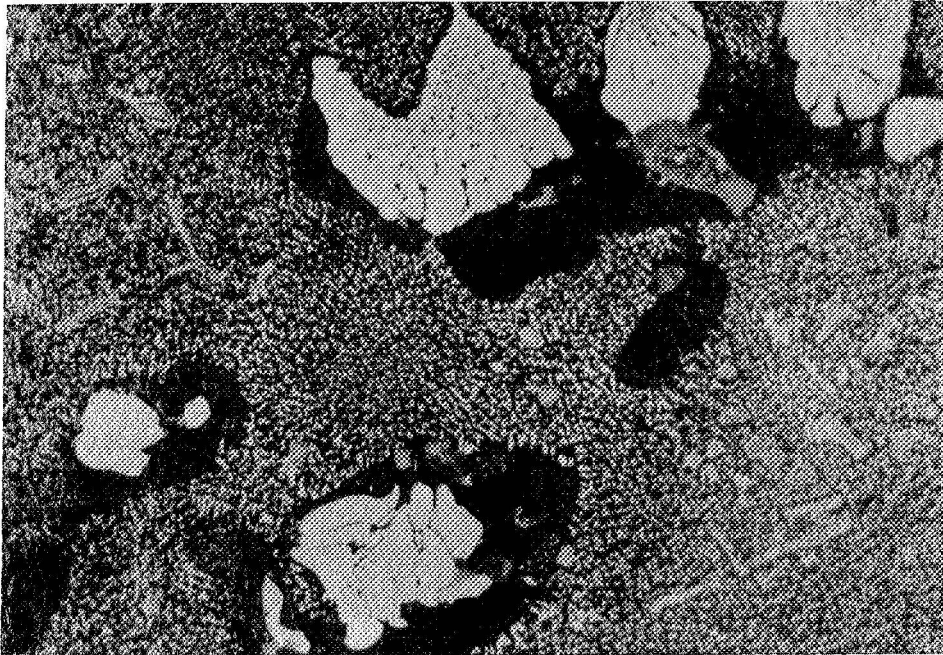
A4232   P6159
(a)   Alloy 3, 0.4 w/o Mn
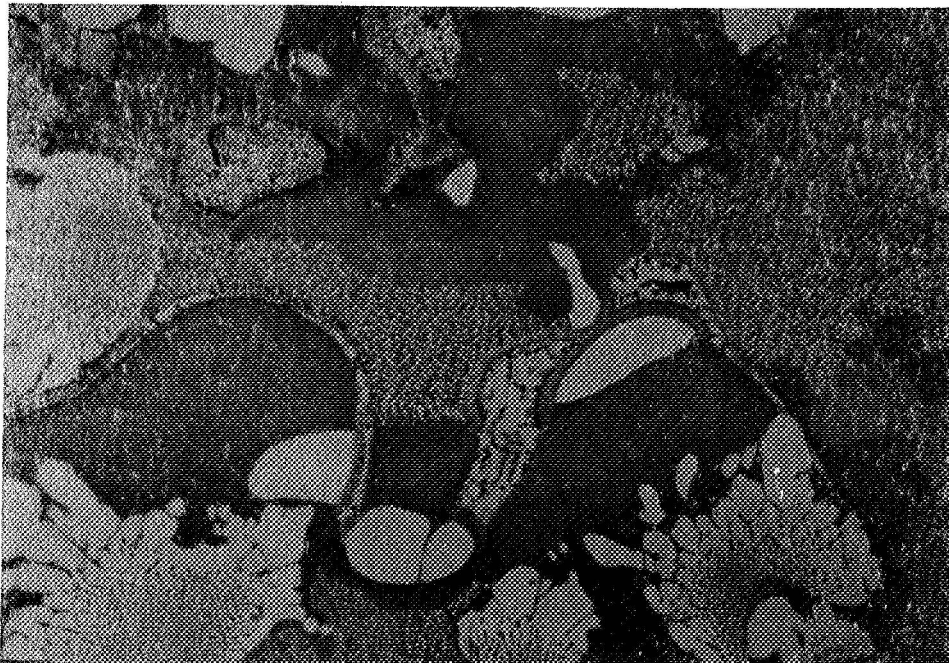
A4256   P6172
(b)   Alloy 9, 0.3 w/o Ce

Figure 26:   Microstructure of Alloys 3 and 9 after Heat Treatment
             1 hr. at 2300F. Etched,   500X

A4260   P6173

(a) Alloy 10, 0.04 w/o Y
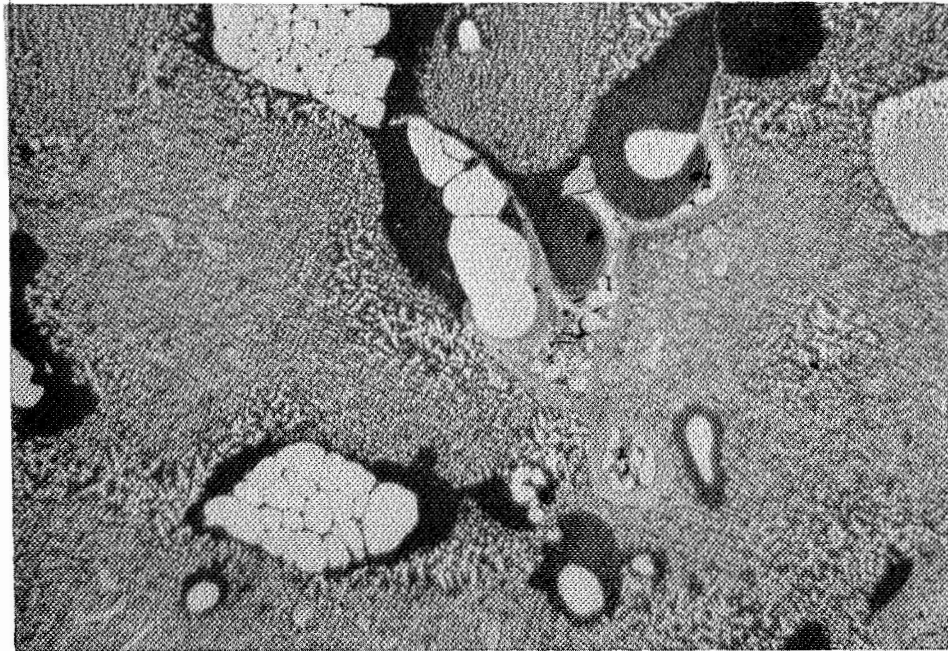
A4264   P6372

(b) Alloy 12, 0.21 w/o Y

Figure 27: Microstructures of Alloys 10 & 12 Containing Yttrium,
after Heat Treatment 1 hr. at 2300F. Etched, 500X
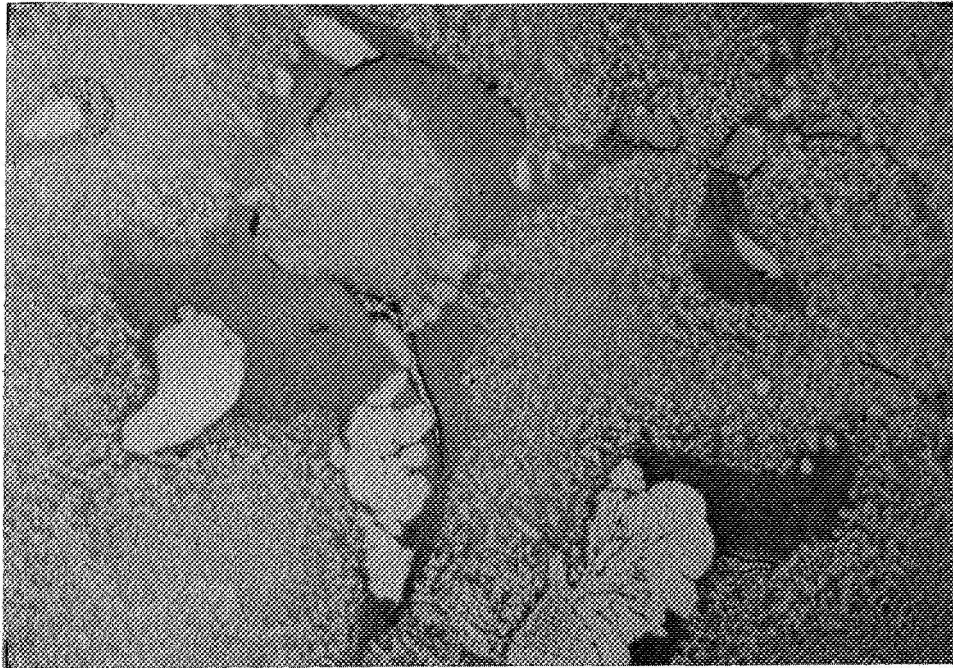
(a)   Alloy 13, 0.23 w/o Gd   P6377
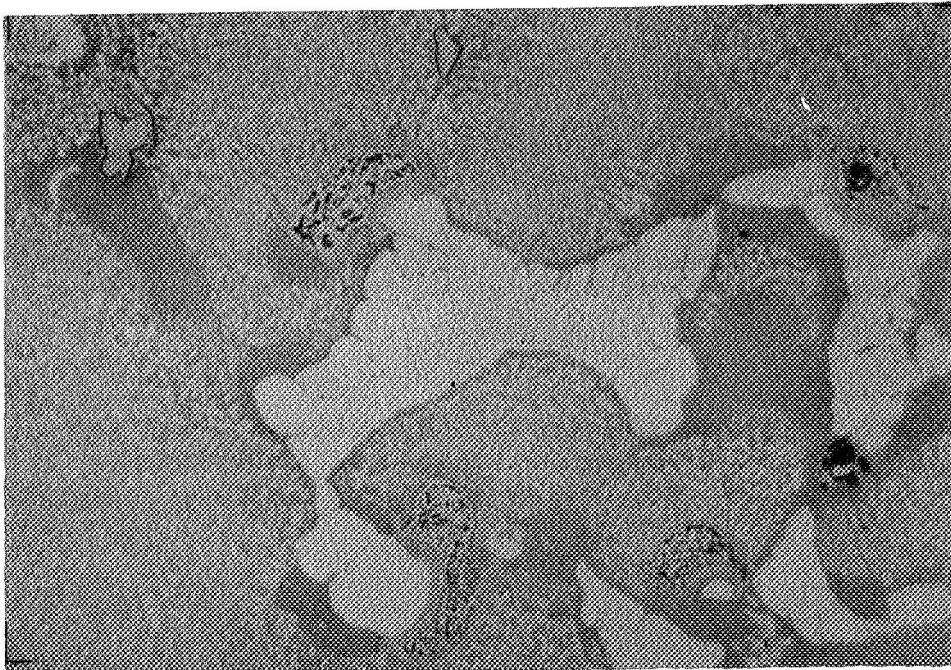
(b)   Alloy 14, 0.23 w/o Th   P6381

Figure 28:   Microstructures of Alloys 13 & 14 after Heat Treatment
2300F, 1 hr.   Etched, 500X
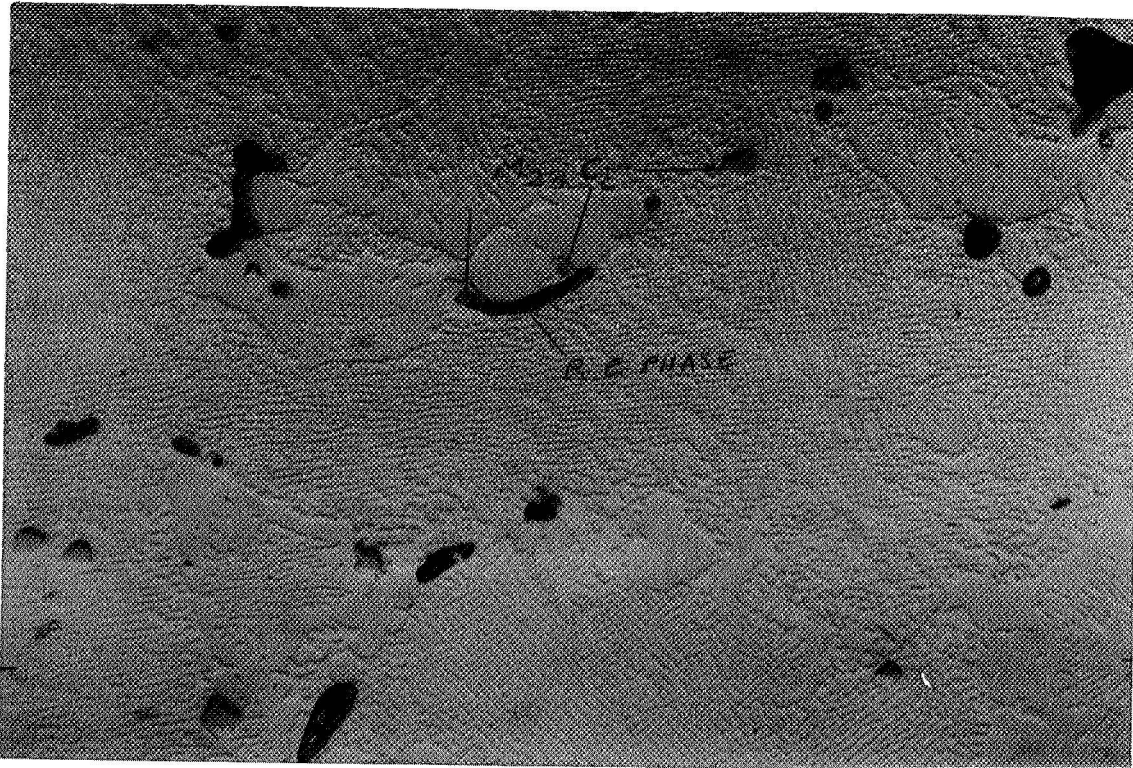
J1697

P2492

Figure 29:   Microstructure of Alloy Containing 0.5% La
After Aging for 500 Hrs. at 1800F, Showing
ɣ ' Envelopment of Carbide Particles.   Etched.
1000X
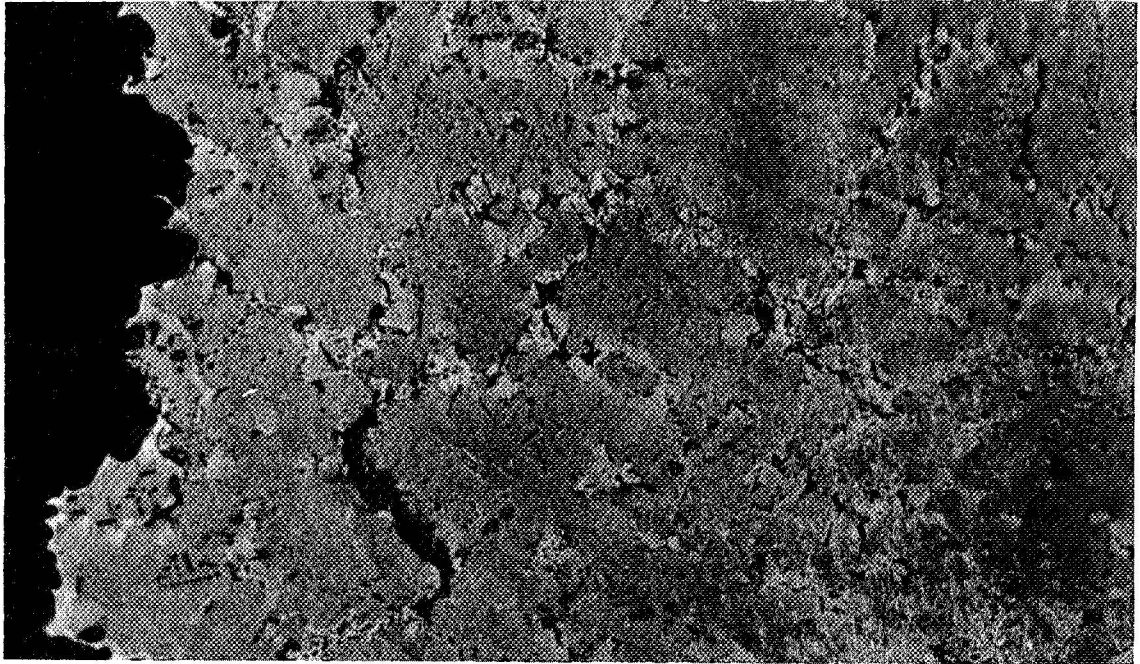
J2246   P2473

Figure 30:   Fracture of Base Alloy after 1800F Rupture Test
             Showing Intergranular Cracking. Etched. 250X
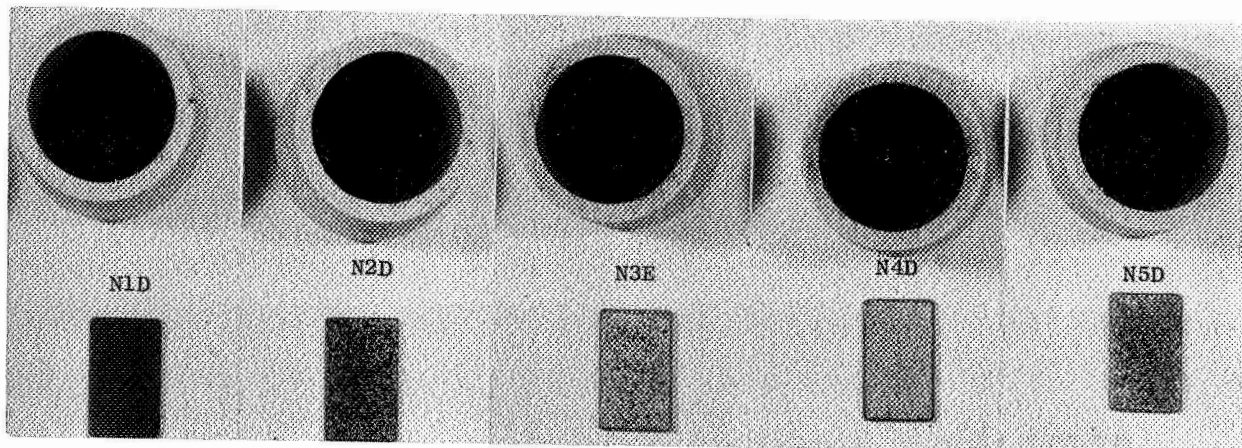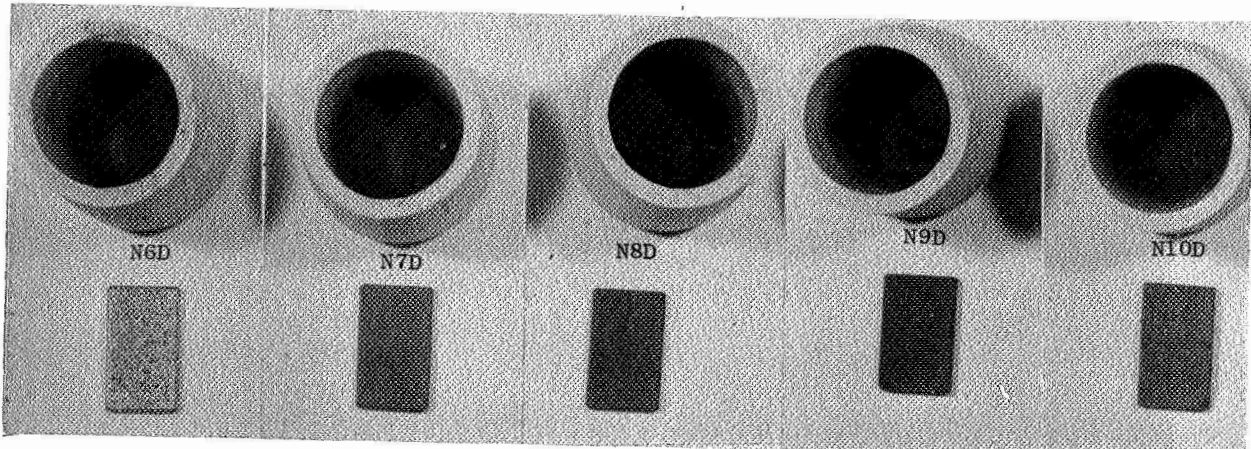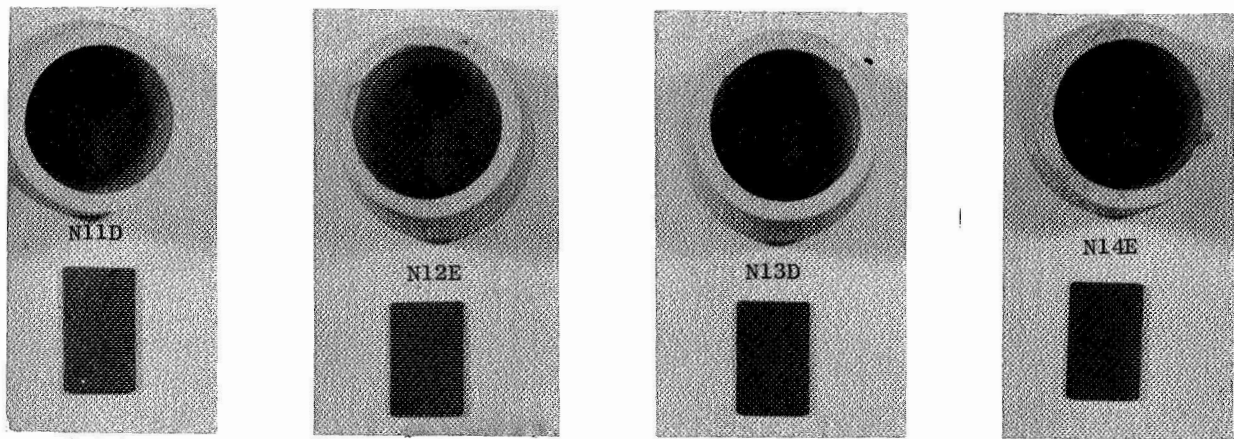
Figure 31: Oxidation Specimens after 400 Hrs. at 2000F in Cyclic Tests.
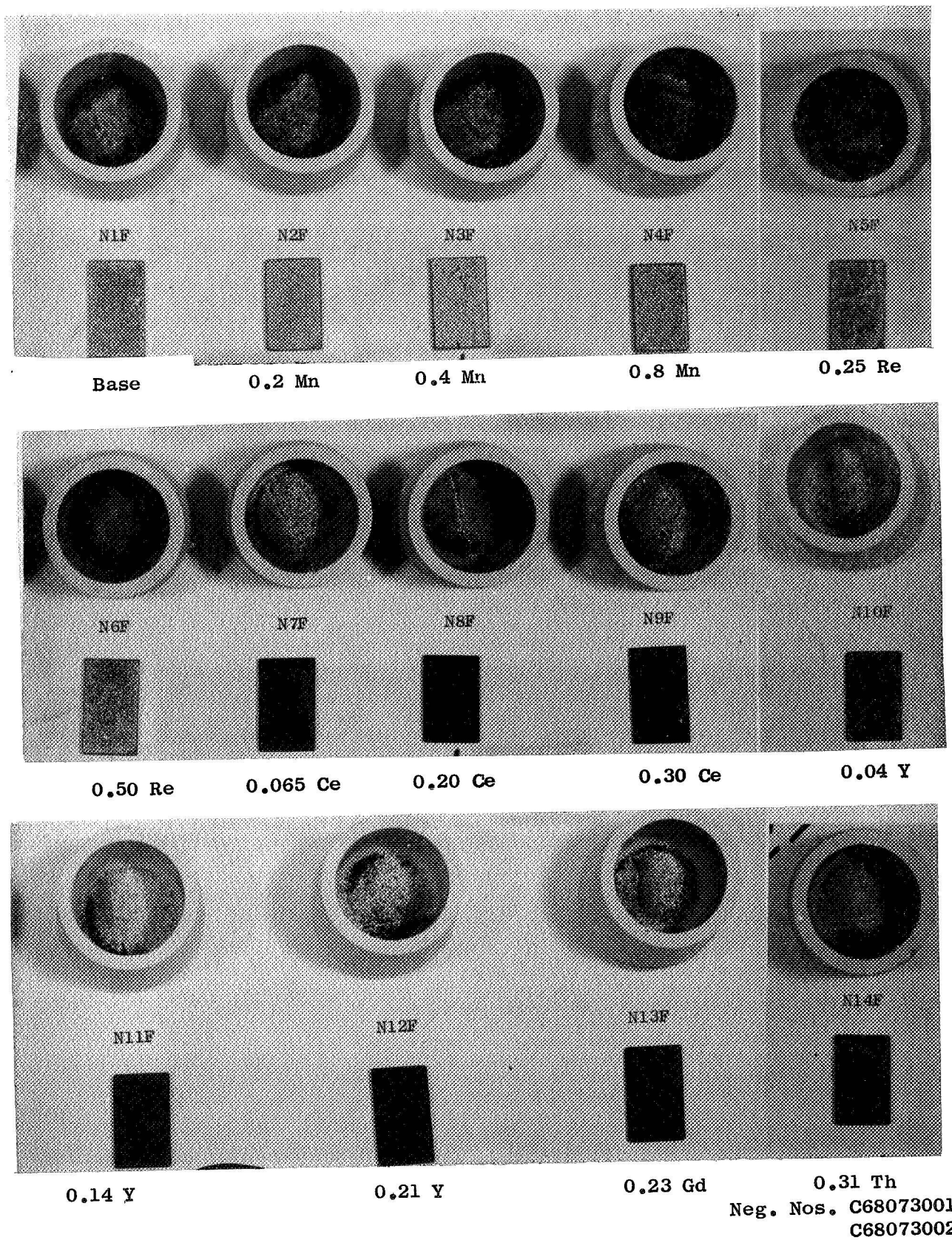
Figure 32: Oxidation Specimens after 400 Hrs. at 2000F in Isothermal Tests.

81

A11414   B10393
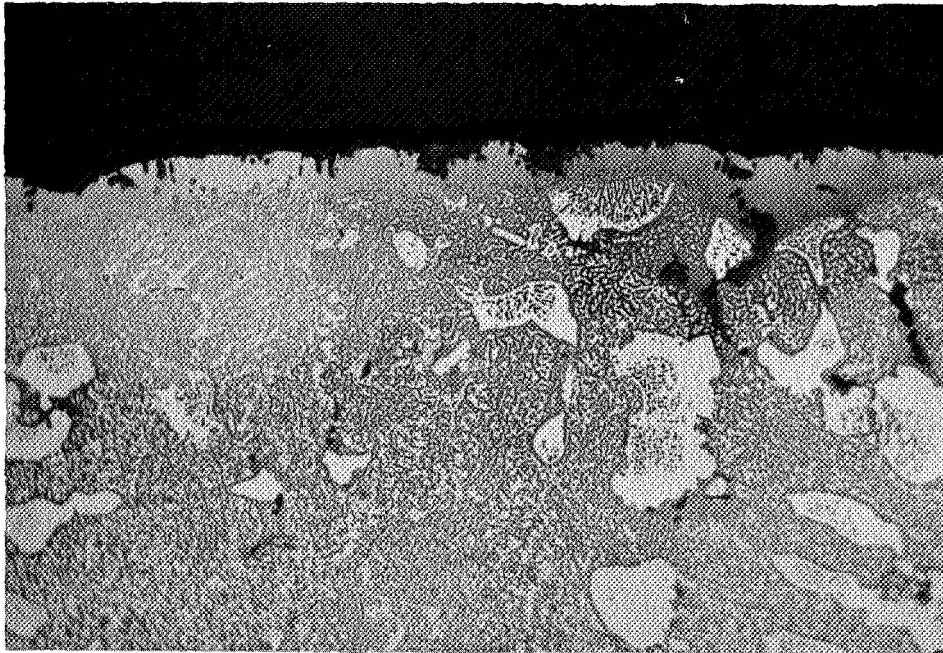
(a)   Alloy #15 (0.05 La)

A11397   B10382

(b)   Alloy #17 (0.3 La)

Figure 33: Microstructures of Oxidation Specimens
            after 400 Hrs. at 2000F. Etched. 250X
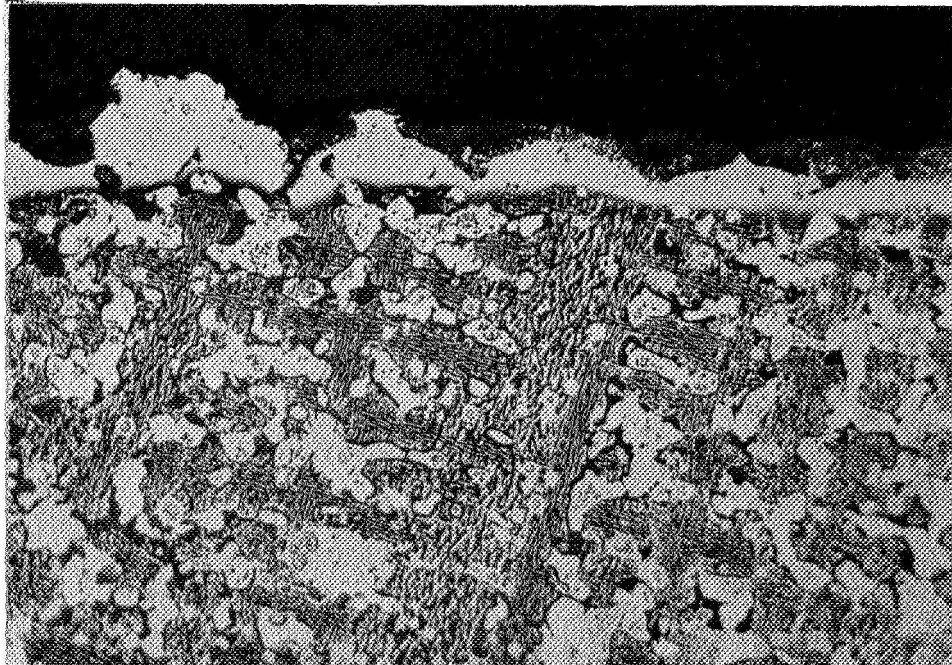
A11408   B10390

(a)   Alloy 2Q 0.5 La + 1 Mn, (50F Superheat)

A11412   B10392

(b)   Alloy 18, 0.5 La + 1 Mn (225F Superheat)

Figure 34:   Microstructures of Oxidation Specimens
after 400 Hrs. at 2000F. Etched. 250X
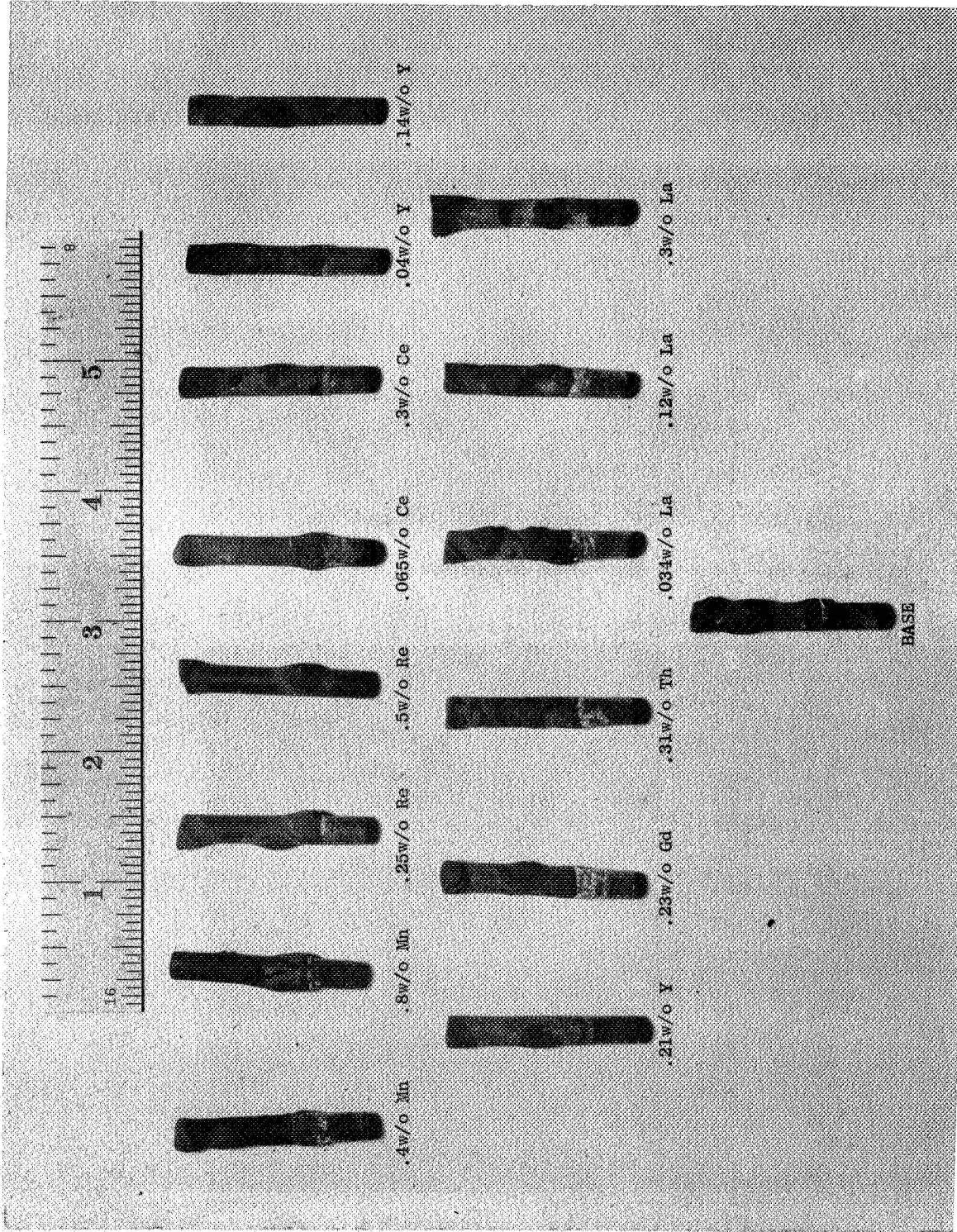
Neg. No. C68110741

Figure 35: Test Specimens after Hot Corrosion at 1750F/50 Hrs./100 ppm.
Showing Overall Appearance. Drop Cast Alloys.   1X

84
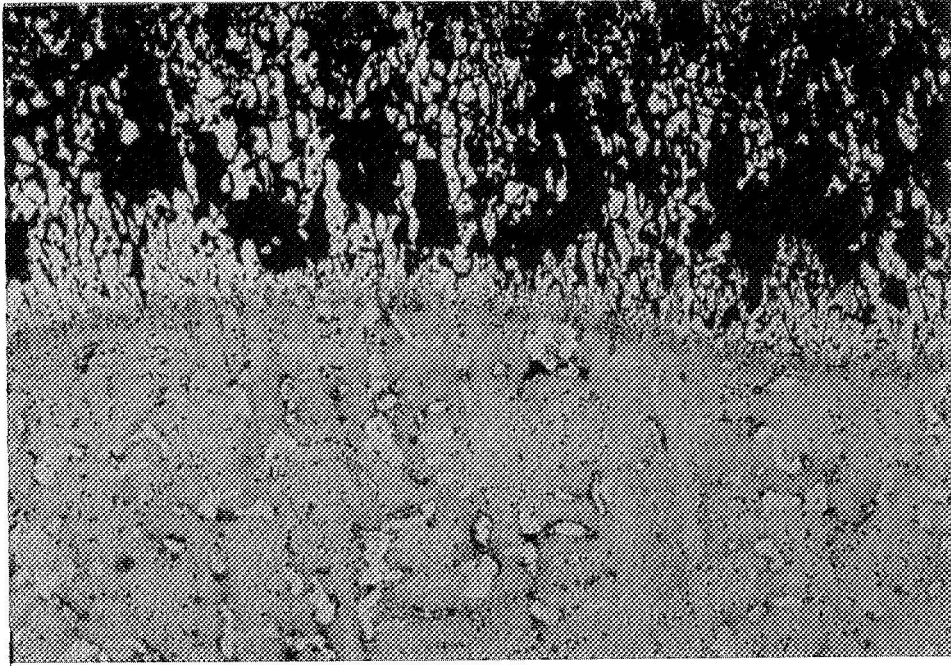
J9152   P8262
(a)   Base Alloy #1, Investment Cast
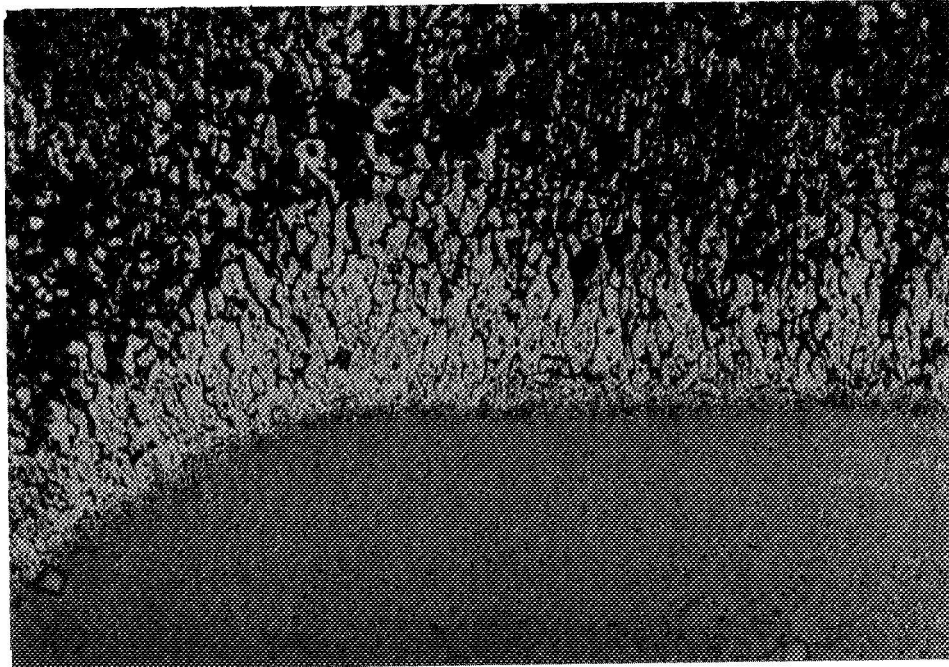
J9705   P8283
(b)   Alloy #12, Drop Cast

Figure 36:   Microstructures of Alloys 1 & 12 after Corrosion Testing
              at 1550F/50 Hrs., 100 ppm Salt. Etched. 100X

.23w/o Gd + .4w/o Mn   .23w/o Gd + .8w/o Mn   .25w/o Re + .4w/o Mn   .25w/o Re + .8w/o Mn   .04w/o Y + .4w/o Mn

.04w/o Y + .8w/o Mn   .14w/o Y + .4w/o Mn   .14w/o Y + .8w/o Mn   .21w/o Y + .4 w/o Mn   .21w/o Y + .8w/o Mn

.31w/o Th + .4w/o Mn   .31w/o Th + .8w/o Mn
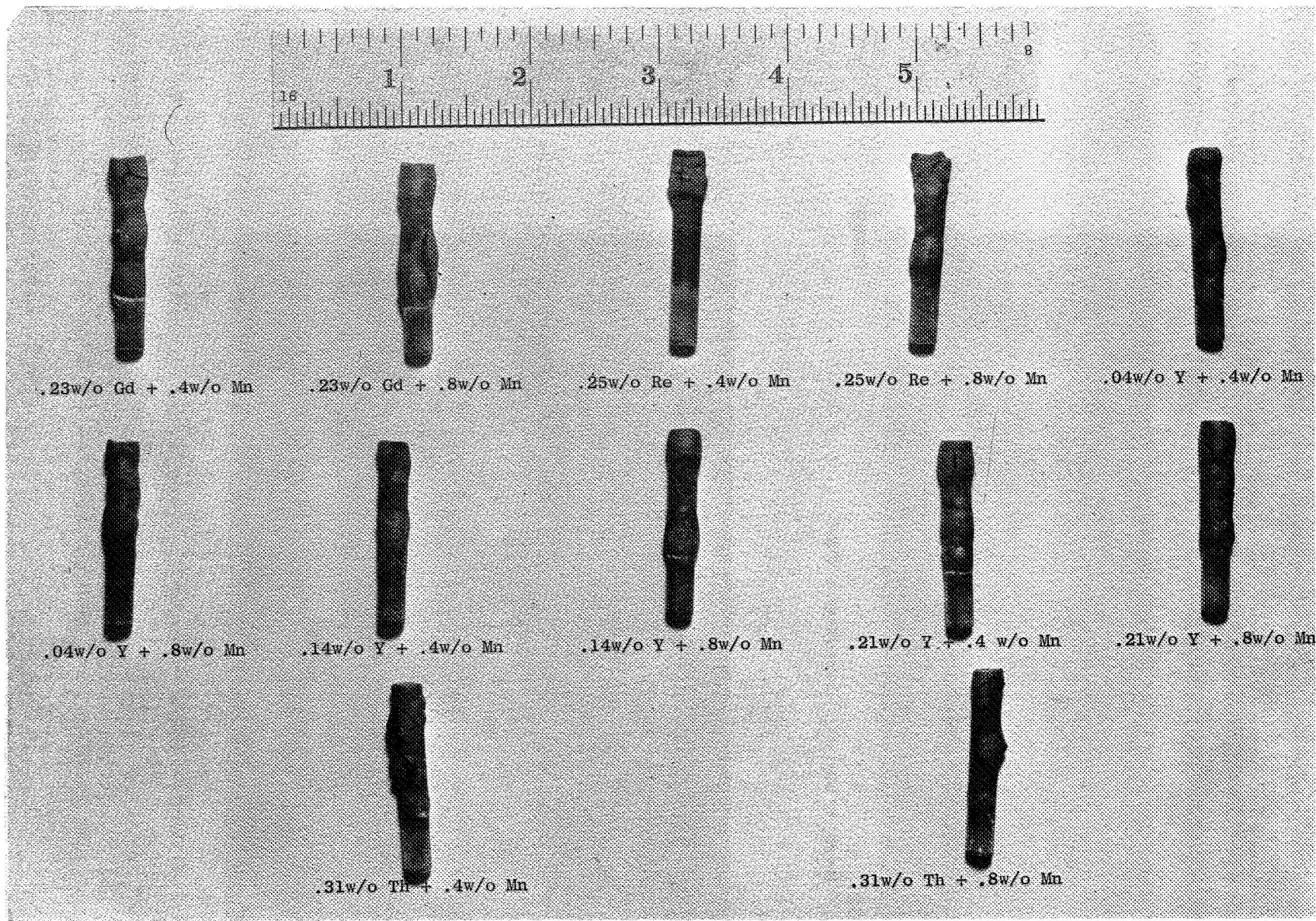
Neg. No. C68110742

Figure 37:   Test Specimens after Hot Corrosion at 1725F/50 hrs./100 ppm.
             Drop Cast Alloys Containing Combination of Doping Elements. 1X

.5 Y   .75 Y   1.0 Y   .5 Ce   .75 Ce   1.0 Ce   .5 La   .75 La   1.0 La

.75 Y
. 5 Mn

.75 Ce
. 5 Mn

.75 La
. 5 Mn

Rene' 77
(Wrought)

.5 Y   .75 Y   .5 Ce   .75 Ce   .5 La   .75 La
.5 Mn   1.0 Mn   .5 Mn   1.0 Mn   .5 Mn   1.0 Mn
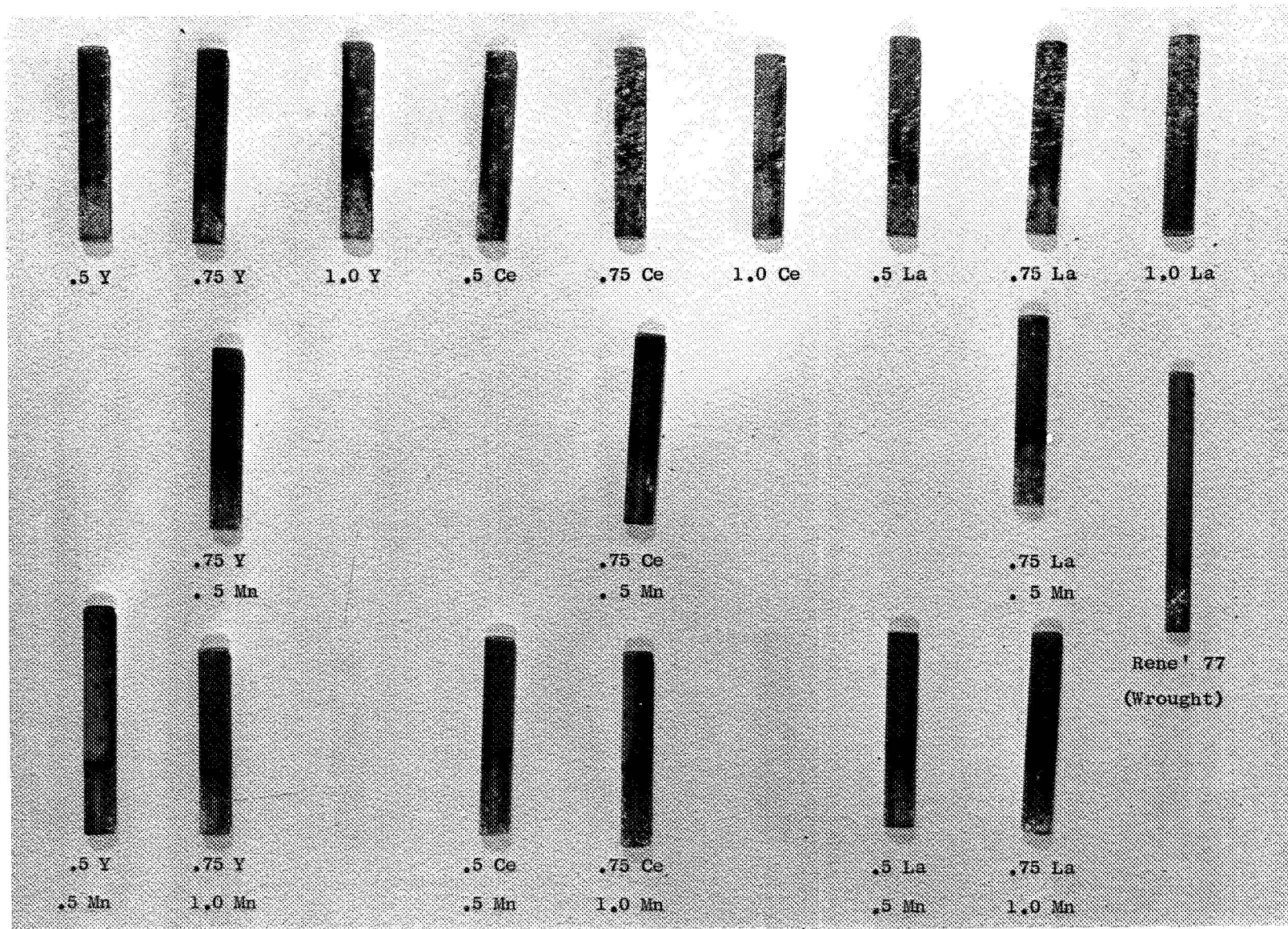
Neg. No. C69040733

Figure 38: Test Specimens after Hot Corrosion at 1550F/50 hrs./100 ppm.
            Drop Cast Alloys.   1X

87

.5 Y   .75 Y   1.0 Y   .5 Ce   .75 Ce   1.0 Ce   .5 La   .75 La   1.0 La

.75 Y
.5 Mn

.75 Ce
.5 Mn

.75 La
.5 Mn

Rene' 77
(Wrought)

.5 Y
.5 Mn

.75 Y
1.0 Mn

.5 Ce
.5 Mn

.75 Ce
1.0 Mn

.5 La
.5 Mn

.75 La
1.0 Mn
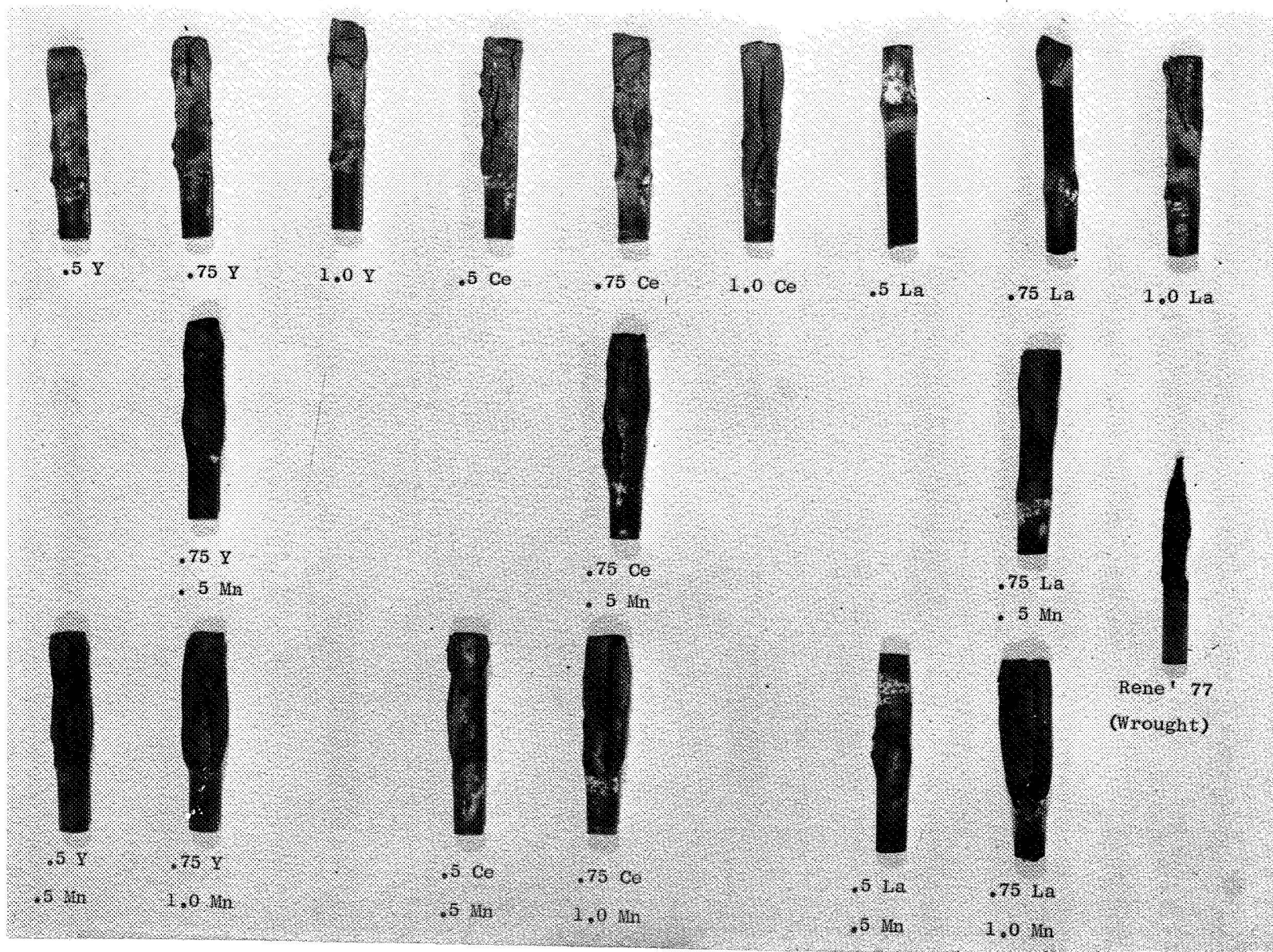
Neg. No. C69040734

Figure 39: Test Specimens after Hot Corrosion at 1725F/50 hrs./100 ppm.
Drop Cast Alloys.   1X

88
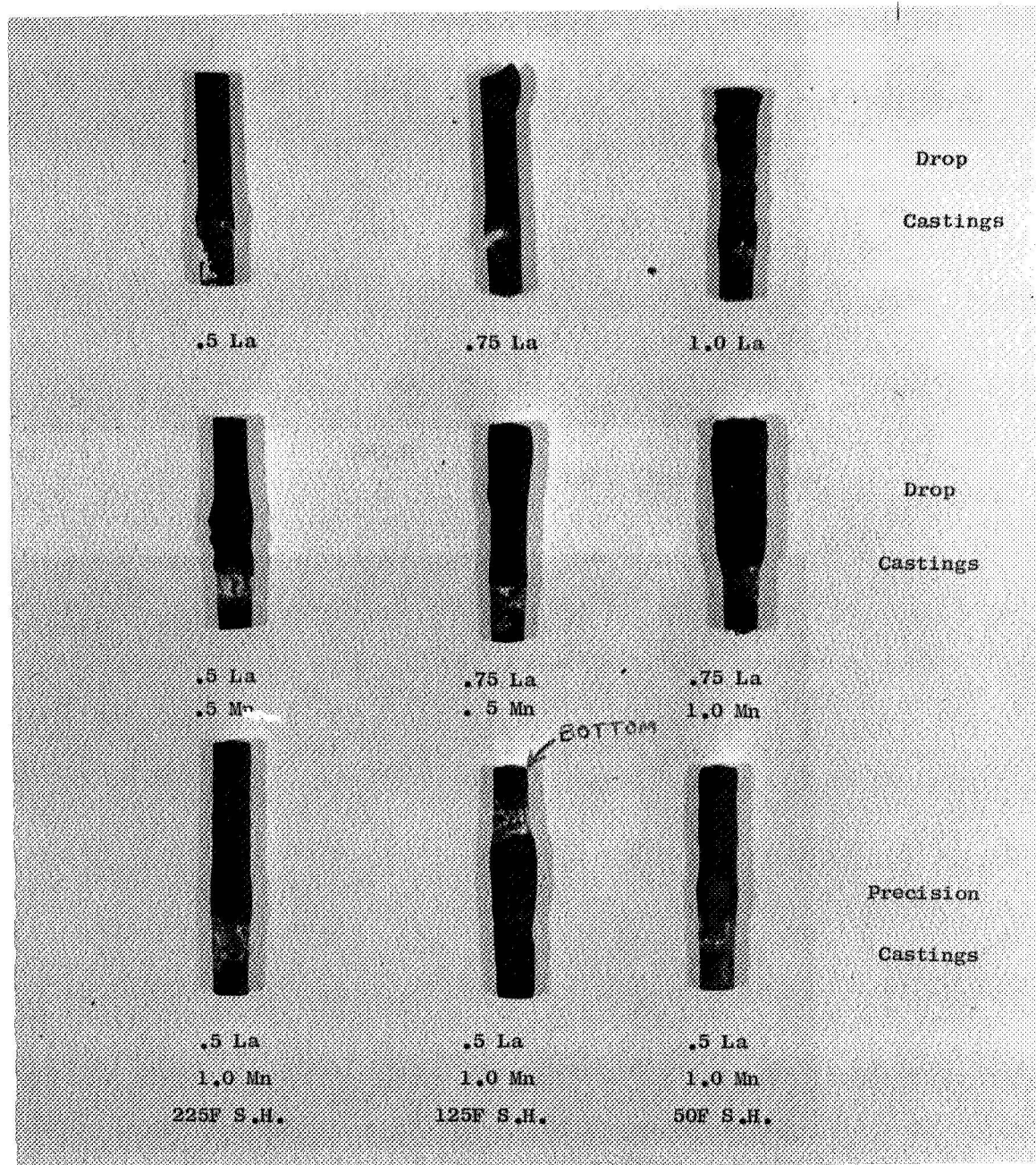
Neg. No. C69040732

Figure 40: Test Specimens after Hot Corrosion at 1725F/50 hrs./100 ppm
Effect of La & Mn in Investment and Drop Castings. 1X
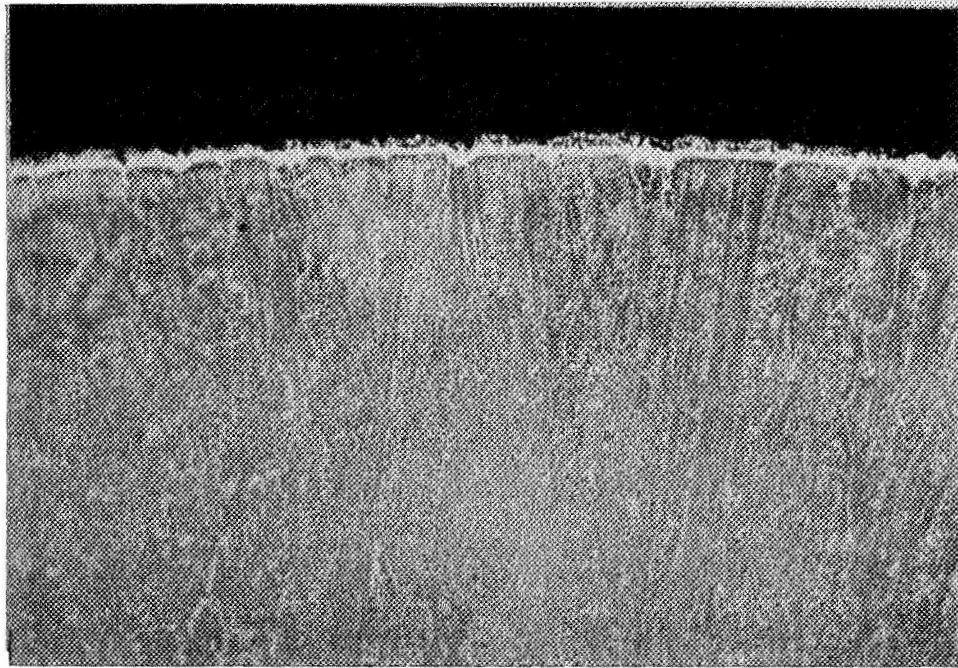
A3614   B1040   B10401
(a)   Etched, 250X
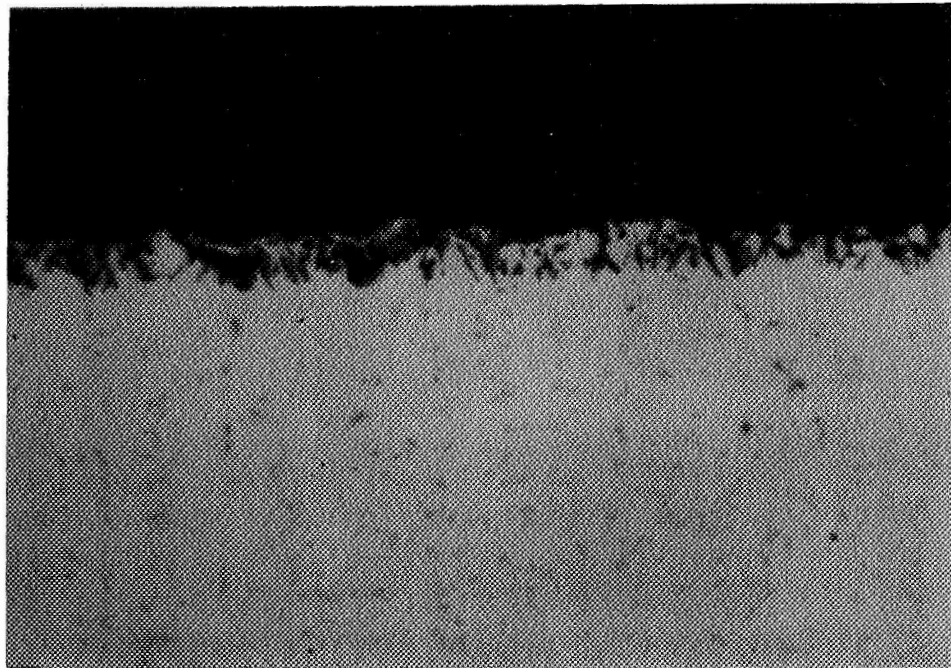
A3614   B10371
(b)   Unetched, 1000X

Figure 41:   Microstructure of a 0.5 w/o La Drop-Cast Alloy after
             Hot Corrosion for 30 Hrs. at 1725F/100 ppm Salt.
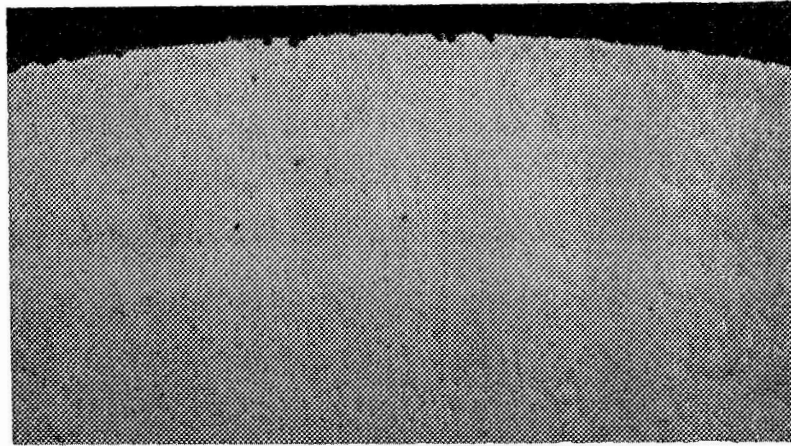
A3616   B10367
(a)   0.75% La Alloy, Negligible Corrosion
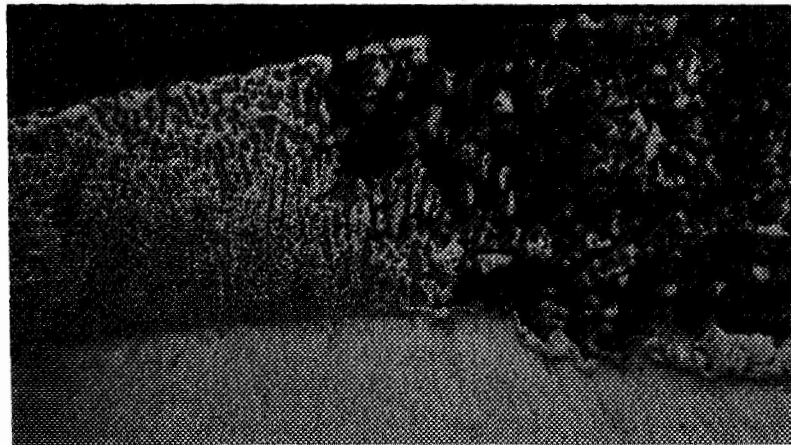
A3615   B10318
(b)   0.75% La Alloy, Gross Corrosion
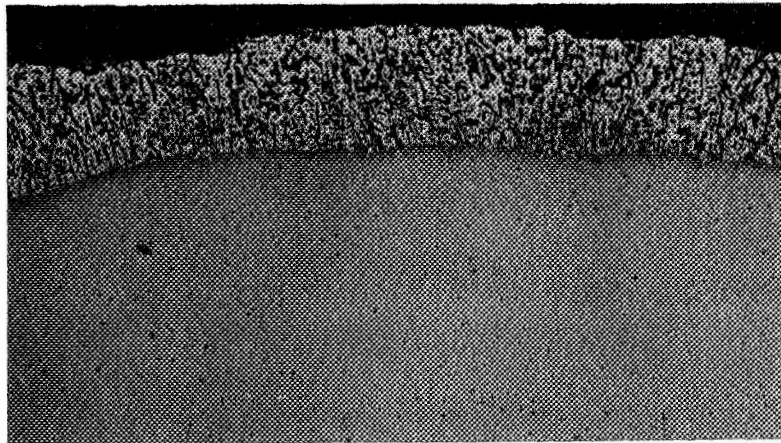
J9713   P8293
(c)   0.5% Re Alloy, Internal Sulfidation

Figure 42:   Microstructures of Various Drop-Cast Alloys after Hot Corrosion
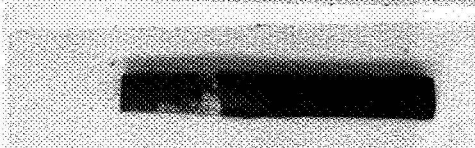   for 30 Hrs. at 1725F/100 ppm Salt. Unetched. 100X
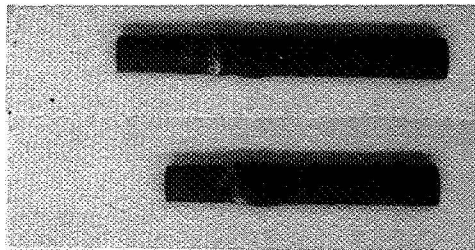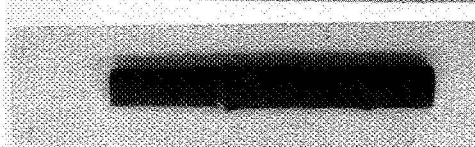
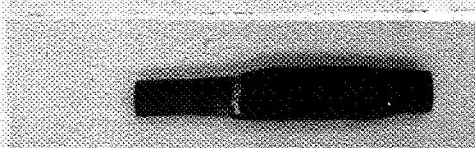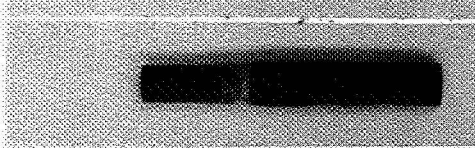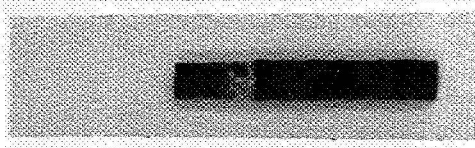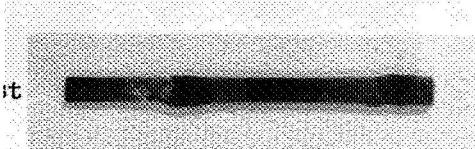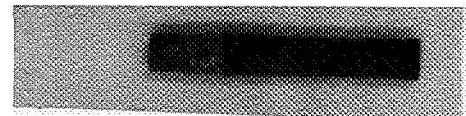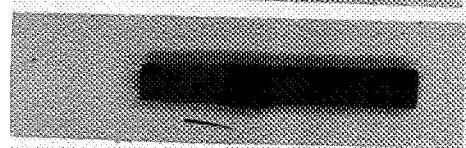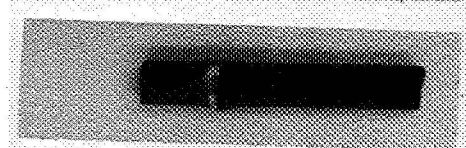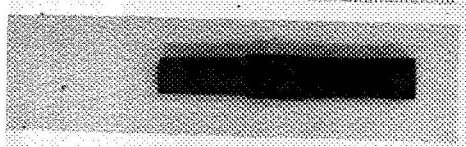| Alloy No.		Alloy No.	
15 .065La		23 0.4La + Re	
16 0.20La		24 0.6La + Re	
17 0.30La		24 D Cast 0.6La + Re	
18 0.5La + Re + Mn		25 0.6La + Re + Mn	
19 0.5La + Re + Mn		25 D Cast 0.6La + Re + Mn	
20 0.5La + Re + Mn		26 0.2La + 0.2Y + Re	
21 0.5La + Re		26 D Cast 0.2La + 0.2Y + Re	
21 D Cast 0.5La + Re		27 0.3La + 0.15Y + Re	
22 0.5La + Re		Rene' 77	
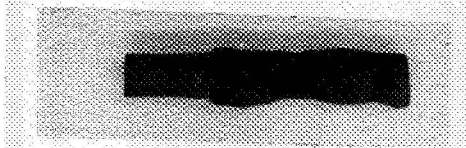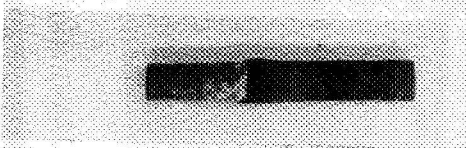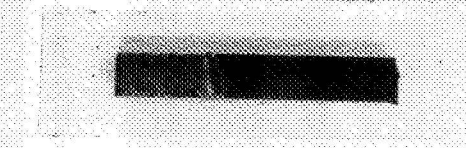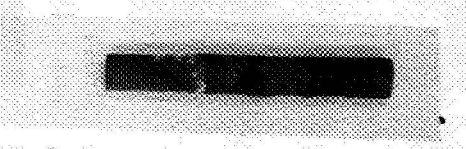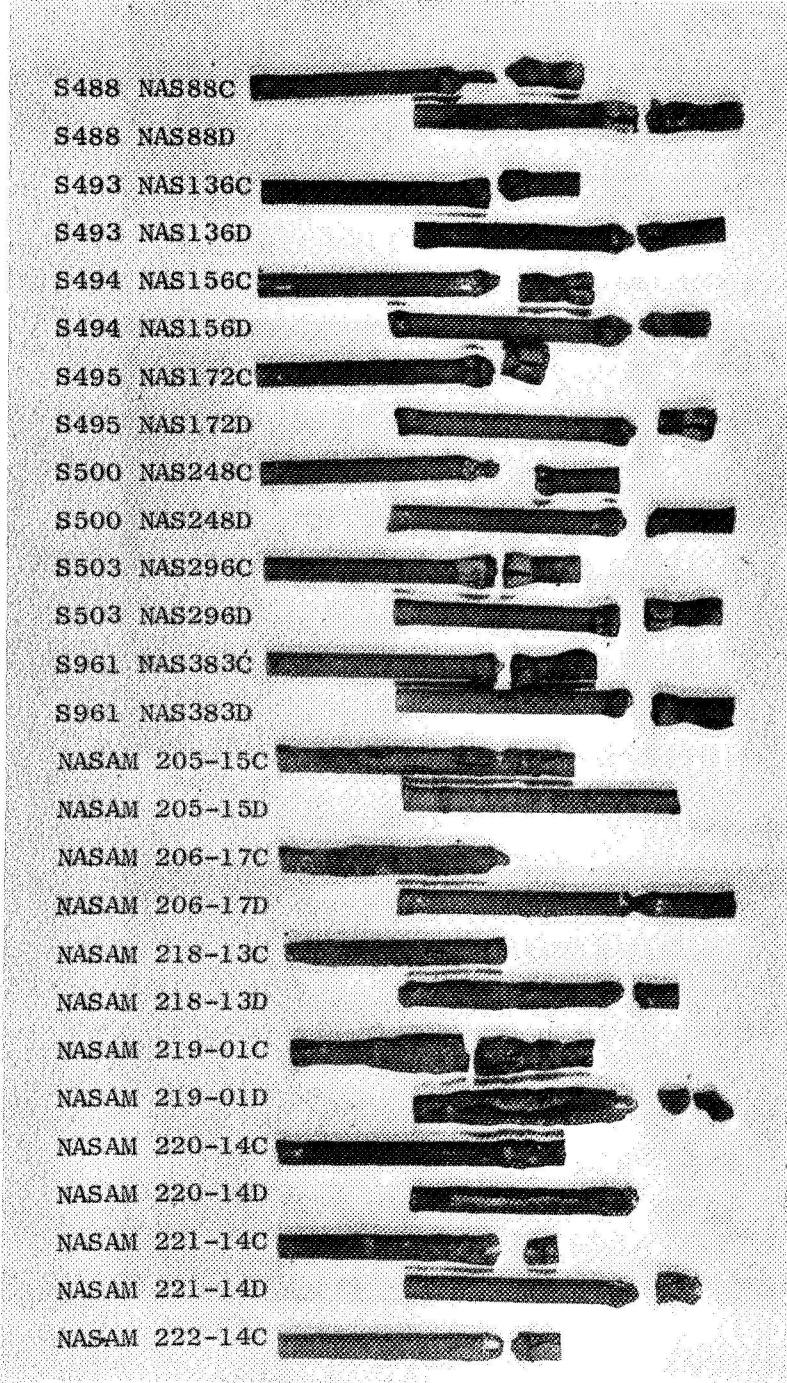
Figure 43:   Hot Corrosion Specimens after Testing at 1725F/100 ppm/30 hrs.

Alloy No.		Dopant Composition
1	S488 NAS88C	Base
	S488 NAS88D	
4	S493 NAS136C	0.8 Mn
	S493 NAS136D	
5	S494 NAS156C	0.25Re
	S494 NAS156D	
6	S495 NAS172C	0.50Re
	S495 NAS172D	
11	S500 NAS248C	0.14Y
	S500 NAS248D	
14	S503 NAS296C	0.31Th
	S503 NAS296D	
17	S961 NAS383C	0.3La
	S961 NAS383D	
21	NASAM 205-15C	0.5La + 0.25Re
	NASAM 205-15D	
22	NASAM 206-17C	0.5La + 0.25Re
	NASAM 206-17D	
23	NASAM 218-13C	0.4La + 0.25Re
	NASAM 218-13D	
24	NASAM 219-01C	0.6La + 0.25Re
	NASAM 219-01D	
25	NASAM 220-14C	0.6La + 0.25Re + 1 Mn
	NASAM 220-14D	
26	NASAM 221-14C	0.2La + 0.2Y + 0.25Re
	NASAM 221-14D	
27	NASAM 222-14C	0.3La + 0.15Y + 0.25Re

C69102228

Figure 44: Hot Corrosion Specimens after Test at
1600F/450 hrs./1 ppm Salt.
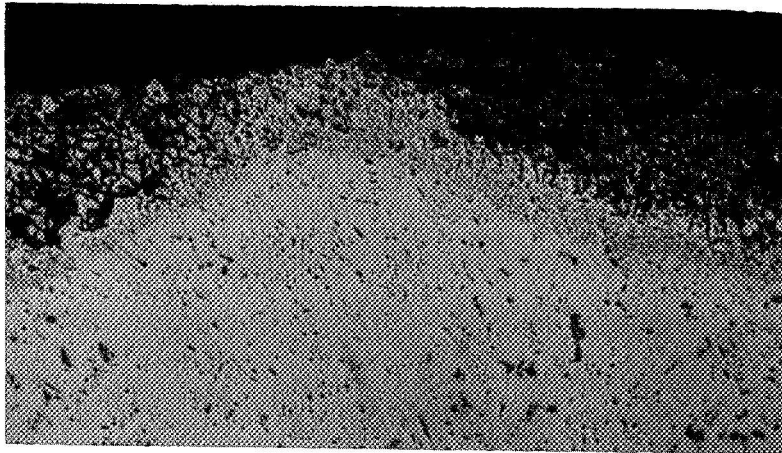
A11432   B10355
(a) Severe Corrosion, Unetched 100X
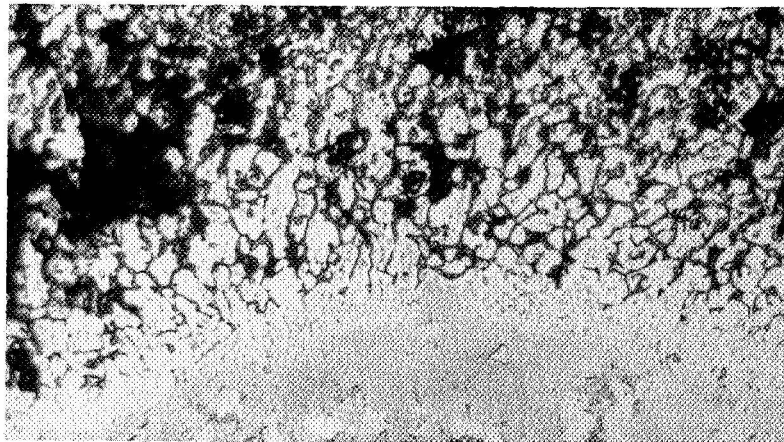
A11432   B10396
(b) Severe Corrosion, Etched 250X
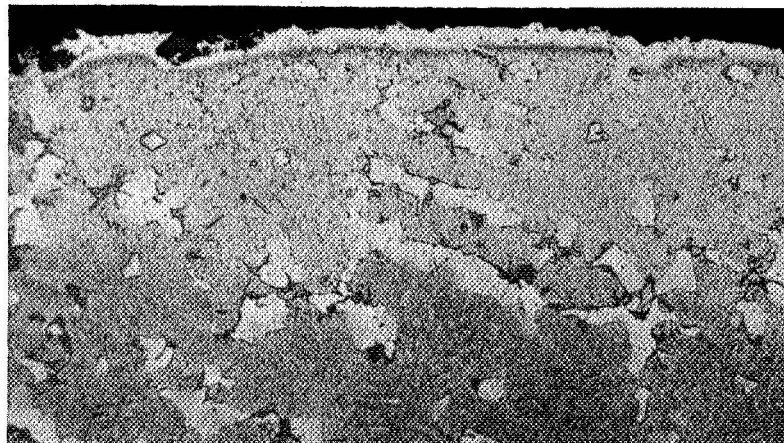
A11449   B10400
(c) Negligible Corrosion, Etched 250X

Figure 45: Microstructures of Base Alloy (#1) after Hot Corrosion
for 450 Hrs. @ 1600F/1 ppm Salt.

94
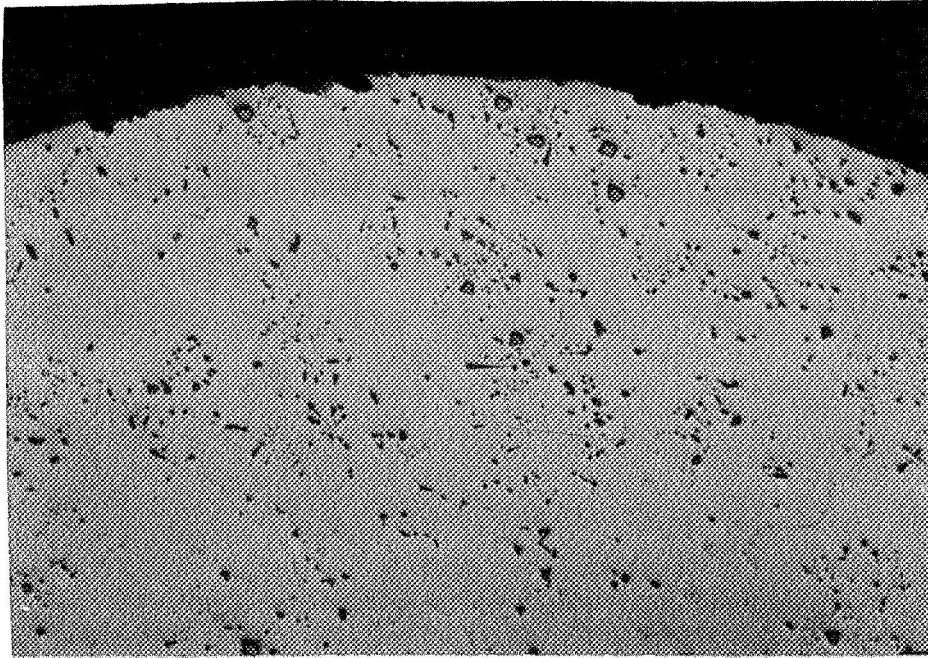
(a)   Alloy No. 5   B10353
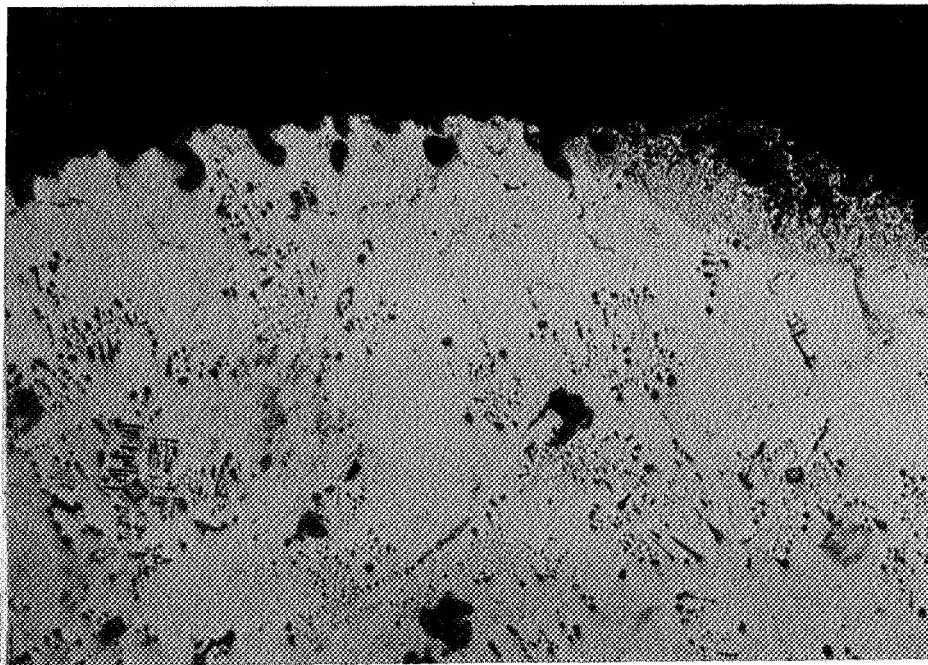
(b)   Alloy No. 6   B10352

Figure 46:   Microstructures of Alloys 5 & 6 (.25 & .5% Re) after
Hot Corrosion for 450 Hrs. at 1600F/1 ppm Salt.
Unetched, 100X
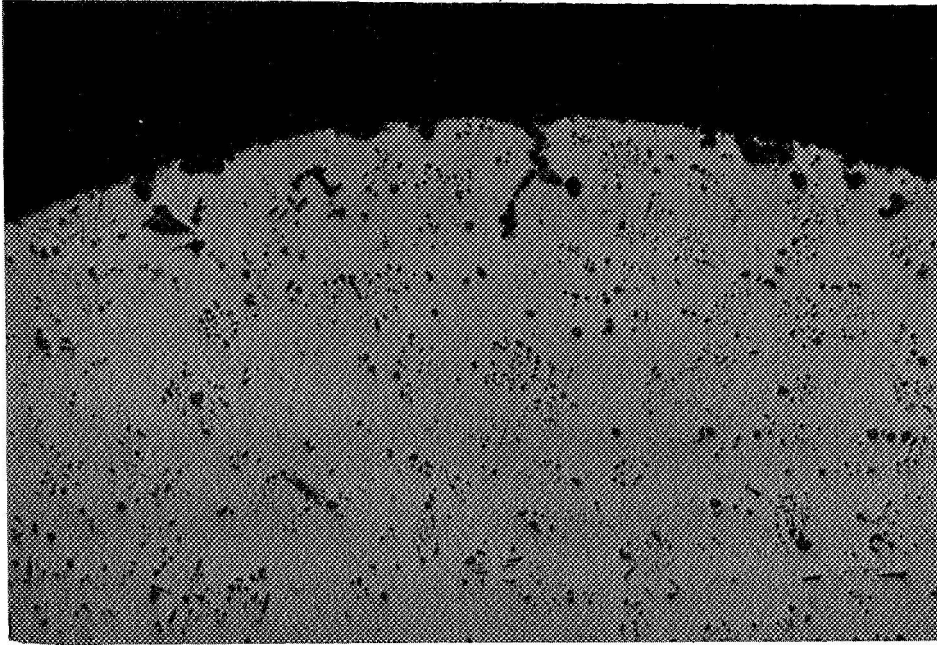
A11437   B10360
(a)   Alloy #11, (.14Y), Unetched, 100X
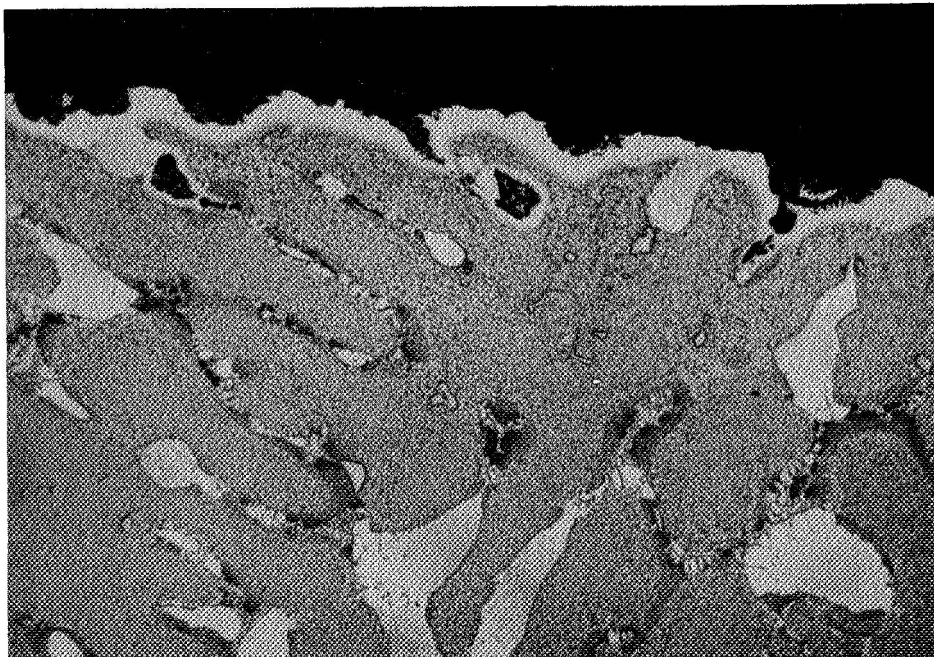
A11443   B10399
(b)   Alloy #21 (.5La) Etched, 250X

Figure 47:   Microstructure of Alloys 11 and 21 after Hot Corrosion
             for 450 Hrs. at 1600F/1 ppm Salt.

Polished
Preoxidized
(2100°F/64 hrs.

Polished

MS-61 (10Cr-6Al-1Y)

MS-60 (10Cr-4Al-1Y)

MS-59 (5Cr-6Al-1Y)

MS-38 (15Cr-4Al-1Y)

C69101505

Figure 48: Fe-Cr-Al-Y Alloy Specimens after Hot Corrosion Testing 1 Hr. at 1800F in 99% Na_2SO_4 + 1% NaCl Solution.

NASA Headquarters
600 Independence Avenue
Washington, D. C.   20546
Attn: G. C. Deutsch/RRM   1
        R. H. Raring/RRM   1
        J. Gangler/RRM   1
        N. Rekos/RAP   1

NASA Lewis Research Center
21000 Brookpark Road
Cleveland, Ohio   44135
Attn: G. M. Ault, MS 105-1   1
        N. T. Saunders, MS 105-1   1
        A. E. Anglin, MS 106-1   1
        F. H. Harf, MS 106-1   5
        C. Blankenship, MS 105-1   1
        R. L. Ashbrook, MS 49-1   1
        J. W. Weeton, MS 49-1   1
        J. C. Freche, MS 49-1   1
        Aeronautics Procurement
           Section, MS 77-3   1
        Library, MS 60-3   2
        Patent Counsel, MS 500-311   1
        Report Control Office,
           MS 5-5   1
        Technology Utilization
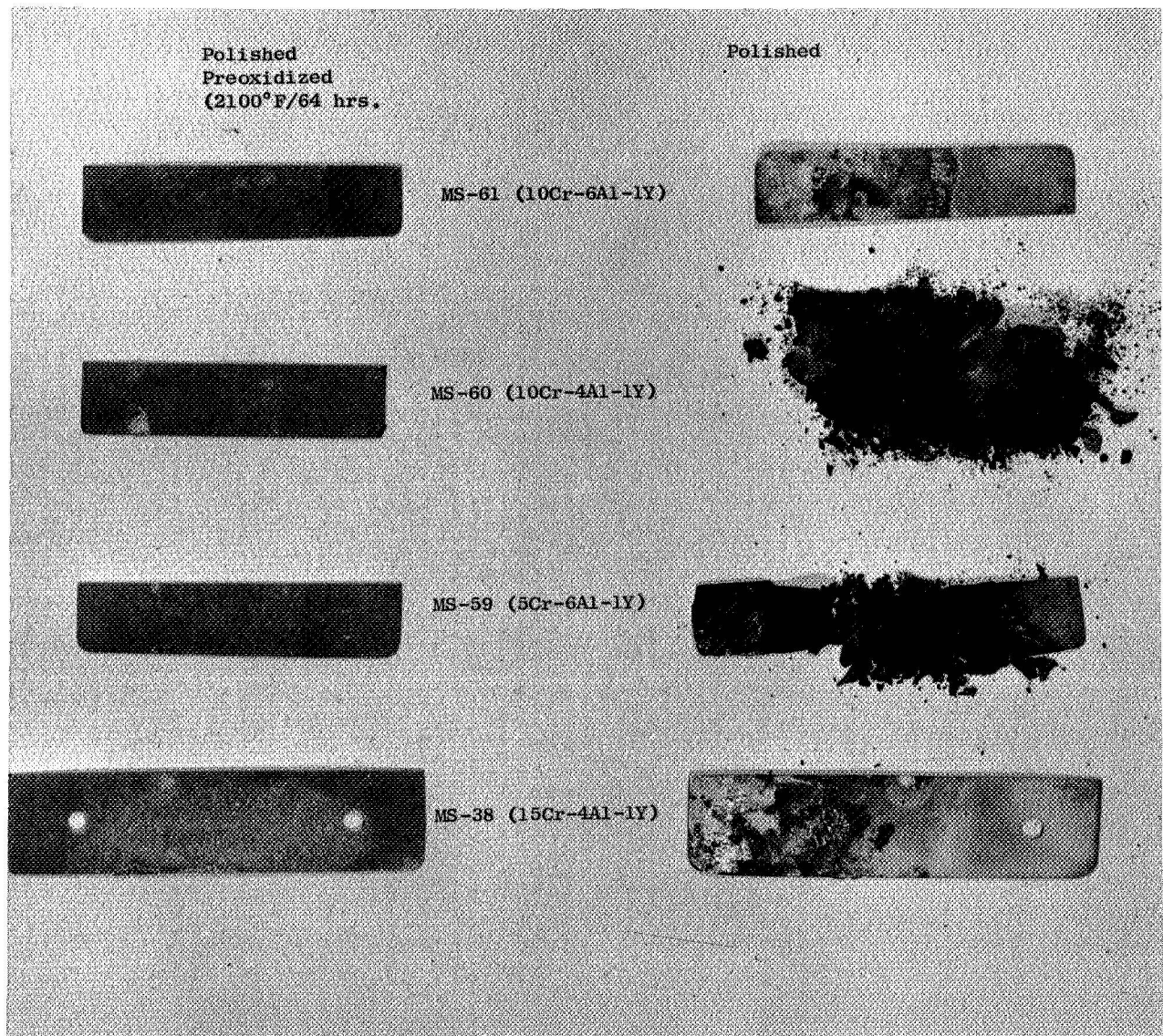   Office, MS 3-19   1
        H. B. Probst, MS 49-1   1
        R. W. Hall, MS 105-1   1

NASA Scientific and Technical
   Information Facility
P. O. Box 3300
College Park, Maryland   20740
Attn: NASA Rep. RQT-2448   6

NASA Langley Research Center
Langley Field, Virginia   23365
Attn: Library   1
        R. Pride, 188A   1

NASA Marshall Space Flight Center
Huntsville, Alabama   35812
Attn: Library   1

Jet Propulsion Laboratory
4800 Oak Grove Drive
Pasadena, California   91102
Attn: Library   1

NASA Ames Research Center
Moffett Field, California   94035
Attn: Library   1

NASA Goddard Space Flight Center
Greenbelt, Maryland   20771
Attn: Library   1

NASA Manned Space Flight Center
Houston, Texas   77058
Attn: Library   1

NASA Flight Research Center
P. O. Box 273
Edwards, California   93523
Attn: Library   1

FAA Headquarters
890 Independence Avenue, SW
Washington, D. C.   20553
Attn: Brig. Gen. J. C. Maxwell   1
        F. B. Howard, SS-210   1
        A. K. Forney   1

Headquarters
Wright Patterson AFB, Ohio   45433
Attn: MAG/A. M. Lovelace   1
        MAM/H. M. Burte   1
        MAAM/Technical Library.   1
        MAMS/C. T. Lynch   1
        MAMP/I. Perlmutter   1
        MAMP/J. K. Elbaum   1

Air Force Office of Scientific Research Propulsion Research Division USAF Washington, D. C. 20525 Attn: M. Slawsky	1

Army Materials Research Agency
Watertown Arsenal
Watertown, Massachusetts 02172
Attn: S. V. Arnold, Director   1

Department of the Army
Frankford Arsenal
Philadelphia, Pennsylvania 19137
Attn: MRL/H. Rosenthal   1

Department of the Navy
NASC Air-5203
Washington, D. C. 20360
Attn: P. Goodwin   1

Department of the Navy
ONR, Code 439
Washington, D. C. 20525
Attn: R. Roberts   1

Department of the Navy
Naval Ship R/D Center
Annapolis, Maryland 21402
Attn: G. J. Danek   1

U. S. Atomic Energy Commission
Washington, D. C. 20545
Attn: Technical Reports
          Library   1
          J. Simmons   1

Oak Ridge National Laboratory
Oak Ridge, Tennessee 37830
Attn: Technical Reports
          Library   1

Defense Documentation Center/DDC
Cameron Station
5010 Duke Street
Alexandria, Virginia 22314   1

Aerojet-General Corporation
Azusa, California 91702
Attn: I. Petker   1

Aerospace Corporation
Reports Acquisition
P. O. Box 95085
Los Angeles, California 90045   1

Allegheny Ludlum Steel Corporation
Research Center
Brackenridge, Pennsylvania 15014
Attn: R. A. Lula   1

American Society for Metals
Metals Park
Novelty, Ohio 44073
Attn: T. Lyman   1

Amsted Research Laboratories
P. O. Box 567
Bensenville, Illinois 60106
Attn: E. J. Zickefoose   1

AVCO Lycoming Division
505 South Main Street
Stratford, Connectcut 06497
Attn: W. H. Freeman   1

AVCO Space Systems Division
Lowell Industrial Park
Lowell, Massachusetts 01851
Attn: Library   1

Battelle Memorial Institute
505 King Avenue
Columbus, Ohio 43201
Attn: R. I. Jaffee   1
          B. Wilcox   1
          Cobalt Info. Center   1
          S. J. Paprocki   1

The Bendix Corporation
Research Laboratories Division
Southfield, Michigan 48075
Attn: Library   1

Boeing Company
P. O. Box 733
Renton, Washington 98055
Attn: W. E. Binz, SST Unit Chief 1

Cabot Corporation
Stellite Division
1020 West Park Avenue
Kokomo, Indiana 46901
Attn: Library 1

Case Institute of Technology
University Circle
Cleveland, Ohio 44106
Attn: Department of Metallurgy 1

Climax Molybdenun Company
1600 Huron Parkway
Ann Arbor, Michigan 48106
Attn: M. Semchyshen 1

Curtiss-Wright Corporation
760 Northland Avenue
Buffalo, New York 14215
Attn: C. Wagner 1

Denver Research Institute
University Park
Denver, Colorado 80210
Attn: Library 1

Denver University
Metallurgy Department
Denver, Colorado 80210
Attn: J. B. Newkirk 1

Douglas Aircraft Company (MSFD)
3000 Ocean Park Boulevard
Santa Monica, California 90406
Attn: Library 1

Falconbridge Nickel Mines, Ltd.
7 King Street, East
Toronto, Ontario, Canada
Attn: L. G. Bonar 1

Federal Mogul Corporation
Research and Development Center
Ann Arbor, Michigan 48106
Attn: J. G. LeBrasse 1

Firth Sterling, Incorporated
Powders Metals Research
P. O. Box 71
Pittsburgh, Pennsylvania 15230 1

Ford Motor Company
Materials Development Department
20000 Rotunda Drive
P. O. Box 2053
Dearborn, Michigan 48123
Attn: Y. P. Telang 1

Fordon McKay Laboratory
6 Oxford Street
Cambridge, Massachusetts 02138
Attn: M. Ashby 1

Garrett-Air Research
Phoenix, Arizona 85034
Attn: Supv. Materials Engineering,
     Department 93393 1

General Electric Company
Advanced Technology Laboratory
Schenectady, New York 12305
Attn: Library 1

General Electric Company
Materials and Processes Laboratory
Schenectady, New York 12305
Attn: C. T. Sims 1

General Electric Company
Materials Development Laboratory
  Operations
Advance Engine and Technical
  Department
Cincinnati, Ohio 45215
Attn: L. P. Jahnke 1
     R. E. Allen 1

General Motors Corporation
Allison Division
Indianapolis, Indiana 46206
Attn: K. K. Hanink, Materials   1
    Laboratory

IIT Research Institute
10 West 35th Street
Chicago, Illinois 60616
Attn: N. M. Parikh   1

Industrial Materials Technology
127 Smith Place
West Cambridge Industrial Park
Cambridge, Massachusetts 02138
Attn: R. Widmer   1

International Nickel Company
67 Wall Street
New York, New York 10005
Attn: R. R. Dewitt   1

International Nickel Company
P. D. Merica Research Laboratory
Sterling Forest
Stuffern, New York 10901
Attn: F. Decker   1

Ladish Company
Government Relations Division
Cudahy, Wisconsin 53110
Attn: C. Burley, Jr.   1

Latrobe Steel Company
Latrobe, Pennsylvania 15650
Attn: E. E. Reynolds   1

Lockheed-Georgia Company
Research Laboratory
Marietta, Georgia 30060
Attn: W. S. Cremens   1

Lockheed Palo Alto Research Laboratories
Materials and Science Laboratory, 2-30
3251 Hanover Street
Palo Alto, California 94304
Attn: Technical Information Center 1

Martin Metals
250 North 12th Street
Wheeling, Illinois 60090
Attn: C. H. Lund   1

McDonnel-Douglas Corporation
3000 Ocean Park Boulevard
Santa Monica, California 90406
Attn: R. Johnson   1

McDonnel-Douglas Corporation
P. O. Box 516
St. Louis, Missouri 63166
Attn: R. E. Jackson   1

Michigan Technical University
Department of Metallurgical
    Engineering
Houghton, Michigan 49931
Attn: R. W. Guard   1

Micromet Laboratories
202 South Street
West Lafayette, Indiana 47906
Attn: J F. Radavich   1

North American Rockewell Corporation
Rocketdyne Division
6633 Canoga Avenue
Canoga Park, California 91304
Attn: E. D. Weisert   1

North Star Research and Development
    Institute
3100 Thirty Eight Avenue South
Minneapolis, Minnesota 55406
Attn: J. W. Clegg   1

Ohio State University
Department of Metallurgical
    Engineering
Columbus, Ohio 43210
Attn: R. A. Rapp   1

Nuclear Materials Company
West Concord, Massachusetts 01781
Attn: Library   1

Philco-Ford Corporation
Ford Road
Newport Beach, California 92663
Attn: R. A. Harlow   1

Polymet Corporation
11 West Sharon Road
Cincinnati, Ohio 45346
Attn: G. J. Wile   1

Reactive Metals, Incorporated
100 Warren Avenue
Niles, Ohio 44446   1
Attn: H. D. Kessler

Solar Division
International Harvester Corporation
San Diego, California 92112
Attn: J. V. Long, Director of
       Research   1

Special Metals Corporation
New Hartford, New York 13413
Attn: W. J. Boesch   1

Stanford Research Institute
Menlo Park, California 94025
Attn: E. S. Wright   1

Stanford University
Department of Materials Science
Palo Alto, California 94305
Attn: O. Sherby   1

Sylvania Electric Products, Incorporated
Chemical and Metallurgical Division
Towanda, Pennsylvania 18848
Attn: J. S. Smith   1

Tem-Pres Research, Incorporated
1401 South Atherton Street
State College, Pennsylvania 16801
Attn: R. I. Harker   1

TRW, Incorporated
Materials Technology
23555 Euclid Avenue
Cleveland, Ohio 44117
Attn: Library   1
       E. A. Steigerwald   1

Union Carbide Corporation
Speedway Laboratories
P. O. Box 24184
Indianapolis, Indiana 46224
Attn: Technical Library   1

United Aircraft Corporation
400 Main Street
East Hartford, Connecticut 06108
Attn: Research Library   1
       E. F. Bradley, Chief,
       Materials Engineering   1

United Aircraft Corporation
Pratt and Whitney Aircraft
Advanced Materials R/D Laboratory
Middletown, Connecticut 06458
Attn: C. P. Sullivan   1

United Aircraft Corporation
Pratt and Whitney Aircraft Division
West Palm Beach, Florida. 33402
Attn: Library   1

Universal-Cyclops Steel Corporation
Bridgeville, Pennsylvania 14017
Attn: C. P. Mueller   1

Westinghouse Electric Corporation
Steam Division
P. O. Box 9175
Lester, Pennsylvania 19113
Attn: F. J. Wall   1

Wyman-Gordon Company
North Grafton, Massachusetts 01436
Attn: W. H. Couts   1

Homogeneous Metals, Incorporated
West Canada Boulevard
Herkimer, New York 13350
Attn: R. J. Nylen   1